When Art Auctions Overlap: Impact of Creator-Linked Concurrency in Singular Goods Online Auction Markets

Abhishek Deshmane[1] Haimeng Hester Zhang[2]

Abstract

Markets for singular goods—art, fine wine, collectibles—face radical valuation uncertainty. Online auctions aggregate independent sellers at scale, routinely creating overlapping listings of one creator's works, termed *concurrent auctions*, that can both intensify and resolve it. Unlike coordinated releases by movie studios and labels, concurrency emerges unscheduled from uncoordinated consignments, leaving demand cannibalization and cross-work spillovers in ambiguous tension. We formalize two forces: a *search channel* lowering discovery costs, and a *co-disclosure channel* whereby a sibling's public bidding history serves as an affiliated signal mitigating uncertainty, forming an endogenous *judgment device*. Using bid-level data on over 277,000 artworks from a major European platform for moderately priced works (mean estimate €260), we exploit the staggered onset of artist-linked concurrency in a difference-in-differences design with propensity-score-matched controls. Concurrency raises bidding on extensive (more unique bidders) and intensive margins (more bids, larger increments), lifting revenue by at least 3.5% (€3.9) per item, without cannibalizing same-category contemporaries: concurrency expands attention rather than diverting it. Both mechanisms are validated. Bidder entry triples when the sibling nears its close, signifying search facilitation; lagged sibling bidding predicts focal bidding, amplifying once the reserve is met. Both strengthen with form proximity until substitution dominates among near-identical works, a suggestive inverted-U. Gains rise monotonically in pre-sale estimate as common value dominates, reversing in the lowest quintile, where value is purely private taste. Wherever creator affiliation transfers reputational capital—wines by château, NFTs by creators—platforms may already generate judgment devices through release timing alone, enhancing platform and seller welfare, without deliberate design.

Keywords: Digital markets; Market innovation; Online auctions; Art market; Cultural operations

1 Introduction

Across creative industries, the release timing of works vying for the same audience is managed rather than incidental: film studios select release dates in explicit anticipation of competing titles (Krider and Weinberg 1998, Einav 2010), video game publishers space releases against their own catalogues (Haviv et al. 2020), and content creators pace output against their prior posts (Caro and Martínez-de Albéniz 2020). Traditional art auctions impose this discipline structurally:

[1]abhishek.deshmane@scheller.gatech.edu. Georgia Institute of Technology, Scheller College of Business, 800 W Peachtree St NW, Atlanta, GA 30308, USA.

[2]hzhang@iese.edu. IESE Business School, Av. Pearson 21, 08034 Barcelona, Spain.

facing buyers who can attend only one saleroom at a time, houses space their sale events and rarely release same-artist works together, sustaining participation and avoiding cannibalization. Since lots are called sequentially, even a sale holding several of an artist's works never puts two of them before a bidder at once.

The digital disruption of the past decade has radically changed this. Third-party platforms such as Auctionet, Invaluable, and LiveAuctioneers aggregate dozens of independent houses into a single marketplace, hosting tens of thousands of timed auctions before a large, geographically dispersed pool of bidders who browse asynchronously over days. Global online art sales nearly doubled from $6 billion in 2019 to $10.5 billion in 2024, after COVID-19 lockdowns (Art Basel and UBS 2025). What changed was not merely the channel but the market's architecture: in-person formats are sequential by necessity, digital aggregation is simultaneous by construction. On a platform hosting 40,000 live listings, a bidder browsing a particular artist routinely encounters several artworks at once. We call this *artist-level concurrent auctions*: distinct works by the same creator whose auction periods overlap. We study overlap at the artist level because, for singular goods, creator identity rather than any observable attribute anchors value and provides inference across listings, as we develop in §3. Such concurrency is not a designed feature but an emergent property of aggregating many sellers' listings at scale—a market innovation infeasible under sequential in-person formats, whose consequences for bidder behavior and market outcomes remain unexamined.

The revenue consequences of concurrency are theoretically ambiguous. Overlapping auctions may raise the focal auction's visibility, intensify competition, and generate real-time public information about artist-level demand, lifting revenue through higher participation and more aggressive bidding (Sorensen 2007, Hendricks and Sorensen 2009). Alternatively, concurrency may fragment scarce bidder attention, induce substitution when concurrent works appear interchangeable, or strain budgets, producing self-cannibalization that leads auction houses, studios, and labels alike to stagger related releases (Krider and Weinberg 1998, Bayus and Putsis 1999).

These competing forces matter most where institutional intermediation is thinnest. Art markets follow a steep Pareto distribution: a handful of blue-chip artists account for the bulk of value, a long tail of regional artists for the bulk of transactions (McAndrew et al. 2012). Blue-chip works have specialist dealers, indexed sale histories, and catalogue scholarship, the judgment apparatus buyers need to fix valuations (Karpik 2010). Long-tail works do not: a regional Swedish landscape from the 1950s has no price index, comparable sale, or specialist to consult. Concurrent auctions, we propose, fill this gap. When a sibling listing by the same artist is live, its publicly observable bidding history becomes a creator-anchored, real-time signal of

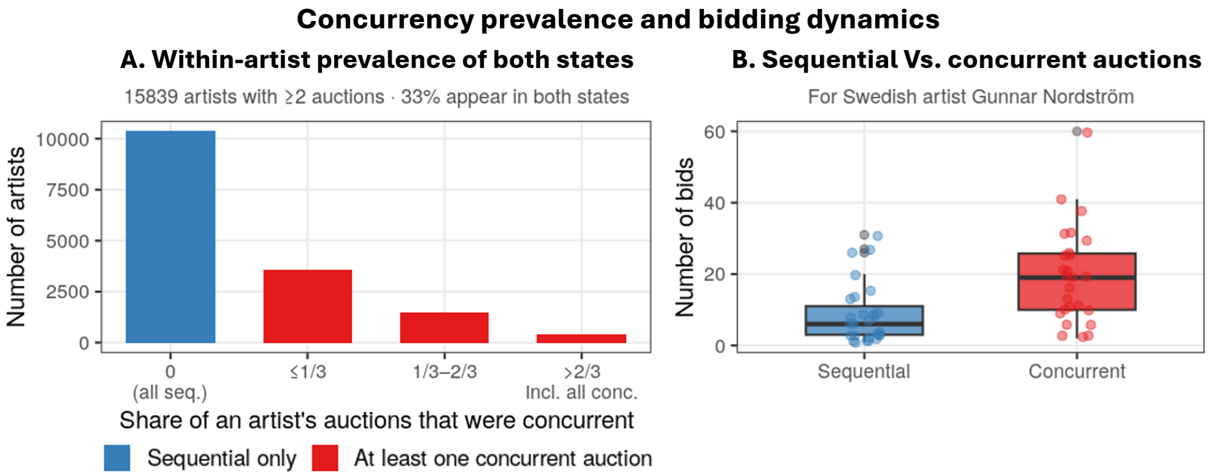

Figure 1: Panel A shows the distribution of 15,839 artists' portfolios by concurrency exposure: one-third appear in both states, with some auctions running concurrently with a same-artist sibling listing and others running without any overlap. Panel B shows the distribution of total bids received across auctions for a randomly chosen artist, Gunnar Nordström (55 works; 26 concurrent), separately for concurrent and non-concurrent episodes.

collective demand, an endogenous *judgment device* the platform generates without engineering it. Past work on overlapping auctions has focused on *identical goods* (Bapna et al. 2009), leaving unresolved the non-identical, and indeed singular, case. The setting also relieves a difficulty that has kept the broader question open: where producers schedule their own releases, timing is chosen in anticipation of the very forces one wishes to measure, whereas here overlap follows from the uncoordinated intake of independent consignors. Hence, we pursue three research questions. RQ1: Does the onset of artist-level concurrency amplify or cannibalize bidding activity and revenue in the focal auction? RQ2: Through what mechanisms does the dominant effect operate? RQ3: Under what conditions, of form proximity (aesthetic, in our case) with the concurrent works and of the value at stake in the focal one, does the dominant effect reverse?

Scope of artist-level concurrency. Figure 1 provides model-free evidence on the scope and bidding consequences of concurrency. Panel A shows that out of 15,839 artists with at least two items, one-third experience some concurrency when independent partner houses' auction schedules happen to overlap. Because these houses do not coordinate consignments, concurrency reflects timing rather than a property of the artist or work. Panel B illustrates the consequences for a randomly chosen artist, Gunnar Nordström, a Swedish painter with 55 works, 26 auctioned off with mutual concurrencies. His concurrent works drew a median of 19 bids against 6, a systematic difference being whether a sibling work was listed simultaneously. These patterns ground RQ1 but cannot rule out selection: *concurrent works may differ in quality*, and while sellers do not coordinate, *the platform's intake processes could shape when works go live in correlation with demand.* These concerns, and our aim of analyzing the mechanisms holistically

(RQ2 and RQ3), require a structured theoretical and empirical exploration.

Theoretical and empirical frameworks. We develop a theoretical framework and bring it to bid-level data from Auctionet, a Swedish third-party platform aggregating 82 independently consigning partner houses and hosting approximately 40,000 simultaneous auctions daily. Our dataset covers over 277,000 items spanning paintings, drawings, graphics, and photographs. The platform specializes in the long-tail secondary market of regional artists (mean pre-sale estimate €260), where seller-provided estimates are backward-looking and of variable reliability (Beggs and Graddy 1997) and institutional intermediation is largely absent, precisely where we propose the stakes of concurrency are highest. Building on affiliated values (Milgrom and Weber 1982), the framework formalizes two channels. A *search channel* raises the focal auction's discovery probability and draws additional bidders, enriching bid history. An *information co-disclosure channel* makes the sibling's observable bid path a creator-anchored affiliated signal, raising expected revenue bid by bid. Both operate against the *winner's curse*: because valuations share an artist-linked common value component, the winner tends to be whoever most overestimated it, and rational participants shade their bids accordingly. Cross-auction information about artist demand, we propose, lets them update toward the common value and bid less cautiously, mitigating the curse and raising expected revenue.

Since treatment assignment is non-random, we combine propensity-score matching with a staggered difference-in-differences design. We match each treated auction to controls of comparable pre-treatment bidding trajectories, pre-sale estimates, listing timing, and genre. The empirical design then exploits the precise moment a sibling listing appears within an ongoing auction, generating within-auction treatment variation.

Results and contributions. The onset of concurrency produces immediate and sustained increases in bidding activity against flat pre-trends, supporting a near-causal reading. *Treated auctions gain on all four bidding margins on average.* New bidder entry rises by 0.6% per 3-hour window and bidding frequency by 1.0%, while mean bid increment rises by 3.4%. Overall revenue increment increases by 3.5% under baseline and up to 5.5% under alternative specifications, translating into an average revenue lift of €3.9 to €6.2 per item, respectively. We find *no cannibalization of non-concurrent same-category listings*, whose bidding activity is statistically indistinguishable from different-category controls: concurrency expands the pool of attention rather than merely redistributing it. Survival analyses confirm the acceleration in the time domain, with concurrency raising the per-window rate at which a treated auction meets its reserve by 79.7% ($\widehat{\mathrm{HR}} = 1.797$) and more than tripling the rate at which it attracts an additional unique bidder ($\widehat{\mathrm{HR}} = 3.136$). We show that the *search channel* appears in timing, as the entry effect triples when the concurrent sibling is in its attention-rich closing hours, sniping-generated traffic spilling over via shared artist tags. Lagged bidding on the sibling listing significantly impacts bidding on the focal one, confirming the co-disclosure channel, which intensifies once the reserve is met and the item is confirmed to sell. Finally, the participation margins trace a suggestive inverted-U in form proximity, peaking at moderate similarity and attenuating to insignificance in bidder entry among near-identical pairs, consistent with entry deterrence and substitution offsetting amplification at the top of the range. The effect on bid increments rises monotonically in the focal item's pre-sale estimate. Concurrency thus cannibalizes at the bottom of the value distribution and amplifies at the top.

Our work makes two main contributions. First, we document a market innovation without deliberate design. Platforms aggregate independent consignors for reach; a byproduct is that a creator's works come to market together, and live bidding on one becomes a public, contemporaneous signal of demand for the other. This signal is economically consequential: concurrency lifts bidding on every margin and expands attention rather than diverting it, supplying to the long tail, at no incremental cost, the judgment that dealers, indices, and appraisers price out of reach. This emergent structure is distinct from directed engineering that dominates market design—recommendation systems, reputation scores, reserve rules. We propose that in institutionally thin markets, recognizing existing structure may matter as much as building new mechanisms. Second, we develop the first theoretical framework for *concurrent auctions in non-identical goods markets*, formalizing the search and co-disclosure channels under affiliated values, and identify two conditions under which a creator's co-present works complement rather than cannibalize each other: the works must differ enough in form that bidders do not treat them as substitutes, and the focal work must carry enough common value for a sibling's bidding to be informative. Where either fails—among near-identical works, or in the lowest quintile of pre-sale estimates—we recover the substitution result known from identical goods (Bapna et al. 2009). Across most of our sample both conditions hold, and co-presence is complementary.

This work proceeds as follows. §2 reviews related literature. §3 develops the theoretical framework and hypotheses. §4 describes the setting, data, and descriptive patterns. §5 presents the empirical strategy and baseline results with mechanisms and boundary conditions explored in §6. §7 reports robustness tests and §8 provides managerial implications before the conclusion.

2 Related Literature

2.1 Transition to Digital Platforms as Market Innovation

As aggregator platforms displace conventional auction houses, the digital disruption is not merely one of channel but of market and process innovation, restructuring competition, search, and information (Sting et al. 2024). For standardized, readily compared goods, online shopping lowered and dispersed prices (Brynjolfsson and Smith 2000) and made niche titles profitable once search costs fell (Bakos 1997, Brynjolfsson et al. 2011). For idiosyncratic goods such as used items and collectibles, platforms sustained liquid markets that physical channels served poorly, with eBay auctions persisting precisely where competitive bidding discovers prices sellers cannot otherwise observe (Einav et al. 2018). And for goods too uncertain in quality to trade without manufactured trust (Luca et al. 2026), accumulated reviews substituted for the assurance of brands, as on Airbnb (Farronato and Fradkin 2022), while lenders and backers in online credit and crowdfunding inferred quality from the observable choices of those before them (Zhang and Liu 2012, Agrawal et al. 2015). The commonality across streams is informational.

None of these settings, however, features goods at once (i) non-identical, so no reference unit *reliably* informs valuation, and (ii) creator-linked, so reputation rather than any observable attribute anchors value. Existing work falls short here: reviews are retrospective; price indices require comparable units (Noparumpa et al. 2015); pre-sale estimates, anchored to concluded sales, are imperfect even for established artists (Beggs and Graddy 1997, Ashenfelter and Graddy 2002). For long-tail artists with sparser histories this impedes calibration. None supplies a forward-looking valuation of what the market will pay right now. Creative-goods research comes closest, treating the producer as the unit of inference—audiences carry what one release reveals to the next in music (Hendricks and Sorensen 2009)—but the producer schedules the releases, so what is revealed, and when, are jointly chosen. Auction platforms instead supply real time contemporaneous bidding on a live same-creator listing, rather than a critic, index, or concluded sale. Online market design can thus synthesize the evaluative apparatus these markets have procured from intermediaries, not merely cut search costs or disclose information.

2.2 Online Auctions: Market Design to Emergent Concurrency

Operations management has long treated online auction design as a prescriptive revenue management lever through optimal dynamic auctions for fixed capacity (Vulcano et al. 2002), auction–posted-price mixes (Caldentey and Vulcano 2007), and repeated ad auctions (Balseiro et al. 2015, Balseiro and Gur 2019). We instead document concurrency's impact and mechanisms when independent sellers' auctions of non-substitutable goods overlap, leaving prescription to future work. The closest precedents study overlap among *identical goods* (Bapna et al. 2009, Einav et al. 2015) or near-substitutes: Pilehvar et al. (2017) show bidders infer price signals across concurrent auctions but restrict comparability to unit counts and retail values, leaving the non-identical case open. We exploit the onset of same-artist concurrency, with controls matched on prior bidding paths, grounding the signal in creator reputation and affiliated values.

A parallel literature in innovation management studies value that owners did not anticipate but nonetheless provisioned deliberately, whether by granting developers access or devolving platform control (Boudreau 2010, 2012), or, as with Landsat imagery, by supplying public data that reduced exploration uncertainty and raised entrants' share of gold discoveries (Nagaraj 2022). Both are deliberately provisioned. Our judgment device is instead a byproduct of ordinary structure: aggregating independent sellers' timed listings at scale. Spillovers between listings usually trace back to platform promotion (Boudreau and Jeppesen 2015). But this is infeasible in our case since the 82 houses do not coordinate schedules and the platform ranks and sorts items deterministically. The externality is thus informational, running through creator identity rather than ranking, and substitutes for costly appraisal in markets too thin to support it.

2.3 Product Portfolios and Release Strategy

Although concurrency emerges from platform architecture, it can become a strategic lever once sellers understand its revenue impacts (Negus 1997). Across creative industries that decision is deliberate (film: Einav 2010; music: Deshmane and Martínez-de Albéniz 2025; social media: Caro and Martínez-de Albéniz 2020 and Deshmane and Barriola 2025). The product-variety literature supplies the rationale: greater variety can raise matching costs and dilute a firm's own demand (Randall and Ulrich 2001, Moreno and Terwiesch 2017, Liu et al. 2025), suggesting that simultaneous same-artist listings should divide bidder attention. However, a creator's works are also informationally linked. A successful new release induces discovery of others sharing a creator (Elberse 2007, Deshmane and Martínez-de Albéniz 2023). Releasing together thus dilutes demand through one force and amplifies it through the other, and which dominates is hard to settle where the question is usually posed, since release dates are chosen in anticipation of both (Einav 2010). Concurrency on an aggregation platform is not chosen: partner houses consign independently, and overlap follows from the coincidence of their intake flows.

Which force prevails depends on two properties: similarity in form, which governs whether the works substitute (Hoberg and Phillips 2016, Chan et al. 2018, Askin and Mauskapf 2017); and, unique to our setting, how much of the focal work's value is common across bidders rather than private taste. A sibling's bidding reveals what the market will pay for the artist, so concurrency's gains grow with the common share, which rises with item value; for cheap works bought on taste, a sibling merely competes for the buyer. Under moderate differentiation, we find, concurrency amplifies demand with gains rising in the estimated item value.

3 Theory and Hypothesis Development

3.1 Concurrency as Unscheduled Portfolio Overlap

Creative works, such as paintings, novels, and music albums, reach the market as entries in a creator's evolving portfolio (Sorensen 2007), priced under radical quality uncertainty (Karpik 2010). Traditionally, labels and studios space a creator's works to limit self-competition, and galleries and appraisers supply price discovery (McAndrew et al. 2012, Renneboog and Spaenjers 2013). In the long-tail online auction market we study, neither role is filled: the portfolio arrives by coincidence, from the intake flows of independent houses that never consult one another, with no agent to manage it and little infrastructure to price it. We develop a framework for concurrent listings in such markets, where creator identity rather than observable attributes anchors value. When no identical reference unit exists, the market must create a reference in real time; concurrent same-creator listings, as we discuss next, do exactly that.

Why artist-level concurrency? Concurrency could be defined by genre, medium, period, or auction house. For singular goods, we propose that the creator is the fundamental unit. A conventional differentiated good is a bundle of observable characteristics (Bakos 1997): similarity in shoe size or style renders two items comparable. A singular good is not: a 60×80 cm oil landscape might be worth €200 or €200,000 depending on whose name is on it. Creator identity works like a brand, transferring reputational capital across works. It is one attribute among many through which all others acquire meaning (Bourdieu 1986). The artist level therefore captures the choice set bidders face and the affiliation justifying cross-listing inference.

Art markets are Pareto-distributed: a few blue-chip artists account for headline value, a long tail of regional artists for the bulk of transactions (McAndrew et al. 2012). Auctionet specializes in this long tail of moderately priced works (mean estimate ≈ €260, Table B.4) by regional, largely Nordic artists. Blue-chip works enjoy the judgment apparatus Karpik (2010) describes—specialists, catalogue scholarship, indexed sale histories; *the long tail has almost none*, a regional Swedish landscape painter of the 1950s having no price index, monograph, or dealer. Here existing frameworks say the least and concurrency's stakes are highest.

Concurrency may fragment attention and cannibalize within-creator demand (Bapna et al. 2009), or reduce search costs (*search effect*) while disclosing collective demand through live bidding (*co-disclosure effect*). We formalize how this unscheduled overlap operates where intermediary judgment is thinnest, and characterize when its benefits dominate.

3.2 Hypothesized Base Effect

We predict that concurrency raises bidding intensity and revenue in the focal auction through two channels. The first is a *search effect*. Concurrency makes the focal auction easier to find, drawing in bidders who would not otherwise have encountered it. Wider participation not only increases the probability of drawing in a high-value bidder, but also enriches the bid history so bidders shade less against the winner's curse under affiliated values. The second is a *co-disclosure effect*. Concurrency generates a public signal of demand for the artist. In Milgrom and Weber (1982)'s framework, public information affiliated with bidders' private signals ties bids more closely to fundamentals: bidders incorporate the sibling's visible bid path into their valuations; the mere availability of this signal raises revenue on average.

Karpik (2010, pg. 44) offers a complementary view: singular goods markets rely on *judgment devices*—rankings, reputations, expert reviews—that *"decrease ignorance associated with multi-dimensional singularities"* and *"authorize the comparisons without which consumers would be limited to random choices."* Concurrent listings are such a device, which is emergent rather than curated. Live cross-auction bidding renders collective assessment of an artist publicly observable in real time. Concluded sales, like reviews, are imperfect substitutes: collector attention, sentiment, and creator salience shift, so prior prices reflect an outdated demand environment. Sibling auctions reveal how bidders value related works under the same conditions. Cross-work inference is otherwise sequential—a new release draws attention onto its predecessors only once its own outcome settles—whereas concurrency makes it contemporaneous and reciprocal.

Co-disclosure also differs from standard auction-theoretic disclosure, which operates *intra*-auction through pre-sale revelation, reserve publication, and dropout sequences. Co-disclosure is *cross*-auction and creator-anchored, existing only because the platform makes sibling listings simultaneously visible and creator identity licenses inference across them. We hypothesize:

Hypothesis 1. *: The onset of artist-level concurrency increases new bidder entry, bidding frequency, and bid increments in the focal auction, thereby raising final revenue.*

3.3 Mechanism Exploration

We develop a stylized model to formalize the two mechanisms; Appendix A presents the full derivations and technical details. The model rests on three interconnected components: an environment with affiliated values, a search channel, and a co-disclosure channel.

Environment. A set of auctions runs simultaneously on the platform. Bidders are risk-neutral with affiliated values in the spirit of Milgrom and Weber (1982): willingness-to-pay combines a private taste component with a common value component tied to artist-level demand and resale value. Because the common value component is uncertain and shared, the setting is exposed to the *winner's curse*: the winner tends to be whoever most overestimated it, so rational bidders shade below their valuations, depressing revenue. Milgrom and Weber (1982) show that publicly releasing any signal affiliated with the item's true value raises expected revenue, since it lowers uncertainty about the common value component and curbs this shading. Greater participation and richer public bid histories therefore raise expected revenue—the principle the two mechanisms below make operational.

Mechanism 1: Search effect. The first channel through which concurrency operates is through search. Although digital platforms drastically lower the per-listing search cost relative to physical sales, they host listings at a scale, where tens of thousands of items are simultaneously open to bid on a typical day. This makes bidder attention itself the binding scarce resource (Anderson and De Palma 2012). When two auctions by the same artist run concurrently, shared artist tags and overlapping search keywords raise the probability that a bidder encountering one listing also encounters the other within the same search episode. Concurrency thus increases focal auction's visit probability and draws in bidders who would otherwise have remained unaware of it, subsequently raising expected revenue (Kuruzovich et al. 2010, Overby and Kannan 2015).

A platform-level subtlety is critical. With total platform visits in any interval treated as fixed, raising one listing's visit share mechanically reduces another's due to *attention-diversion*. This effect is expected to be stronger on *contemporaneous non-concurrent listings in the same category than those in a different one*: at a certain time, the impact of Painting A having a creator-based concurrent item A' may divert attention from a same-category Painting B more than from a different-category Photograph C. We hypothesize the following.

Hypothesis 2. *: Concurrency decreases contemporaneous bidder participation in same-category listings without concurrent auctions, in line with attention diversion phenomenon.*

A further implication of the search channel concerns where the concurrent auction sits in its auction life cycle. Online auctions do not attract attention uniformly over time. Instead, bidder monitoring and bid arrival rates tend to intensify as the auction approaches its close, a pattern commonly associated with *sniping*—the strategic concentration of bids in the final moments of an auction (Roth and Ockenfels 2002). Thus, the concurrent auction's late-stage life cycle creates a temporary surge in bidder attention: more bidders are actively watching the listing, platform visits to the item increase, and bid updates make the auction more salient in search environments. This late-stage traffic can spill over to the focal auction when the two listings are connected by artist tags and search keywords. The search channel therefore predicts that concurrency should have a larger effect when the concurrent auction is close to ending—not because the focal auction itself is near its own closing stage; rather, the concurrent auction's life-cycle position changes the amount of attention it can channel toward the focal listing.

Hypothesis 3. *: The treatment effect of concurrency on new bidder entry and bidding frequency in the focal auction is larger when the concurrent auction is in its closing hours.*

Mechanism 2: Co-disclosure effect. The second channel through which concurrency operates is informational. In the canonical English auction, bidders update their valuations by inferring rivals' private signals from the observable dropout sequence (Milgrom and Weber 1982). Online auctions, however, lack observable dropout: bidder exit is inferred only imperfectly from inactivity, and is contaminated by sniping, the strategic withholding of bids until the closing minutes (Roth and Ockenfels 2002). Bidders therefore update from a richer public history of current standing price, distinct bidder count, bid arrival rate, and bid increment size rather than from clean exit times. Under concurrency, this public history is augmented by an analogous stream of signals from the sibling listing, which under shared artist identity is positively affiliated with the focal item's value (Gagnon-Bartsch et al. 2021). Further, because the cross-auction signal is updated bid by bid, its effect should propagate dynamically: bidding activity on the concurrent listing should predict bidding activity on the focal listing.

Hypothesis 4. *: Following concurrency onset, bidding intensity (new bidder entry, bidding frequency, and bid increments) in the focal auction is increasing in the corresponding bidding dynamics of the concurrent listing.*

3.4 Boundary Conditions: Form Proximity and Valuation Stakes

Two properties bound the amplification developed so far, which we discuss next.

Form proximity. So far we have treated a bidder's valuations of the two items as independent. In practice, same-artist works can be substitutes, and concurrent listings then risk cannibalization: in overlapping auctions of identical goods, Bapna et al. (2009) find that overlap depresses prices as bidders withhold bids across auctions to hunt for bargains, and they flag the non-identical case as open. We use form proximity as a proxy for substitutability since works close in palette and subject are likelier to satisfy the same collector's desire than distant works merely sharing an artist.[1] Our wider consideration encapsulates both identical substitutes and non-identical siblings. Similarity is the measurable counterpart of the lever managers utilize by judgment when spacing a creator's simultaneous offerings. Here, style is economically consequential (Chan et al. 2018), differentiation yields an interior optimum for performance (Askin and Mauskapf 2017), and measured similarity predicts substitutability (Hoberg and Phillips 2016).

Rising similarity raises cannibalization risk through two channels. First, entry deterrence: a bidder active in the concurrent auction has less reason to enter the focal one when the items serve the same aesthetic purpose, the comparison shifting from "which do I want?" to "which is the better deal?". Second, bid alternation: bidders in both auctions avoid holding the high bid in both, in case they win twice, and alternate rather than escalate in parallel. Yet higher similarity also strengthens the search and co-disclosure channels: visually coherent works are more readily clustered by platform algorithms, and bidding on a similar item is more diagnostic of the focal item's value. The prediction is therefore non-monotone: over most of the range the gains dominate; at the upper end substitutability pulls participation back down. We hypothesize:

Hypothesis 5. *: The treatment effect of concurrency on bidding intensity (new bidder entry, bidding frequency and bid increments) in the focal auction is inverted-U-shaped in form proximity with the concurrent item, as search and co-disclosure gains are overtaken by substitution-driven cannibalization at high similarity.*

Valuation stakes. A second property, belonging to the focal work alone, governs how strong the co-disclosure effect is: the item's worth. A bidder's valuation combines a common value component—the artist's resale value and market standing, shared across bidders—with a private one, her own taste. Since a sibling's live bidding reveals only the common value component, the weight placed on it rises with the share of a bidder's valuation *uncertainty* that is common—a variance share, not a mean share. Variance is what matters: a sibling's bidding helps only insofar as it resolves uncertainty, so a common value component that is large but known in advance shifts all valuations alike and leaves nothing to learn.

That share rises with the item's worth because, in the long tail, the uncertainty at stake in a more valuable work increasingly concerns its common value—what an artist commands in today's market, genuinely in doubt and shared across bidders—rather than private taste, which each bidder settles for herself and whose spread does not grow with value. The common share of valuation uncertainty therefore rises with the pre-sale estimate—an unbiased proxy for value (McAndrew et al. 2012, Ashenfelter and Graddy 2019)—and with it the informational return to a sibling's bidding. At the bottom of the range, where the little uncertainty there is concerns private taste alone, a concurrent listing reveals nothing and merely competes for the same buyer. Appendix A formalizes this decomposition and the conditions under which the common share rises with value. This bounds what an emergent judgment device can substitute for. Provisioned infrastructure covers the entire market (Nagaraj 2022). An emergent device does not: it works only where valuation carries enough common-value uncertainty to disclose. It stops short of the cheapest lots, whose value is so low that paid appraisal itself is unjustified in the first place.

Hypothesis 6. *: The treatment effect of concurrency on bidding frequency and bid increments in the focal auction is increasing in the focal item's pre-sale estimate, as the common value component, on which co-disclosure operates, grows with item value.*

4 Data Description

4.1 Online art auctions

Online art sales reached $10.5 billion in 2024, roughly half through online auctions and the rest through dealers' online channels (Figure B.1; Art Basel and UBS 2025). Aggregation platforms such as Invaluable, LiveAuctioneers, and Barnebys are dominated by *timed* auctions, in which each lot has a fixed closing time and bidding proceeds asynchronously over days, eBay-style, rather than *live* auctions replicating the saleroom. Aggregation combined with extended listing duration produces the concurrency we study: at any moment a platform may host thousands of overlapping auctions, including multiple same-artist listings.

4.2 The platform

Auctionet, a Swedish third-party platform established in 2011, supplies the digital infrastructure (bidding, payments, standardized shipping) through which local European auction houses sell fine art, furniture, design objects, and collectibles. Partner houses handle inspection, description, and photography. As of October 2025 it had roughly 900,000 subscribers and sold over 2,000 items daily. Its 82 partner houses span Sweden, Germany, the UK, Spain, Denmark, and Finland (Table B.1), mostly small-to-medium operations consigning from local estates and private collectors, though a few, including Balclis in Barcelona and Stockholms Auktionsverk—among the world's oldest auction houses—handle higher-value prestige sales. Regional houses thus provide intake and cataloguing while Auctionet supplies the marketplace and international reach, monetizing through commission: 6% of the hammer price (excl. VAT) plus a €4.83 hammer fee per item. Because intake is governed by what each house happens to receive rather than by any shared calendar, no party has cross-coordinated overlapping schedules. Crucially for identification, the platform ranks listings deterministically by genre, category, and time-to-close, running *no behavioral recommendation engine* of the kind streaming services deploy: it neither personalizes to browsing history nor popularity-ranks on aggregate demand.[2] Because we control for these ranking primitives throughout, a bidder's discovery of a concurrent listing reflects shared artist tags, search keywords, and catalogue browsing rather than an algorithm that learns from and amplifies latent demand.

4.3 Auction format and bidding rules

Auctions follow an ascending-bid (English) format; the bidding page (Figure B.2) displays item details, the current high bid, pre-sale estimate, closing time, minimum next bid, delivery fee, and bid history. Reserves, when present, are disclosed only upon being met, and items go unsold if the reserve is unmet at close. Bidders may submit manual bids or use an autobid feature that places incremental bids automatically up to a specified ceiling. Withdrawal and payment rules are strict: private individuals (not companies) hold a 14-day right of return at their own expense, and failure to pay within five days constitutes breach, allowing cancellation or resale. Shill bidding, where sellers bid on their own items directly or through agents, is prohibited.

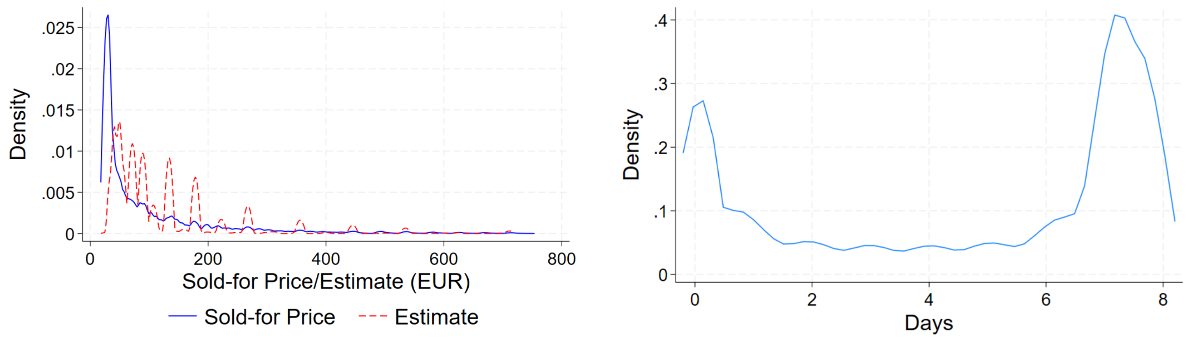

(a) Density distribution of sold-for price and estimate.

(b) "Sniping" in online bidding.

Figure 2: Price distribution and bidding dynamics on Auctionet.

Notes: Panel (a) shows the density distribution of 0 to 95th percentile. Panel (b) includes auctions lasting 7 to 8 days.

4.4 Data

Auctionet targets the secondary market for everyday, lower-value art: final prices and pre-sale estimates are heavily right-skewed, with most items estimated below €200 and selling for less (Figure 2a, top-5% winsorized). Measured between first and last recorded bid, which is a lower bound on the listing window, since start times are unobserved, active bidding spans 7-8 days (Figure B.3), with concentration in the final 24 hours (Figure 2b), consistent with the presence of a common value component that makes early bidding costly (Bajari and Hortaçsu 2004).

The dataset covers 277,036 auctions listed between 2011 and 2024, of which 119,388 (43%) overlap temporally with at least one same-artist auction—a high share reflecting the platform's Scandinavian roots, where works by regional artists recur across partner houses. We scrape all bidding dynamics, item metadata, and photographs on each listing page; within an auction, bid timestamps and within-auction bidder identifiers are fully observed, as illustrated in Figure B.2, where bidder 5's bids at 12:59 and 18:31 on 3 June are recorded. No persistent identifier, anonymized or otherwise, is available, making cross-auction bidder behavior tracking infeasible. This constraint does not affect our empirical design: all outcome variables are measured at the auction-window level, and identification exploits within-auction variation in concurrency onset rather than individual bidding trajectories across auctions.

Non-concurrent auctions carry higher and more dispersed prices (€298.1 vs. €207.5) and estimates (€332.6 vs. €206.1), suggesting higher-value items are less likely to have a concurrent same-artist listing. Concurrent auctions have longer durations (6.9 vs. 5.3 days) and attract more bids (10.0 vs. 7.1) and bidders (3.5 vs. 2.6) (Table B.2). OLS estimates relating final price to three concurrency measures—a binary indicator, a count, and a cross-house indicator—each yields positive correlations (Table B.3). However, these are not causal: independent listing-time decisions by partner houses mean demand-driven self-selection or scheduling coordination could confound concurrency with latent quality—precisely the threat the matched difference-in-differences design in the next section addresses.

5 Estimating Baseline Effects of Concurrency

We aim to estimate the causal effect of concurrency onset on bidding outcomes in ongoing auctions. The central identification challenge is endogenous timing: sellers and houses may strategically *choose when to list items*, clustering high-demand works, and if unobserved quality or anticipated demand correlates with both concurrency and bidding outcomes, naïve concurrent-versus-non-concurrent comparisons are severely biased.

We therefore pair a difference-in-differences (DiD) design with propensity score matching (PSM), exploiting two sources of variation: the precise timing of onset within an auction's lifecycle, which generates staggered treatment heterogeneity, and observably similar controls that never experience concurrency. Matching treated auctions to counterfactuals on the linear propensity score and comparing outcomes around onset isolates the causal effect from time-invariant confounders and common time trends. Cox proportional hazards models then recast the effect as time-to-threshold, testing whether concurrency accelerates relevant bidding dynamics.

5.1 Treatment Definition

We partition the auction lifecycle into 3-hour windows ($\Delta = 3$ h), focusing on auctions whose observed bidding window spans at least 7 days (56 windows). Robustness to $\Delta \in \{1, 6\}$h is reported in §7. Auction a is *treated* if, at some window starting at time w, at least one other auction by the same artist $i(a)$ runs concurrently: $[w, w + \Delta) \cap [t^s_{a'}, t^e_{a'}] \neq \emptyset$ for some $a' \neq a$ which starts at $t^s_{a'}$ and ends at $t^e_{a'}$, with $i(a') = i(a)$. Treatment onset is $w^*_a = \min\{w : \text{Concurrent}_{a,w} > 0\}$, where $\text{Concurrent}_{a,w}$ counts the same-artist auctions overlapping window

w, and the episode ends at $w_a^{**} = \max\{w : \text{Concurrent}_{a,w} > 0\}$. For cleaner identification auction a remains continuously treated from w_a^* onward. We replicate our analyses with a separate sample in which the concurrent auction ends before the focal one, producing a post-treatment period of non-concurrency. We require at least $\underline{W} = 24$ pre-treatment windows (72 h) per treated auction for pre-trend estimation.

Measuring listing windows. The platform does not record the calendar time at which a lot is posted, so t_a^s and $t_{a'}^s$ are proxied by the first recorded bid on each listing. Closing times t_a^e, $t_{a'}^e$ are provided. Two features of the data indicate that this proxy is appropriate. First, the measured first-to-last-bid span concentrates sharply at 7–8 days (Figure B.3), matching the platform's standard listing length; a systematically late first bid would shift that mass downward. Second, bids arrive throughout the listing window rather than only at the close (Figure 2b), so listings are rarely without bids for long stretches after posting. The proxy is also conservative: any gap between posting and the first bid truncates the *pre*-treatment portion of the panel, which tightens the $\underline{W} = 24$ window requirement rather than relaxing it, and cannot manufacture a spurious break at w_a^*.

5.2 Matching: Dual Control Pools and Propensity Score

For each treated auction a, we identify candidate controls c that: (i) start within 168h of w_a^* (ensuring common market conditions at treatment onset); (ii) are works by a different artist; (iii) carry at least $\underline{W} = 24$ pre-treatment windows and remain active through w_a^{**}; and (iv) are never themselves concurrent (no auction by their artist overlaps another same-artist auction at any point in the sample). We then partition eligible controls into two structurally distinct pools:

- **T' (same category, different artist):** Auctions competing for the same category-specialist bidders but unaffected by artist-specific spillovers.
- **C (different category, different artist):** Auctions with orthogonal bidder pools whose artists have no concurrent activity in any category.

Both contrasts are estimated against C: T vs. C identifies the effect of artist-level concurrency on the focal auction (Hypothesis 1), while T' vs. C identifies the category-level spillover onto non-concurrent peers (Hypothesis 2). The T' pool therefore enters the design as a second treatment arm rather than as the counterfactual for T.

Within each pool, we estimate a pool-specific logistic propensity score model (detailed in Appendix C) and match on the *linear predictor* (log-odds) rather than the raw probability, following Austin and Stuart (2015). Matching uses greedy nearest-neighbor without replacement subject to a tight caliper of $\delta = 0.10$ standard deviations of the control group's linear predictor. For each treated auction we retain up to $K = 5$ matches per pool, yielding triads $\{T_k,\, T'_{k,1}, \ldots, T'_{k,5},\, C_{k,1}, \ldots, C_{k,5}\}$.

Our matching strategy produces 4950 triads, amounting to 4950 *Treated* (T) items, 12,517 *SameCategory* (T') items, and 13,056 Control_a (C) items. Tables C.1 and C.2 present covariate balance statistics across treatment and control groups post-matching. We also verify parallel pre-trends by estimating event-study specifications (§5.3.2) and confirming that treated and control groups exhibit statistically indistinguishable trajectories prior to treatment.

5.3 Difference-in-Differences Specification

5.3.1 Baseline Model

Let $\tau = w - w_k^*$ denote time relative to the onset of treatment in triad k, where w indexes absolute 3-hour windows and w_k^* is the onset window of the treated auction in that triad. All auctions in a triad, treated and control alike, are aligned to this common relative grid, so $\tau = 0$ is the onset window throughout. Replacing T_a, T'_a, and C_a with $\text{Treated}_a, \text{SameCategory}_a$, and Control_a, respectively for the ease of interpretation, our primary estimating equation is:

$$
\begin{aligned}
Y_{a\tau} = {} & \beta_1\, \text{POST}_\tau + \beta_2\, \text{Treated}_a + \beta_3\, \text{SameCategory}_a \\
& + \beta_4\, (\text{POST}_\tau \times \text{Treated}_a) + \beta_5\, (\text{POST}_\tau \times \text{SameCategory}_a) \\
& + \boldsymbol{\delta}'\mathbf{X}_{a\tau} + \gamma_{k(a)} + \gamma_\tau + \gamma_{r_{a\tau}} + \gamma_{\text{DOW}} + \gamma_H + \gamma_M + \gamma_Y + \gamma_{Cat} + \gamma_{S(a)} + \varepsilon_{a\tau},
\end{aligned}
\tag{1}
$$

where $Y_{a\tau}$ is the outcome for auction a in time window τ. We analyze four primary outcomes: for auction item a in a given window, new bidder entry through $NewBidders_{a\tau}$, number of bids received through $Bids_{a\tau}$, mean increment per bid through $\Delta_{a\tau}^{Mean}$ and total increment in bidding amount through $\Delta_{a\tau}^{Total}$. These are window-level bidding-process outcomes rather than the final selling price, allowing a granular study of temporal impact of concurrency. A single end-of-auction price cannot be aligned to τ and conflates the onset effect with late-stage sniping. Revenue implications are recovered by aggregating per-window increment effects over the lifecycle. To account for skewness in raw distributions, these dependent variables are log-transformed. Control_a pool is the omitted baseline.

$\mathbf{X}_{a\tau}$ includes time-varying controls: $ReserveMet_{a\tau}$ (indicator for reserve price met), $NBidders_{a\tau}$ or $NBidders_{a,\tau-1}$ (cumulative or lagged unique bidders; latter used as a control for $NewBidders_{a\tau}$), $AuctionAge_{a\tau}$, and $(AuctionAge_{a\tau})^2$ (auction maturity and its square).

Triad fixed effects $\gamma_{k(a)}$ absorb all time-invariant heterogeneity within matched sets. Relative-window fixed effects γ_τ absorb the average bidding profile relative to onset. Since POST_τ is a linear combination of these indicators, it is not separately identified and dropped in estimation.

Countdown-to-close fixed effects $\gamma_{r_{a\tau}}$, where $r_{a\tau}$ is hours remaining until auction a closes, are critical: matched auctions end at different times, a given τ may coincide with the final hours of one auction and an early period of another. Without $\gamma_{r_{a\tau}}$, the end-of-auction sniping acceleration would contaminate the treatment effect estimate. These fixed effects absorb that lifecycle nonparametrically. We further include fixed effects for day of week, hour of day (since the platform and most of its users are European), month, and year (γ_{DOW}, γ_H, γ_M, γ_Y), which account for calendar patterns in bidding intensity. Finally, because our triads contain both within- and across-category and across-seller comparisons, we include category and auction-house fixed effects, γ_{Cat} and $\gamma_{S(a)}$, respectively. Standard errors are clustered at the triad (k) and relative window (τ) level to account for serial correlation within matched sets and potential cross-sectional dependence among auctions in the same triad.

5.3.2 Validating the Parallel Trends Assumption: Event-Study Specification

To assess the parallel trends assumption, we estimate:

$$Y_{a\tau} = \sum_{j\neq -1} \theta_j \,\mathbf{1}[\tau = j] \times \text{Treated}_a + \sum_{j\neq -1} \phi_j \,\mathbf{1}[\tau = j] \times \text{SameCategory}_a + \gamma_{k(a)} + \gamma_\tau + \gamma_{r_{a\tau}} + \varepsilon_{a\tau}, \quad (2)$$

normalizing $\theta_{-1} = \phi_{-1} = 0$. The coefficients $\{\theta_j\}_{j<-1}$ and $\{\phi_j\}_{j<-1}$ trace differential pre-trends for Treated_a and SameCategory_a relative to Control_a; we test $H_0 : \theta_j = 0 \ \forall j < -1$ and $H_0 : \phi_j = 0 \ \forall j < -1$ via joint Wald F-tests. Figure 3 plots $\{\hat{\theta}_j, \hat{\phi}_j\}$ with 95% confidence intervals over $\tau \in [-24, 36]$.

5.4 Survival Analyses

To complement the DiD analysis and characterize treatment *dynamics*, we estimate Cox proportional hazards models (Cox 1972) for the speed at which three events occur after treatment onset: (i) $ReserveMet_{a\tau}$, the auction reaching its minimum acceptable price, a marker of seller protection and market validation; (ii) $EstimateMet_{a\tau}$, the auction reaching the auctioneer's pre-sale estimate, signaling strong demand and the potential for above-estimate outcomes; and (iii) $NewBidderEntry_{a\tau}$, the arrival of an additional unique bidder, reflecting the visibility and competitive dynamics induced by concurrency.

We measure duration on the same relative-window grid as the DiD: the survival clock is τ, with origin $\tau = 0$ at treatment onset, and estimation restricted to $\tau \geq 0$. The risk set therefore comprises post-onset auction-windows, which isolates treatment-induced acceleration from pre-existing baseline differences across pools. We estimate:

$$h_a(\tau \mid \cdot) = h_{0,Cat(a)}(\tau) \exp\Big(\beta_1 \,\text{Treated}_a + \beta_2 \,\text{SameCategory}_a + \boldsymbol{\psi}'\mathbf{X}_{a\tau} + \boldsymbol{\eta}'\mathbf{D}_{a\tau} + \theta_{k(a)}\Big), \qquad \tau \geq 0, \quad (3)$$

where $h_{0,Cat(a)}(\cdot)$ is a baseline hazard over windows-since-onset, stratified by category $Cat(a)$; $\mathbf{X}_{a\tau}$ denotes the time-varying controls of Eq. (1), *excluding any variable that mechanically defines the event in question*; $\mathbf{D}_{a\tau}$ includes day-of-week, hour, month, and year dummies absorbing calendar patterns in bidding intensity; and $\theta_{k(a)}$ is a triad-level shared frailty, the survival analogue of our triad-clustered DiD errors. Concretely, $ReserveMet_{a\tau}$ is dropped from the $ReserveMet$ model, and the cumulative bidder count $NBidders_{a\tau}$ is replaced by its one-window lag $NBidders_{a,\tau-1}$ in the $NewBidderEntry$ model, so that no covariate is a deterministic function of the outcome at the same instant; the remaining models retain the full control set. Hazard ratio e^{β_1} compares treated auctions to different-category controls, with values above one indicating that concurrency raises the instantaneous rate at which the event occurs. Appendix E details the risk-set construction and right-censoring at window containing auction close (t_a^e).

5.5 Results for Baseline Treatment Effects

Table 1 reports the DiD estimates from Equation (1), where the coefficients of interest are for interactions $\text{POST}_\tau \times \text{Treated}_a$ and $\text{POST}_\tau \times \text{SameCategory}_a$.

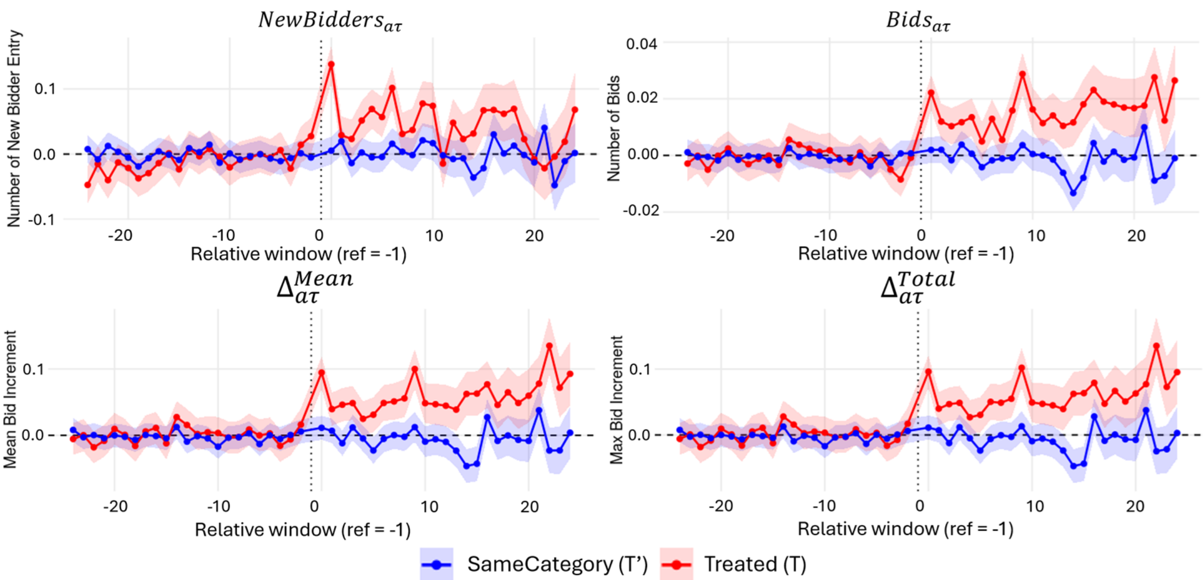

Figure 3: Treatment effects on bidding dynamics estimated across time as per Equation 2. Full results available in Appendix Table I.1.

Notes: Plots show estimated coefficients for event analyses for Treated_a (in **red**) and SameCategory_a (in **blue**) with respect to Control_a (relative window -1). Shaded regions represent 95% confidence intervals. Treatment and same category items do not differ significantly from true controls in the windows prior to the treatment. This validates parallel trends and the efficiency of the matching strategy.

Treated and control auctions evolve in parallel before onset. Before exploring the main results, we first verify the identifying assumption of parallel trends using the event-study specification in Equation (2). Across all four outcomes, the pre-treatment coefficients $\{\hat{\theta}_j\}_{j<-1}$ for treated auctions and $\{\hat{\phi}_j\}_{j<-1}$ for the same-category pool fluctuate tightly around zero, with no visible drift in the 24 windows (72 hours) preceding onset (estimated results in Table I.1 are presented in Figure 3). Joint Wald F-tests fail to reject $H_0 : \theta_j = 0 \; \forall j < -1$ for every outcome ($p > 0.1$), with analogous null results for $\{\phi_j\}_{j<-1}$. Combined with the post-matching covariate balance documented above, the absence of differential pre-trends supports interpreting the post-onset interactions as causal effects of concurrency rather than artifacts of selection or trending unobservables. The coefficients for treated auctions turn sharply positive at $\tau = 0$ and persist thereafter, locating the effect precisely at the moment a sibling listing appears.

Concurrency raises bidding intensity. Table 1 shows that concurrency onset produces positive, highly significant increases on all four bidding outcomes, validating Hypothesis H1. New bidder entry rises by 0.6% ($[e^{0.006} - 1] \times 100$ in Model (1), $p < 0.001$) per 3-hour window and bidding frequency by 1.0% by similar logic (Model (2), $p < 0.001$). We also see in Models (3) and (4) that the mean and total bid increments increase by 3.4% and 3.5%, respectively (both at $p < 0.001$). Concurrency thus moves the focal auction on three margins the theory targets—entry, frequency, and increment size—establishing that the onset of a sibling listing is not a passive coincidence of timing but an active force on the focal auction's bidding process. Since onset is proxied by the sibling's first bid, the jump could reflect a common artist-level demand shock rather than the sibling itself. Such a shock would have to arrive exactly at $\tau = 0$ across thousands of staggered onset dates, which is highly implausible, and platform's regional artists rarely attract coverage or collector surges that blue-chip listings do.

The relative magnitudes are worth exploring more. The entry and frequency effects are the participation margins: concurrent listings raise the focal auction's discoverability through shared artist tags and recommendation surfaces, drawing in bidders who would otherwise have remained unaware of it (Kuruzovich et al. 2010). Were search the whole story, gains would concentrate on participation. Instead, the increment effects are roughly six times larger than the entry effect. This wedge is indicative of how the publicly observable bid path on the sibling listing functions as a value-relevant signal that bidders impound directly into higher willingness-to-pay, not merely into more frequent bidding. The baseline therefore already points toward co-disclosure as the dominant channel, motivating the formal decomposition that follows in §6.

The 3.5% per-window effect on bid increments implies a proportional increase in the bid-up an item accumulates after onset. Among matched control auctions, the standing bid rises from €168.5 at onset to €280.1 at close, a bid-up of €111.6; scaling this counterfactual by the estimated effect yields approximately €3.9 per treated auction. The consignor retains €3.7 after the 6% commission, and the platform earns €0.23 at no cost, since concurrency requires no listing fee, promotion, or additional infrastructure. At roughly 2,000 items sold daily, this corresponds to €7,800 in additional daily hammer value and €470 in daily commission, though our estimates are identified on four categories, so the platform-wide figure is illustrative. The figure is also conservative. The specification without controls in Table G.2 yields effects as high as 5.5%, or €6.2 per auction. Finally, Table G.3 shows that these effects do not vary with the number of concurrent auctions: once treated, the effect is essentially invariant to how many siblings are live.

	Dependent Variable			
	$NewBidders_{a\tau}$	$Bids_{a\tau}$	$\Delta^{Mean}_{a\tau}$	$\Delta^{Total}_{a\tau}$
	(1)	(2)	(3)	(4)
Treated_a	0.000	-0.004^{***}	-0.011^{**}	-0.011^{**}
	(0.001)	(0.001)	(0.004)	(0.004)
SameCategory_a	0.000	0.000	-0.001	-0.001
	(0.000)	(0.000)	(0.002)	(0.002)
$\text{POST}_\tau \times \text{Treated}_a$	0.006^{***}	0.010^{***}	0.034^{***}	0.035^{***}
	(0.001)	(0.003)	(0.008)	(0.008)
$\text{POST}_\tau \times \text{SameCategory}_a$	0.000	0.000	-0.002	-0.002
	(0.000)	(0.001)	(0.004)	(0.004)
Controls	*Yes*	*Yes*	*Yes*	*Yes*
Fixed Effects				
$\gamma_{k(a)}$	*Yes*	*Yes*	*Yes*	*Yes*
γ_τ	*Yes*	*Yes*	*Yes*	*Yes*
$\gamma_{r_{a\tau}}$	*Yes*	*Yes*	*Yes*	*Yes*
γ_{DOW}	*Yes*	*Yes*	*Yes*	*Yes*
γ_H	*Yes*	*Yes*	*Yes*	*Yes*
γ_M	*Yes*	*Yes*	*Yes*	*Yes*
γ_Y	*Yes*	*Yes*	*Yes*	*Yes*
γ_{Cat}	*Yes*	*Yes*	*Yes*	*Yes*
$\gamma_{S(a)}$	*Yes*	*Yes*	*Yes*	*Yes*
Observations	1,233,876	1,233,876	1,233,876	1,233,876
Adj. R^2	0.077	0.107	0.079	0.080

Notes: Observations are at the auction-relative time level ($a \times \tau$). Standard errors (in parentheses) are clustered at the auction triad (k) and relative window (τ) level. $^{***}p < 0.001$; $^{**}p < 0.01$; $^{*}p < 0.05$.

Table 1: Impact of concurrency on bidding dynamics: Difference-in-Differences estimation of matched triads as per Equation 1. Detailed results are in Appendix G, Table G.1.

Impact on non-concurrent category peers. The $\text{POST}_\tau \times \text{SameCategory}_a$ coefficient compares non-concurrent listings in the *same* category as a treated auction against non-concurrent listings in a *different* category. Both groups are free of concurrency, so the coefficient isolates how same-category peers move *relative to* different-category peers. Hypothesis 2 is not supported: these coefficients are negligible and indistinguishable from zero across outcomes (≤ 0.002, $p > 0.1$), so same-category peers show no differential change in bidding intensity.

A null differential, however, is not an absence of diversion. Since bidders are more likely to search within categories, attention drawn to a concurrent listing comes disproportionately from same-category substitutes, leaving different-category peers insulated. Pure diversion would therefore push same-category peers *below* the different-category baseline, yielding a negative coefficient. We observe no such depression, not because diversion fails but because a countervailing force offsets it in the same channel: as derived in Appendix A, concurrency does not merely redistribute attention but *creates* it, since cheaper discovery through overlapping tags, shared ranking surfaces, and co-occurrence in search episodes draws fresh attention that likewise concentrates among same-category peers. The two approximately cancel, yielding the observed null. Revenue gains are then net creation, expanding the attention pie rather than reallocating it.

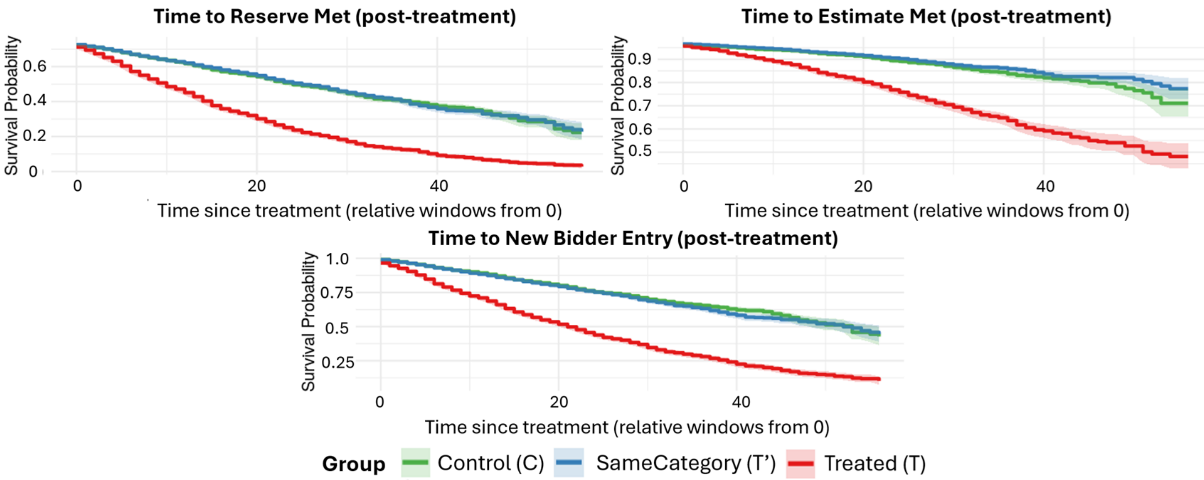

Figure 4: Treatment effects on time to threshold: Kaplan-Meier survival curves. Results from estimating the Cox Proportional Hazard model from Equation 3 are in Appendix Table G.4.

Notes: Curves show the proportion of items that have not yet experienced the event, starting from treatment onset (relative window 0). The treatment group (red) shows systematically lower survival probabilities, indicating faster time to threshold. Shaded regions represent 95% confidence intervals.

Results from survival analyses. The hazard models in Table G.4 recast the treatment effect as time-to-threshold and reinforce the intensity results. Among auctions yet to cross a given threshold, concurrency raises the per-window rate of doing so: by 79.7% for meeting the reserve ($\widehat{\text{HR}} = 1.797$), 68.1% for reaching the pre-sale estimate ($\widehat{\text{HR}} = 1.681$), and 213.6% for attracting an additional unique bidder ($\widehat{\text{HR}} = 3.136$; all $p < 0.001$). Hazard ratios scale the instantaneous rate at which risk is realized, so the implied reduction in expected time-to-event is smaller than these percentages. The Kaplan–Meier curves in Figure 4 make the point nonparametrically: treated survival functions (red) lie everywhere below the controls, and the gap widens with windows-since-onset rather than reflecting a one-time level shift.

The acceleration is largest by far for new-bidder entry, consistent with the disproportionate intensity gains in $NewBidders_{a\tau}$: a concurrent listing operates most directly through visibility that pulls fresh participants into the focal auction, and the downstream price thresholds—reserve, and the more demanding estimate (met by only 10.2% of items)—are crossed faster by that thicker, faster-forming pool. Restricted to the post-onset risk set, these accelerations cannot reflect pre-existing differences between matched pools, a reading reinforced by the flat pre-trends above. Finally, the SameCategory_a hazard ratios are indistinguishable from one in every column ($\widehat{\text{HR}} = 0.91$–$1.06$). Hence, the acceleration is specific to the artist-level concurrency treatment, not extending to non-concurrent peers, further supporting invalidation of Hypothesis 2.

Together, these results show that artist-level concurrency increases focal-auction bidding across all margins without cannibalizing same-category demand. Robustness tests in §7 reinforce these findings. Next, we study mechanisms driving these results and boundary conditions.

6 Scope of Concurrency and Relevant Mechanisms

6.1 Additional Empirical Considerations

Moderation analyses. Although Equation (1) identifies the average treatment effect of concurrency, our hypotheses also (H3–H6) predict heterogeneity along auction-lifecycle, information-revelation, item-similarity, and item-value dimensions. We therefore augment Equation (1) with a battery of triple interactions of the form $\text{POST}_\tau \times \text{Treated}_a \times M_{a\tau}$, where $M_{a\tau}$ is one of four moderators defined below. All lower-order interactions and main effects are retained, and the full set of fixed effects and clustering structure from Equation (1) is preserved. Each moderator is constructed window-by-window so that variation is identified within the relative-time grid.

The first moderator partitions each *concurrent* auction's lifecycle into $\text{EarlyStage}'_\tau = \mathbf{1}[r_{a'\tau} > 12\text{h}]$ and $\text{LateStage}'_\tau = \mathbf{1}[r_{a'\tau} \leq 12\text{h}]$, where $r_{a'\tau}$ is hours remaining until close for sibling; testing attention spillover from a closing rival's bidding-intensive period drives entry into focal auction (H3). For multiple concurrent siblings, $\text{LateStage}'_\tau = 1$ as long as there is one item in its terminal 12h window. The second set of moderators are one-window lags of the concurrent auction's own bidding dynamics—$\text{Bids}'_{a,\tau-1}$, $\text{NewBidders}'_{a,\tau-1}$, ${\Delta^{\text{Mean}}}'_{a,\tau-1}$, and ${\Delta^{\text{Total}}}'_{a,\tau-1}$—each interacted with the corresponding focal-auction outcome to test information-spillover channel of H4; lagging by one window rules out mechanical contemporaneous correlation.

The third moderator, $\text{Similarity}_{(a,a')}$, captures *form* proximity between the focal and concurrent items. We embed each item's primary listing image using DINOv2 (Oquab et al. 2023), a self-supervised vision transformer (`facebook/dinov2-base`), taking the `[CLS]` token from the final hidden state as a 768-dimensional content representation, and compute the cosine similarity $s_{a,a'} = \langle e_a, e_{a'} \rangle / (\|e_a\| \, \|e_{a'}\|)$ between focal and concurrent embeddings. A detailed treatment of the model choice, preprocessing pipeline, embedding extraction, and validation against human

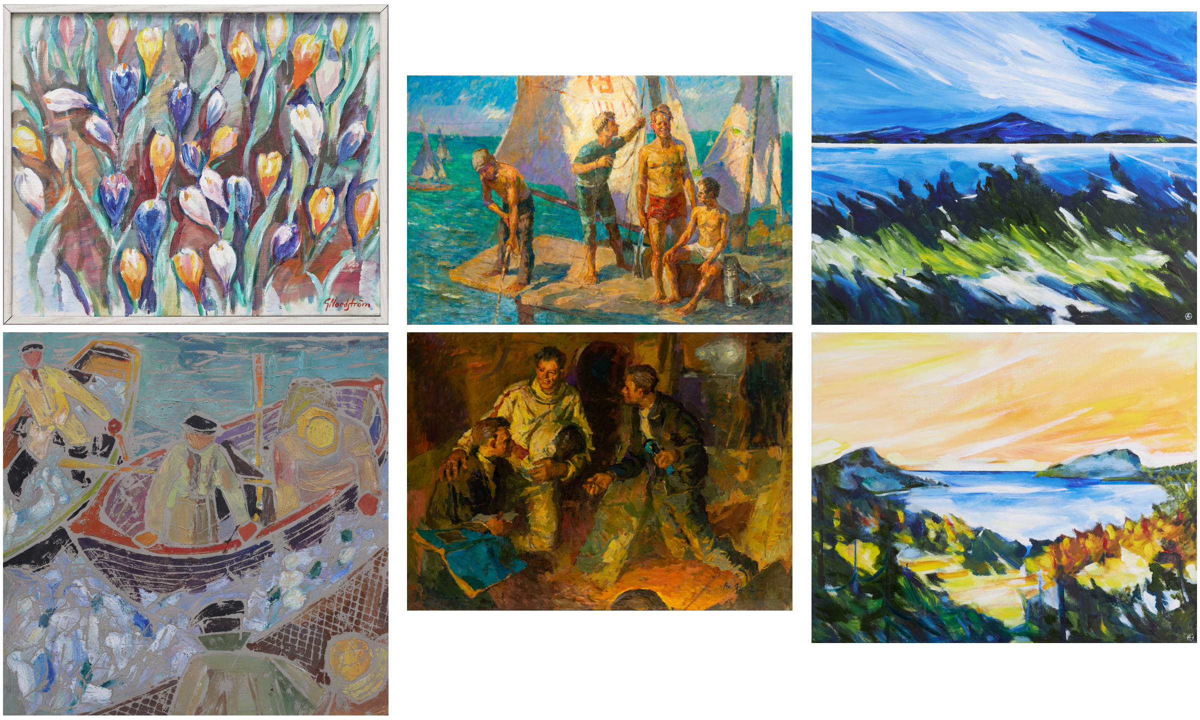

(a) Low similarity (Q1) (b) Moderate similarity (Q3) (c) High similarity (Q5)

Figure 5: Illustrative same-artist pairs across the form proximity distribution. Each panel shows a focal–concurrent pair from the bottom (quintile 1, *left*), middle (quintile 3, *center*), and top (quintile 5, *right*) of the DINOv2 cosine-similarity distribution, visual proximity increasing left to right. Both images in a panel are by the same artist by construction. Three artists left to right are Gunnar Nordström, Anatoly Nikitovich Janev, Anita Fröding.

judgments is provided in Appendix D; cosine similarity correlates at 0.71 with average human similarity ratings of 50 randomly drawn painting pairs, close to the agreement between the two raters themselves (correlation at 0.88). To avoid imposing linearity on a similarity scale, we discretize $s_{a,a'}$ into sample quintiles indexed 1 (least similar) through 5 (most similar) and enter five separate triple interactions $\text{POST}_\tau \times \text{Treated}_a \times \mathbf{1}[\text{Similarity}_{(a,a')} = q]$ for $q \in \{1, \ldots, 5\}$. Figure 5 illustrates the similarity measure with representative same-artist pairs drawn from the bottom, middle, and top similarity quintiles.

Finally, EstimateLevel_a is the sample quintile of the focal item's pre-sale estimate. It is a property of the focal work alone and fixed at listing. It is one of the covariates on which treated and control auctions are matched—so the contrast it identifies is not confounded by differences in item value between the arms. Table F.1 summarizes each moderator, its construction, and the hypothesis it targets.

6.2 Results: Exploring Mechanisms

Evidence for search channel. H3 predicts that the search channel is stronger when the concurrent auction is in its closing hours. The empirical results provide direct support for this mechanism. Table G.5 shows that new bidder entry in the focal auction rises from 0.6% when the concurrent auction is in its early stage to 1.9% ($p < 0.01$) when it is in its late stage. This reinforces the search friction story: because sniping behavior independently concentrates visitor traffic in the final hours of any auction, a concurrent listing in its late stage generates a larger pool of potential bidders who may discover and enter the focal auction as a by-product of their search. Consequently, number of bids and bid increments increase (2.6%–5.2%, all $p < 0.05$). This is not generic live-platform traffic as we control for it by various fixed effects (including day-of-week, hour, month and year) in Equation (1).

The survival analysis in Table G.4 provides a complementary perspective: treated auctions attract an additional unique bidder at more than three times the per-window rate of controls ($\widehat{\mathrm{HR}} = 3.136, p < 0.001$), underscoring that concurrency compresses the time it takes for a focal auction to become discovered by participants outside its initial audience.

Evidence for co-disclosure channel. Co-disclosure treats the concurrent listing's live bidding history as a public signal from which focal bidders update beliefs about artist-level demand. Table G.6 tests this period-by-period propagation most directly, lagging the concurrent auction's dynamics by one window to rule out mechanical simultaneity. Beyond the average treatment effect in $\mathrm{POST}_\tau \times \mathrm{Treated}_a$, a lagged rise in the concurrent listing's bid count predicts an additional rise in the focal auction's ($0.012, p < 0.01$), and a lagged rise in its mean increment an additional focal increment ($0.007, p < 0.05$). Signal strength transmits dynamically as bidding history accumulates on the sibling listing. Event study in Figure 3 corroborates this at onset: concurrency immediately raises bidding frequency and mean increment—hence the standing price—persisting until close, consistent with continuous updating as the sibling's history evolves. The alternative reading, a common artist shock such as press coverage or surging collector interest generating correlated momentum across listings, is implausible here: the platform's low-value works by regional artists, unlike blue-chip market artists, rarely attract coverage.

If concurrent bidding is informative, its value should peak when uncertainty about the focal item resolves. On Auctionet the reserve is undisclosed until the current bid reaches it, whereupon a public message confirms the item will sell. This removes the risk that even a winning bid yields no transaction, sharpening cross-auction signals: bidders who know the item will sell have both motive and clarity to calibrate against the concurrent listing's trajectory. The three-way interaction $\mathrm{POST}_\tau \times \mathrm{Treated}_a \times \mathrm{ReserveMet}$ in Table G.7 confirms this, reserve-meeting raising the treatment effect on bidding frequency, mean increment, and total increment by a further 5.7%, 12.5%, and 13.0% (all $p < 0.01$). Table G.4 reinforces the logic at the auction level, treated auctions crossing the reserve ($\widehat{\mathrm{HR}} = 1.80, p < 0.001$) and the expert estimate ($\widehat{\mathrm{HR}} = 1.68, p < 0.001$) at higher per-window rates, reflecting cumulative information-driven upward revisions. These results, despite being descriptive as ReserveMet itself is affected by concurrency, strongly support Hypothesis 4. Partitioning the focal auction by its own clock, by contrast, yields only weak support. Co-disclosure should intensify toward the close, but Table G.8 shows treatment effects significant only early (over 12 hours remaining)—bid count up 0.8%, mean increment 3.2%, total increment 3.2% (all $p < 0.001$)—the late-stage coefficients larger (2.3%, 5.4%, 5.7%) yet insignificant ($p > 0.05$). We expect this result to be an econometric artifact. The late stage comprises only four 3-hour windows against roughly fifty-two in the early stage, so under 8% of the panel identifies the late-stage coefficient and its standard errors are inflated accordingly; the point estimates are in fact *larger* late than early on all three outcomes, ordered as co-disclosure predicts, but the cell is too thin to distinguish them from zero.

Evidence for form proximity boundary. Form proximity moderates both channels through competing forces: stylistic coherence strengthens search and co-disclosure, while at very high similarity substitutability counteracts these gains through entry deterrence and strategic bid alternation. Results for comparisons between one focal and concurrent painting siblings are in Figure 6 (left panel) and Table G.9, discretizing similarity into five levels. The entry effect rises from 0.6% at levels 1 and 2 to a 1.3% peak at level 3, then declines to 0.8% at level 4 (all $p < 0.05$) and an insignificant 0.3% at level 5; bids likewise peak at level 3 (2.2%) and fall at levels 4 and 5 (1.7% and 1.4%). The inverted-U is specific to these participation outcomes—who enters and how often they bid—while mean and total increments remain large even at the highest similarity. This resilience is informative: high similarity appears to select bidders resolved to win at most one item, who, once engaged, bid no less aggressively than without a concurrent listing. The pattern broadly reproduces across all category pairs rather than painting-to-painting alone (Table G.11). Though the estimates differ in clustering and are not strictly comparable, the contrast is what substitution implies: a work is a plausible alternative only if comparable in kind as well as close in form, and pooling dilutes the highest-similarity cell with pairs visually alike yet not competing for the same purchase. Hypothesis 5 remains partially validated.

The shape warrants caution. Quintile effects are positive throughout and significant against different-category controls, but adjacent quintiles do not differ significantly at the 5% level; replacing quintiles with linear and quadratic terms yields predicted negative quadratic on every outcome without statistical significance (Table G.10), leaving a formal interior-peak test uninformative. We see this as a *suggestive* inverted-U—a boundary condition under which amplification weakens—and claim no threshold where concurrency turns cannibalizing.

Evidence for the valuation-stakes boundary. Hypothesis 6 predicts that the treatment effect on bidding frequency and bid increments rises with focal item's pre-sale estimate. Results are given in Figure 6 (right panel) and Table G.12. With $\text{POST}_\tau \times \text{Treated}_a$ omitted so that each estimate level enters as its own triple interaction, mean increments run -4.5%, 0.4%, 3.7%, 5.6%, and 12.2% across the estimate quintiles—rising monotonically, significant at every level but the second, and a jump of over sixteen percentage points—and frequency traces the same increase (-1.4% to 2.4%). The continuous specification in Table G.13 reproduces this result: the interaction with $Estimate_a$ is 0.064 on mean increments and 0.013 on frequency (both $p < 0.01$).

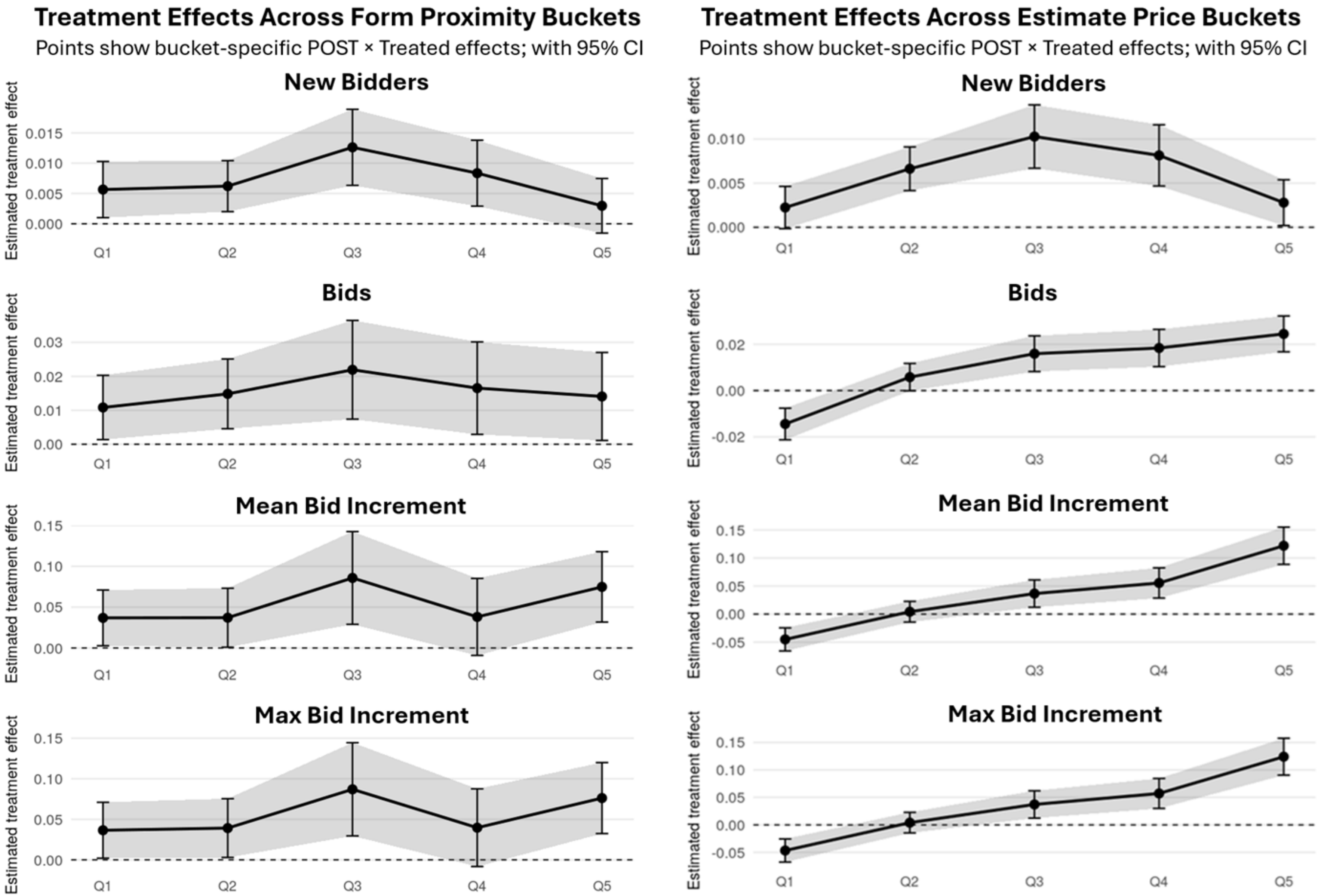

Figure 6: Moderation of the concurrency treatment effect by form proximity and valuation stakes. Each panel reports estimated treatment effects on the four bidding outcomes—new bidder entry, bidding frequency, and mean and total bid increments—across five quintiles of the moderator, with 95% confidence intervals. Left panel uses quintiles of DINOv2 cosine similarity between the focal and concurrent items and right panel uses quintiles of the focal item's pre-sale estimate. Full estimates are reported in G.9 and Tables G.12.

New bidder entry is 0.2%, 0.7%, 1.0%, 0.8%, and 0.3% across the five quintiles, peaking in the middle. The lowest quintile is indistinguishable from zero and the highest, though significant, falls below every interior level; the continuous interaction is precisely zero, consistent with an interior peak. Entry alone captures pure discovery; repeated bidding and bid size instead reflect valuation responses that scale with how much bidders can learn. Discovery requires both an item worth searching for and bidders who have not yet been reached, conditions that weaken at both ends of the value range. The margins therefore diverge here.

We note that the decomposition reproduces the baseline: equal-weight averaging of the quintile effects on $\Delta_{a\tau}^{Mean}$ gives 3.5%, against the 3.4% average treatment effect in Table 1—the specification resolves the existing result into parts rather than introducing a new one. Second, the lowest quintile is genuinely negative, not merely small: -4.5% on mean increments, -1.4% on frequency, both $p < 0.001$. For the least valuable fifth of the catalogue, a sibling listing carries too little common value content to be worth reading, leaving a second lot competing for the same buyer. Hence, cannibalization from identical overlapping-auctions literature (Bapna et al. 2009), is recovered as a bounded regime rather than a general property.

7 Extension and Robustness Tests

7.1 Extension: Does Co-Disclosure Persist After the Concurrent Auction Closes?

We exploit a complementary sample in which concurrency ends before the focal auction closes: a within-auction reversal from non-concurrent to concurrent and back. Because this requirement caps how much sibling bidding a focal auction can accumulate, we retain only episodes carrying a readable signal, those whose concurrent listing drew at least one bid over at least 24 hours of overlap, yielding 630 treated auctions matched to 1,933 SameCategory_a and 2,047 Control_a auctions (Appendix H). The design tests whether co-disclosure is a *flow*, contingent on a sibling remaining live, or a *stock* retained once acquired: we replace POST_τ with two phases, Concurrent_τ and PostRemoval_τ, each interacted with Treated_a and SameCategory_a.

All four outcomes rise while concurrency is live—entry by 0.4%, bids by 0.9%, and mean and total increments by 2.9% and 3.0%. Every post-removal interaction is statistically insignificant (Table H.1). The signal is a flow: bidding responds to a live sibling and reverts once it closes, as co-disclosure implies, since a bid path informs valuations only while it is being updated. SameCategory_a peers, sharing the category but not the creator, show no entry gain but do gain 0.7% on bids and 2.5% on both increment margins (all $p < 0.001$). Discovery thus travels along creator-linked paths such as shared artist tags, while the intensification of bidding is diffuse, elevating activity across the category. Live bidding on a same-artist pair may supply reference prices to bidders for comparable works, or episode may coincide with elevated category-level activity affecting both arms. However, our results with continuous treatment show no such pattern, suggesting it is particular to the short episodes this sample selects.

7.2 Robustness Tests

In addition to our event study employing Equation 2 (Appendix I.1), we conduct additional robustness tests to ensure the baseline findings are not driven by event-time construction, lifecycle dynamics, matching choices, or aggregation windows.

Placebo event study. We estimate a placebo event study on pure Control_a auctions alone (Table I.2). These are never exposed to concurrency. Figure I.1 shows that the pure controls exhibit no discrete, persistent increase after $\tau = 0$, in contrast to treated auctions, where bidding activity and bid increments rise sharply at onset. The main results are therefore not artifacts of relative-time normalization or common auction lifecycle patterns.

Synthetic control estimation. Next, as a diagnostic, we implement a pooled synthetic-control-style comparison of $Treated$ and $SameCategory$ auctions against Control_a (Appendix I.3). The treated-control comparison yields positive post-treatment gaps on all outcomes: 0.022 for new bidders, 0.069 for bids, 0.229 for mean increments, and 0.232 for total increments. The $SameCategory$ gaps are small and insignificant, and pre-treatment gaps are near zero in both comparisons. The divergence is thus concentrated among treated auctions rather than general to matched comparisons.

Alternative matching and estimation specifications. We re-estimate the baseline specification using matched-set weights so that differences in the number of treated, same-category control, and pure control observations within matched triads do not mechanically determine the estimating sample. We see that the results actually strengthen with this additional consideration in Table I.4. For count-based dependent variables ($NewBidders_{a\tau}$ and $Bids_{a\tau}$), we use Poisson Pseudo-Maximum Likelihood Estimation as an alternative to our main specification in Equation 1. Results in Table I.5 show evidence of main treatment effects directionally in line with our expectations. Next, the main specification is altered by using 1-hour and 6-hour aggregation windows to produce the results in Appendix I.6, indicating that the findings are not specific to the 3-hour window used in the main analysis. Similarly, we change the matching caliper from 0.1 SD to 0.25 SD and 1 SD separately, and generate corresponding matched triads to test the robustness around this caliper-related decision. Results in Appendix I.7 also replicate our baseline results. Finally, we vary the matching procedure by using Mahalanobis-distance-based matching in Appendix I.8. The estimated treatment effects remain positive and significant for bids and bid increments across these specifications, providing further evidence that the baseline results are not driven by a particular matching bandwidth or distance metric.

Alternative dimensions of overlap. We re-estimate Equation (1) with triple interactions for three coarser overlap measures: shared category ($TypeOverlap$; Table I.11), shared genre ($GenreOverlap$; Table I.12), and same partner house ($AuctionHouseOverlap$; Table I.13). The baseline effect survives throughout. Hence, the effect operates through creator identity rather than through the coarser category, genre, or seller channels.

8 Discussion on Implications and Conclusion

8.1 Managerial Implications

Our results cast concurrency as a free, technology-enabled judgment device substituting for costly institutional intermediation. The revenue gains are additive rather than redistributive across the catalogue and operate through search and co-disclosure mechanisms.

I. For sellers and auction houses, cluster distinct same-artist works, but manage substitution. Sellers often hesitate to list same-artist works together for fear of "competing with themselves." However, we show that overlap makes demand for the artist visible, concentrates bidder attention, and lets information spill from one auction to another. The key is to cluster works recognizably connected by authorship but differentiated enough in subject, style, palette, or scale that bidders do not treat them as interchangeable. Studios and labels already exercise it by judgment when spacing related releases; here the platform supplies the visibility without coordination, leaving the consignor only the differentiation to manage. Next, gains rise with item value and turn negative in the lowest quintile of pre-sale estimates. So clustering pays for the middle and upper range of a catalogue and works against the least valuable lots, better released alone.

II. For platforms, the implications are more nuanced. The concurrency value we document was not designed in, and platforms should beware of suppressing it inadvertently. Because the lift is additive, scheduling rules that separate same-artist listings to avoid apparent self-competition would forgo revenue the architecture already generates at no cost. Nor does the benefit come at the expense of non-concurrent same-category peers: concurrency expands the pool of bidder attention rather than reallocating a fixed one, so a platform that encourages it grows the market rather than redistributing within it. Whether it can be engineered is a separate question. We have not modeled or tested an allocation mechanism, and bidders who recognize an engineered pairing may behave differently from those encountering one incidentally. Our contribution is identifying a phenomenon a future design exercise would target.

III. Beyond art auctions, the mechanism generalizes to markets where one producer's output recurs across heterogeneous, individually priced lots. Fine wine is the clearest parallel: a château anchors value across vintages as an artist does across works, so the mechanism should matter least in the blue-chip segment, where critic scores and price indices already discipline valuations, and most among producers lacking either. Online wine marketplaces disclose demand (Liv-ex publishes live bid-offer ratios, CultX operates a continuous order book, iDealwine pairs auctions with a three-decade price database), but at the asset level: each vintage is priced in isolation, producer-level demand observable only through lagged indices. Linking a producer's concurrent vintages, so live demand for one informs valuation of the others, would reorient disclosure toward the producer. Two qualifications apply. First, vintage introduces a quality shock without analog among an artist's works, so sibling lots are less comparable and the signal noisier. Second, our valuation-stakes condition yields a test: the mechanism should hold for bottles whose value is largely common, set by vintage scores and resale prospects, and fail for everyday wines, as in the lowest quintile of our estimates. The logic plausibly extends to artist-tagged NFT issuances and screenplay rights, wherever the creator's identity is partly determinant of the price.

IV. The origin of innovation in market design is the broader point. Most value-creating platform features are deliberately engineered: recommendation systems, reputation scores, reserve-price rules. Concurrency, and the cross-listing opportunity it opens in wine, NFTs, or screenplay rights, is instead an unplanned byproduct of aggregating independent sellers' listings at scale; its value-creating property, an endogenous public signal of creator-level demand, was never designed. In film, music, and platform content the same configuration is a scheduling decision whose consequences producers bear; in singular goods markets it arrives unmanaged, leaving its deliberate version an unentered design space. Platforms in thin, high-search-cost markets may thus already possess undesigned affordances substituting for the missing infrastructure. Recognizing and preserving such emergent structure can matter as much as building new mechanisms.

8.2 Conclusion

Markets for singular goods depend on judgment devices: the rankings, reputations, and expert appraisals that discipline valuation when a work cannot be reduced to observable attributes. Such devices have been costly, humanly supplied, and most abundant for the blue-chip works that least require them. The market disruption through emergence of large-scale auction platforms has manufactured a comparable device for free as an unplanned byproduct of their architecture: when distinct works by one artist overlap in time, the live bidding history of one listing becomes a creator-anchored, contemporaneous signal of collective demand that, unlike a concluded sale or lagged index, reveals how the market values the artist now. We term this concurrency and recover its causal effect from the moment overlap begins within an active auction.

Concurrency onset raises bidder entry, bidding frequency, and bid increments, lifting revenue by at least €3.9 per item against flat pre-trends. A search channel operates through scarce attention, tripling the entry effect when the sibling is in its closing hours; a co-disclosure channel operates through information, the sibling's bid path mitigating the winner's curse, propagating dynamically, and strengthening once the reserve is met. The gains are additive, with no same-category cannibalization, and attenuate only among near-identical works, where the participation margins trace a suggestive inverted-U. Two conditions bound the result: the works must be differentiated enough not to read as one purchase, and the focal item must carry enough common value for a sibling's bidding to be worth reading. Where the second fails, in the lowest estimate quintile, the effect reverses and co-presence becomes competition.

The deeper learning concerns the provenance not of artworks but of market value itself. The judgment device was never engineered; it accrued to a marketplace built for scale, working best where designed intermediation is thinnest. Wherever a creator's name prices the work and sibling works may overlap, it can be recognized and preserved rather than invented.

Four limitations point to future work. Evidence from one platform reflects Auctionet's search and ranking design; replication would establish generality. Our matched design accounts for platform-side scheduling, and partner houses consign independently of one another. Whether the effect survives when sellers coordinate their listings is a question for future work. We observe bidding at the auction level; a bidder-level panel would reveal whether search operates through cross-over from the sibling, co-disclosure through monitoring both auctions, and high-similarity substitution through the bid alternation documented by Bapna et al. (2009). A final question is buyer welfare: whether the gains reflect valuation coordination or herd-driven over-revision (Simonsohn and Ariely 2008); resale data could answer whether co-disclosure serves buyers as well as sellers.

Notes

[1]A collector with a fixed budget allocated to an artist has limited appetite for multiple lots; given the moderate prices in our setting, substitutability comes mainly from diminishing marginal utility rather than budget constraints. This holds on average but not everywhere: at the top of the value distribution a single lot can absorb a collector's entire allocation, a case we return to below.

[2]Confirmed directly with Auctionet.

References

Abadie A (2021) Using synthetic controls: Feasibility, data requirements, and methodological aspects. *Journal of economic literature* 59(2):391–425.

Agrawal A, Catalini C, Goldfarb A (2015) Crowdfunding: Geography, social networks, and the timing of investment decisions. *Journal of economics & management strategy* 24(2):253–274.

Anderson SP, De Palma A (2012) Competition for attention in the information (overload) age. *The RAND Journal of Economics* 43(1):1–25.

Art Basel, UBS (2025) *The Art Basel and UBS Global Art Market Report 2025* (Basel: Arts Economics), URL `https://www.artbasel.com/news/the-art-basel-and-ubs-global-art-market-report-2025`.

Ashenfelter O, Graddy K (2002) Art auctions: A survey of empirical studies. Working Paper 8997, National Bureau of Economic Research.

Ashenfelter O, Graddy K (2019) Art auctions. Discussion Paper 13665, Centre for Economic Policy Research.

Askin N, Mauskapf M (2017) What makes popular culture popular? product features and optimal differentiation in music. *American Sociological Review* 82(5):910–944.

Austin PC, Stuart EA (2015) Optimal full matching for survival outcomes: a method that merits more widespread use. *Statistics in medicine* 34(30):3949–3967.

Bajari P, Hortaçsu A (2004) Economic insights from internet auctions. *Journal of Economic Literature* 42(2):457–486.

Bakos JY (1997) Reducing buyer search costs: Implications for electronic marketplaces. *Management science* 43(12):1676–1692.

Balseiro SR, Besbes O, Weintraub GY (2015) Repeated auctions with budgets in ad exchanges: Approximations and design. *Management Science* 61(4):864–884.

Balseiro SR, Gur Y (2019) Learning in repeated auctions with budgets: Regret minimization and equilibrium. *Management Science* 65(9):3952–3968.

Bapna R, Chang SA, Goes P, Gupta A (2009) Overlapping online auctions: Empirical characterization of bidder strategies and auction prices. *MIS Quarterly* 33(4):763–783.

Bayus BL, Putsis WP (1999) Product proliferation: An empirical analysis of product line determinants and market outcomes. *Marketing Science* 18(2):137–153.

Beggs A, Graddy K (1997) Declining values and the afternoon effect: Evidence from art auctions. *The Rand journal of economics* 544–565.

Boudreau K (2010) Open platform strategies and innovation: Granting access vs. devolving control. *Management science* 56(10):1849–1872.

Boudreau KJ (2012) Let a thousand flowers bloom? an early look at large numbers of software app developers and patterns of innovation. *Organization science* 23(5):1409–1427.

Boudreau KJ, Jeppesen LB (2015) Unpaid crowd complementors: The platform network effect mirage. *Strategic Management Journal* 36(12):1761–1777.

Bourdieu P (1986) The forms of capital .

Brynjolfsson E, Hu Y, Simester D (2011) Goodbye pareto principle, hello long tail: The effect of search costs on the concentration of product sales. *Management science* 57(8):1373–1386.

Brynjolfsson E, Smith MD (2000) Frictionless commerce? a comparison of internet and conventional retailers. *Management science* 46(4):563–585.

Caldentey R, Vulcano G (2007) Online auction and list price revenue management. *Management Science* 53(5):795–813.

Caro F, Martínez-de Albéniz V (2020) Managing online content to build a follower base: Model and applications. *INFORMS Journal on Optimization* 2(1):57–77.

Caron M, Touvron H, Misra I, Jégou H, Mairal J, Bojanowski P, Joulin A (2021) Emerging properties in self-supervised vision transformers. *Proceedings of the IEEE/CVF international conference on computer vision*, 9650–9660.

Chan TH, Mihm J, Sosa ME (2018) On styles in product design: An analysis of us design patents. *Management Science* 64(3):1230–1249.

Cox DR (1972) Regression models and life-tables. *Journal of the royal statistical society: Series B (methodological)* 34(2):187–202.

Deshmane A, Barriola X (2025) Frame by fame: Content creation on short video-format platforms. *Manufacturing & Service Operations Management* 27(2):479–495.

Deshmane A, Martínez-de Albéniz V (2023) Come together, right now? an empirical study of collaborations in the music industry. *Management Science* 69(12):7217–7235.

Deshmane A, Martínez-de Albéniz V (2025) Play it again, sam? reference-point formation and product differentiation in the music industry. *Management Science* 71(10):8304–8318.

Einav L (2010) Not all rivals look alike: Estimating an equilibrium model of the release date timing game. *Economic Inquiry* 48(2):369–390.

Einav L, Farronato C, Levin J, Sundaresan N (2018) Auctions versus posted prices in online markets. *Journal of Political Economy* 126(1):178–215.

Einav L, Kuchler T, Levin J, Sundaresan N (2015) Assessing sale strategies in online markets using matched listings. *American Economic Journal: Microeconomics* 7(2):215–247.

Elberse A (2007) The power of stars: Do star actors drive the success of movies? *Journal of Marketing* 71(4):102–120.

Farronato C, Fradkin A (2022) The welfare effects of peer entry: the case of airbnb and the accommodation industry. *American Economic Review* 112(6):1782–1817.

Gagnon-Bartsch T, Pagnozzi M, Rosato A (2021) Projection of private values in auctions. *American Economic Review* 111(10):3256–3298.

Haviv A, Huang Y, Li N (2020) Intertemporal demand spillover effects on video game platforms. *Management Science* 66(10):4788–4807.

Hendricks K, Sorensen A (2009) Information and the skewness of music sales. *Journal of Political Economy* 117(2):324–369.

Hoberg G, Phillips G (2016) Text-based network industries and endogenous product differentiation. *Journal of Political Economy* 124(5):1423–1465.

Karpik L (2010) *Valuing the Unique: The Economics of Singularities* (Princeton, NJ: Princeton University Press), ISBN 9780691137100.

Krider RE, Weinberg CB (1998) Competitive dynamics and the introduction of new products: The motion picture timing game. *Journal of Marketing Research* 35(1):1–15.

Kuruzovich J, Viswanathan S, Agarwal R (2010) Seller search and market outcomes in online auctions. *Management Science* 56(10):1702–1717.

Liu Y, Chen XA, Liu Y, Wang Z (2025) Simultaneous vs. sequential: Optimal assortment recommendation in multistore retailing. *Manufacturing & Service Operations Management* 27(3):825–842.

Luca M, Nagaraj A, Subramani G (2026) Getting on the map: The impact of online listings on business performance. *Management Science* .

McAndrew C, Smith JL, Thompson R (2012) The impact of reserve prices on the perceived bias of expert appraisals of fine art. *Journal of Applied Econometrics* 27(2):235–252.

Milgrom PR, Weber RJ (1982) A theory of auctions and competitive bidding. *Econometrica* 50(5):1089–1122.

Moreno A, Terwiesch C (2017) The effects of product line breadth: Evidence from the automotive industry. *Marketing Science* 36(2):254–271.

Nagaraj A (2022) The private impact of public data: Landsat satellite maps increased gold discoveries and encouraged entry. *Management Science* 68(1):564–582.

Negus K (1997) *Popular music in theory: An introduction* (Wesleyan University Press).

Noparumpa T, Kazaz B, Webster S (2015) Wine futures and advance selling under quality uncertainty. *Manufacturing & service operations management* 17(3):411–426.

Oquab M, Darcet T, Moutakanni T, Vo H, Szafraniec M, Khalidov V, Fernandez P, Haziza D, Massa F, El-Nouby A, et al. (2023) Dinov2: Learning robust visual features without supervision. *arXiv preprint arXiv:2304.07193* .

Overby E, Kannan K (2015) How reduced search costs and the distribution of bidder participation affect auction prices. *Management Science* 61(6):1398–1420.

Pilehvar A, Elmaghraby WJ, Gopal A (2017) Market information and bidder heterogeneity in secondary market online B2B auctions. *Management Science* 63(5):1493–1518, URL `http://dx.doi.org/10.1287/mnsc.2016.2444`.

Randall T, Ulrich K (2001) Product variety, supply chain structure, and firm performance: Analysis of the us bicycle industry. *Management Science* 47(12):1588–1604.

Renneboog L, Spaenjers C (2013) Buying beauty: On prices and returns in the art market. *Management Science* 59(1):36–53.

Roth AE, Ockenfels A (2002) Last-minute bidding and the rules for ending second-price auctions: Evidence from ebay and amazon auctions on the internet. *American economic review* 92(4):1093–1103.

Simonsohn U, Ariely D (2008) When rational sellers face nonrational buyers: evidence from herding on ebay. *Management science* 54(9):1624–1637.

Sorensen AT (2007) Bestseller lists and product variety. *The journal of industrial economics* 55(4):715–738.

Sting FJ, Tarakci M, Recker J (2024) Performance implications of digital disruption in strategic competition. *MIS Quarterly* 48(3):1263–1278.

Vulcano G, Van Ryzin G, Maglaras C (2002) Optimal dynamic auctions for revenue management. *Management Science* 48(11):1388–1407.

Wang H, Song M (2011) Ckmeans.1d.dp: Optimal k-means clustering in one dimension by dynamic programming. *The R Journal* 3(2):29–33.

Zhang J, Liu P (2012) Rational herding in microloan markets. *Management science* 58(5):892–912.

Zhang S, Lee D, Singh PV, Srinivasan K (2022) What makes a good image? Airbnb demand analytics leveraging interpretable image features. *Management Science* 68(8):5644–5666.

When Art Auctions Overlap: Impact of Creator-Linked Concurrency in Singular Goods Online Auction Markets

Appendix

A Theoretical Model

This appendix presents the formal derivations underlying the theoretical framework summarized in Section 3.3.

A.1 Environment and Valuation

Consider a set of auctions $a = 1, \ldots, A$ running on the platform during a given interval t. Each auction sells a unique artwork. Bidders are risk neutral. Bidder valuation of the auction object follows the seminal paper by Milgrom and Weber (1982). Upon visiting auction a, bidder b forms a valuation of the object at U_{ab} (suppressing subscript t for simplicity), but does not observe U_{ab} directly. Instead, each receives a scalar private observation $\tilde{X}_{ab}$ about the object. $\tilde{X}_{ab}$'s are identically distributed across b over the support $(0,\ \bar{X}_a)$ and are strictly affiliated. Intuitively, strict affiliation means that large realized values for some of the variables make the other variables more likely to be large than small. For a general definition of affiliation, see the Appendix of Milgrom and Weber (1982).

Bidder valuations are affiliated in the sense that bidder b's expected value of object a, V_{ab}, is a function of private observations of all bidders that arrive at auction a, i.e. $V_{ab} = v(x_{ab}, \{x_{ab'}\}_{b' \neq b}) = E[U_{ab} \mid x_{ab}, \{x_{ab'}\}_{b' \neq b}]$, where v is continuous and increasing in each argument. By assumption, the value function $v(\cdot)$ is the same for all bidders and across all auctions. This value function encompasses the common value case (which consists of both a private value component and a common value component) and two special cases: the private value case and the pure common value case. For the private value case, $V_b = v(x_b, \{x'_b\}_{b' \neq b}) = v(x_b)$, where bidder b's expected value only depends on her own private observation. For the pure common value case, $V_b = v(x_b, x_k, \{x_{b'}\}_{b' \neq b, b' \neq k}) = v(x_k, x_b, \{x_{b'}\}_{b' \neq b, b' \neq k}), \forall k \neq b$, that is, private observations of all bidders (including bidder b) enter into bidder b's value function symmetrically. In the context of art auctions, the presence of resale value suggests a common value component. Heterogeneity in taste, on the other hand, suggests the presence of a private value component. As a result, we rule out the two special cases and only consider the common value case.

An implicit assumption embedded in this value structure is that each item is valued in isolation: bidder b's valuation of item a does not depend on whether she also acquires any other item. Items are therefore treated as neither complements nor substitutes. Formally, for a bidder who wins a set S of the artist's concurrently listed works, independence amounts to additive separability of the bundle value,

$$V_b(S) = \sum_{m \in S} V_{mb},$$

so that the marginal value of item a conditional on also winning a sibling item m equals its standalone value, $V_{ab|m} = V_{ab}$. This is the maintained assumption throughout the analysis of the two mechanisms below, and it is what permits treating each focal auction's expected revenue in isolation.

The assumption is relaxed by adding a pairwise interaction term $\omega_{b,am}$ to the value of jointly held items:

$$V_b(\{a, m\}) = V_{ab} + V_{mb} + \omega_{b,am}, \qquad V_{ab|m} = V_{ab} + \omega_{b,am}.$$

Items are *complements* when $\omega_{b,am} > 0$, so that owning m raises the marginal value of a ($V_{ab|m} > V_{ab}$), and *substitutes* when $\omega_{b,am} < 0$, so that owning m lowers it ($V_{ab|m} < V_{ab}$). The polar case of perfect substitutability corresponds to single-unit demand,

$$V_b(\{a, m\}) = \max\{V_{ab}, V_{mb}\},$$

in which a bidder derives no incremental value from the second item. We maintain independence ($\omega_{b,am} = 0$) when deriving the search and co-disclosure mechanisms and return to the substitutes case ($\omega_{b,am} < 0$), whose magnitude grows with form proximity, when analyzing the boundary condition that generates the cannibalization force underlying H5.

The value function $v(\cdot)$ admits a second source of variation: the weight bidder b places on other bidders' signals $\{x_{ab'}\}_{b' \neq b}$ relative to her own signal x_{ab}. This weight indexes how common rather than private her valuation is, and the two special cases above delimit it: it is zero in the private value case, where v depends on x_{ab} alone, and equals the weight on her own signal in the pure common value case, where all signals enter symmetrically. Our common value case lies between, and we assume the weight is increasing in the share of the common value component. We further assume this share is increasing in the item's total value. To see when this holds, let $U_{ab} = A_a + t_{ab}$, with common value component A_a (the artist's resale and reference value) and private value component t_{ab} (bidder b's taste); the common share rises if the dispersion of A_a grows with value while that of t_{ab} does not. (This can be formally shown under mild assumptions, including independence of A_a and t_{ab} and finite variances, with normality yielding the updating weight in closed form.) Both hold in our long-tail setting. The dispersion of A_a widens as the value range extends upward, because it brings in higher-quality, more sought-after artists whose resale and reference value varies more widely. The dispersion of t_{ab} does not, provided taste is uncorrelated with quality—plausible for the moderately priced regional works we study, though not for blue-chip works, whose recognized quality itself drives enjoyment.

While total value is unobserved, the pre-sale estimate is a suitable proxy: set by the partner house from the work's attributes and comparable past sold prices (Beggs and Graddy 1997), it is monotone in expected value (McAndrew et al. 2012, Ashenfelter and Graddy 2019). Combining the two assumptions, the weight a bidder places on affiliated signals—both from other bidders in the focal auction and bidders in the *concurrent auction* as formally defined below—is increasing in the pre-sale estimate. The two boundary conditions of §3.4 therefore correspond to two distinct primitives of the model: $\omega_{b,am}$, increasing in absolute magnitude with form proximity, and the weight on affiliated information, increasing with the pre-sale estimate.

Let B_a denote the number of active bidders in auction a. Expected revenue conditional on the realized bidder count satisfies the usual structure:

$$\mathbb{E}[R_a \mid B_a] = r(B_a),$$

where $r(\cdot)$ is increasing in B_a. Two forces underlie this monotonicity, both operating within the ascending-bid (English) format we study. First, an *order-statistic effect*: the transaction price is set where the second-to-last bidder drops out, and drawing more bidders from a fixed distribution stochastically raises this near-top order statistic, so prices rise with participation even absent any informational change. Second, under affiliated values, an *information-aggregation effect*: each active bidder's dropout price publicly reveals a signal affiliated with the common value component, so a larger pool of bidders produces a richer sequence of public signals over the course of the auction. This additional information reduces the remaining bidders' residual uncertainty and attenuates the winner's curse, leading them to bid less cautiously (Milgrom and Weber 1982). Both forces push in the same direction, so greater participation raises expected revenue. The information-aggregation effect is stated here under the canonical assumption that the dropout sequence is publicly observed; the co-disclosure mechanism (§A.3) relaxes this for the timed online format we study, where exit is not directly observed.

Two auctions a and m are said to be *concurrent* if they involve works by the same artist and their auction windows overlap. Let $\chi_{at} = 1$ if auction a has at least one concurrent partner at time t, and $\chi_{at} = 0$ otherwise.

A.2 Mechanism 1: Visibility and Search

During interval t, M_t unique individuals—the *potential bidders*—arrive at the platform. M_t is a non-negative, integer-valued random variable with mean $\mathbb{E}[M_t] = \mu_t$, capturing the size of the platform's active audience during t.

Potential bidders are *ex ante* identical and symmetric in the search process. Each potential bidder commits at the start of her search episode to visiting ν_t auctions. Conditional on making a visit, each draws the auction or auctions visited from the common visit-probability distribution $\{p_{at}\}_{a=1}^{A}$ specified below. We call $\nu_t > 0$ the common *search intensity.*

Search intensity is governed by the platform's search environment. Let $c_t \geq 0$ measure the prevailing *search friction* on the platform during t, and set

$$\nu_t = \nu(c_t),$$

where $\nu(\cdot)$ is decreasing, so that potential bidders sample more auctions when friction is lower.

Aggregating individual search, total visits to the a auctions are $N_t = M_t\,\nu_t$, with mean $\mathbb{E}[N_t] = \mu_t\,\nu_t$ increasing in both the expected audience size μ_t and the search intensity ν_t.

We model the visit probabilities via a nonnegative function f, which represents a visit score. For each visit, let the visit probability to auction a at time t be

$$p_{at} \;=\; \frac{f(x_{at}, y_{at}, \chi_{at})}{\sum_{k=1}^{A} f(x_{kt}, y_{kt}, \chi_{kt})},$$

where x_{at} is a vector of auction specific attributes, including estimate, auction duration, and other searchable attributes (e.g., artist, theme, medium, etc.); y_{at} is a vector of visibility attributes, including the listing position, page number, and whether the auction is specially featured; and χ_{at} is the aforementioned binary concurrency indicator. Notice that by construction, $\sum_{a=1}^{A} p_{at} = 1$. Following the search cost logic in Overby and Kannan (2015), we assume

$$f(x_a, y_a, 1) > f(x_a, y_a, 0).$$

Consequently, $p_{at}(\chi_{at} = 1) > p_{at}(\chi_{at} = 0)$. Concurrency increases the likelihood of discovery of a listing by raising its visit score.

Conditional on N_t, each visit independently lands on auction a with probability p_{at}, so $N_{at} \mid N_t \sim \text{Binomial}(N_t, p_{at})$, which is increasing in p_{at} in the first-order stochastic dominance (FOSD) order. Since $p_{at}(\chi_{at} = 1) > p_{at}(\chi_{at} = 0)$, concurrency shifts the *realized* number of visits to auction a upward,

$$N_{at} \mid \chi_{at} = 1 \ \succeq_{\text{FOSD}} \ N_{at} \mid \chi_{at} = 0,$$

conditional on N_t and hence unconditionally, since FOSD is preserved under mixing over N_t.

Each potential bidder visits any given auction at most once, so N_{at} counts the distinct bidders arriving at a. We abstract from the entry decision—which weighs a bidder's valuation against entry and monitoring costs—and assume each arrival enters independently with positive probability. Independent entry thins the arriving pool, and thinning preserves the FOSD order, so the active-bidder count inherits the shift:

$$B_{at} \mid \chi_{at} = 1 \ \succeq_{\text{FOSD}} \ B_{at} \mid \chi_{at} = 0.$$

Recall that $r(B_{at}) = \mathbb{E}[R_{at} \mid B_{at}]$ is expected revenue conditional on the realized bidder count, so unconditional expected revenue is $\mathbb{E}[r(B_{at})]$. Since $r(\cdot)$ is increasing and first-order stochastic dominance raises the expectation of every increasing function,

$$\mathbb{E}[r(B_{at}) \mid \chi_{at} = 1] \ \geq \ \mathbb{E}[r(B_{at}) \mid \chi_{at} = 0],$$

so concurrency raises expected focal-auction revenue.

Importantly, conditional on the total number of visits N_t, higher visit probabilities for concurrent auctions mechanically reduce visit probabilities for non-concurrent auctions, generating what can be described as *attention diversion.* On the other hand, concurrency also shapes the search friction itself. Writing $s_t = \frac{1}{A}\sum_{a=1}^{A} \chi_{at}$ for the share of concurrent auctions during t, we let

$$c_t = c(s_t),$$

where $c(\cdot)$ is decreasing, that is, a larger share of concurrent listings lowers platform-wide search friction—works by the same artist are easier to locate. Through $\nu_t = \nu(c_t)$, a higher s_t thus raises the common search intensity ν_t, and with it total visits $N_t = M_t \, \nu_t$ and the expected number of visits $\mathbb{E}[N_t] = \mu_t \, \nu_t$. We refer to this offsetting force as *attention creation.* When attention creation is sufficiently strong, it can fully compensate for attention diversion, rendering the net effect of concurrency on non-concurrent auctions neutral.

A.3 Mechanism 2: Information Disclosure

As discussed before, in art auctions, valuations carry a common value component due to uncertainty about resale value, latent market demand, and perceived artistic significance. The presence of the common value component implies that bidders' valuations and information are affiliated. As Milgrom and Weber (1982) has shown, under affiliated values, additional public information that is affiliated with bidders' valuations increases expected revenue by reducing uncertainty and mitigating winner's curse concerns (see Milgrom and Weber (1982), Theorem 13). Concurrent auctions generate such information in real time: the bidding dynamics of one listing provide a noisy but informative signal about the underlying value of works by the same artist.

Updating within an online English auction. Before discussing how information revealed in concurrent auctions leads to dynamic valuation updates by bidders in the focal auction, we first establish how valuation updates take place within the focal auction. Recall that with affiliated values, bidder b's valuation in auction a, which is also the highest price she is willing to pay, is a function of the private signals of all bidders, i.e. $V_{ab} = v(x_{ab}, \{x_{ab'}\}_{b' \neq b}) = E[U_{ab} \mid x_{ab}, \{x_{ab'}\}_{b' \neq b}]$, where U_{ab} is the true latent value of a to bidder b. In the canonical ascending-bid auction model, a bidder forms the anterior expectation at the beginning of the auction by substituting her own private signal x_{ab} in place of the signals of other bidders $\{x_{ab'}\}_{b' \neq b}$ that are not observed by her. She then updates her posterior valuation upon observing the exit of a bidder by inferring the bidder's private signal from inverting his bid function using the dropout price. Online auctions differ in two important respects. First, bidder exit is typically not directly observed; prolonged inactivity is at best an imperfect proxy, especially in the presence of sniping. Second, the number of bidders is not perfectly observed until the auction ends as new bidders can enter as the auction progresses.

To bridge the gap between the canonical model and the online environment, we propose the following updating process to better describe bidder behavior. We represent the bidders' information set at time t in auction a by a public history H_{at}, which includes observable bidding dynamics such as the standing price, the number of observed distinct bidder IDs, the sequence of bids (and their timestamps), and the pattern of bid increments. We then summarize this public history via a sufficient statistic

$$z_{at} = g(H_{at}),$$

where $g(\cdot)$ is increasing in public indicators of competitive intensity and value-relevant information. Concretely, z_{at} rises when the auction attracts more unique bidders, when bid arrivals are more frequent, and when bid increments are larger (including "jump bids," i.e., bids that exceed the minimum amounts required by the platform). This also delivers the information-aggregation effect posited in the environment (§A.1) without requiring an observable dropout sequence: because z_{at} is increasing in the number of unique bidders, greater participation enriches the public history from which bidders update and raises expected revenue even though individual bidder exits are not observed.

We model bidder b's time-t valuation in auction a as the posterior expectation

$$\tilde{V}_{abt} \;=\; \tilde{v}(x_{ab}, z_{at}),$$

where $\tilde{v}(\cdot)$ is increasing in both arguments. This representation captures the idea that online bidders rationally map the observable bid path into an updated belief about the value-relevant state U_{ab}. When observed bidding dynamics exceed what bidder b expected given her prior and x_{ab}—for example, when many bidders arrive early or when increments are unusually aggressive—she revises upward the component of her valuation tied to market demand and resale prospects; conversely, unexpectedly weak bidding leads to downward revisions. Importantly, unlike the pure "dropout inference" mechanism in standard theory, this updating is driven by *observable bid histories* rather than perfectly observed exits.

Cross-auction updating under concurrency. Now consider a concurrent auction k for a different work by the same artist as a. Under concurrency, bidders who discover or monitor both listings observe not only H_{at} but also the public history H_{kt} in the concurrent auction. Let $z_{kt} = g(H_{kt})$ be the analogous sufficient statistic for auction k.

We then extend the bidder b's valuation in auction a to incorporate the concurrent-auction signal:

$$\tilde{V}_{abt} \;=\; \tilde{v}\big(x_{ab},\, z_{at},\, \rho_{ak}\, z_{kt}\big), \qquad \rho_{ak} \in (0,1).$$

The weight ρ_{ak} captures imperfect comparability: works are not identical, so information from k is less directly value-relevant than information generated within a. Nonetheless, when the two works share the same artist, z_{kt} is positively affiliated with the private signal x_{ab} and therefore increases $\tilde{V}_{abt}$ on average. Intuitively, bidding intensity in k reduces bidders' uncertainty about the state of demand for the artist and mitigates the perceived winner's-curse of "overpaying" relative to the market; this increases willingness-to-pay on average and can manifest as more frequent bids and larger increments.

This cross-auction updating also yields clear timing implications. First, the onset of concurrency creates a discrete informational shock: once auction k becomes visible while a is still active, bidders in a can condition on an additional stream of public signals, leading to an immediate change in bidding behavior. Second, as long as k continues to receive bids, z_{kt} keeps evolving, so the informational effect can persist throughout the overlap.

B Data Details

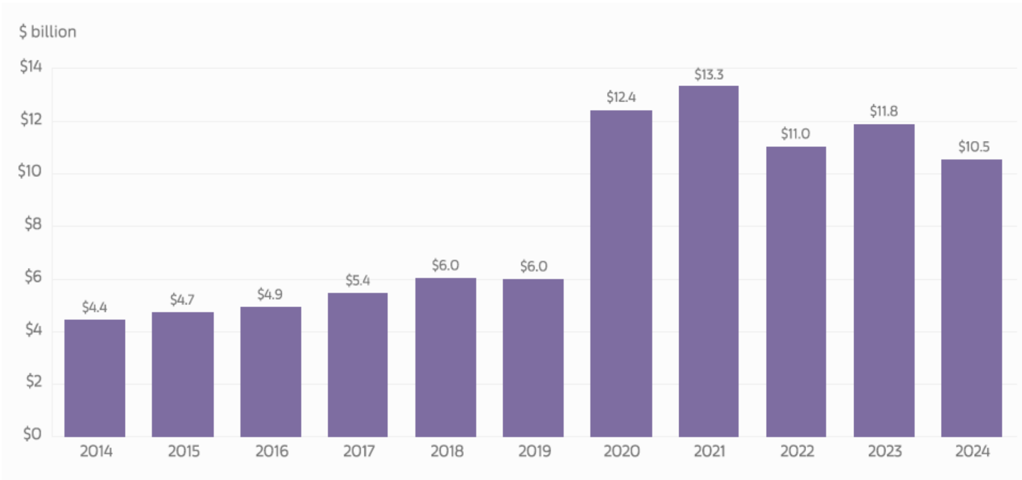

Figure B.1: The Global Online Art Market 2014–2024.

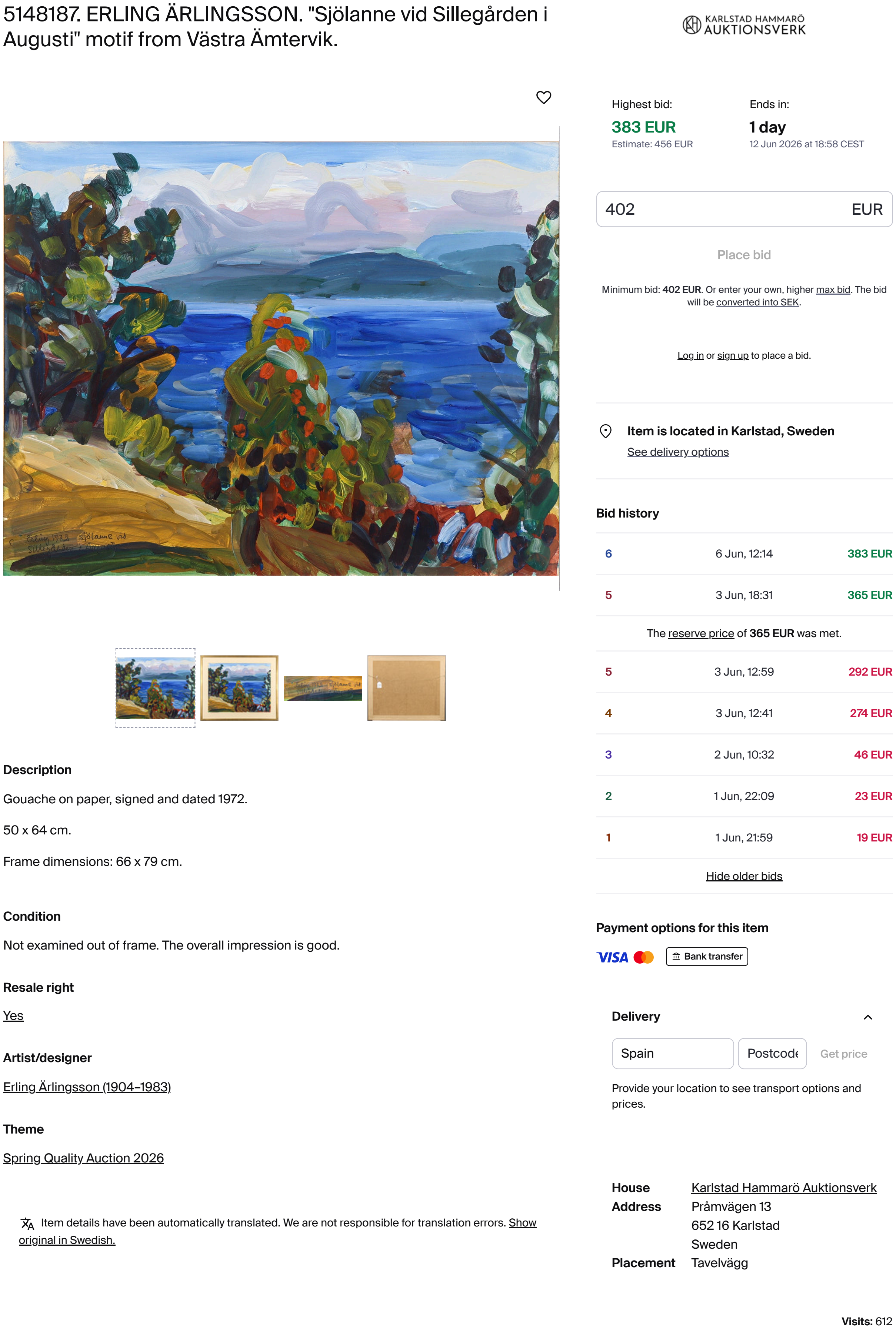

Figure B.2: Example of a bidding screen on Auctionet.

No.	Country	City	Auction house	No.	Country	City	Auction house
1	Denmark	Copenhagen	Palsgaard Kunstauktioner	42	Sweden	Linköping	Gomér & Andersson Linköping
2	Denmark	Holbæk	Woxholt Auktioner	43	Sweden	Lund	Björnssons Auktionskammare
3	Denmark	Køge	Bidstrup Auktioner	44	Sweden	Lund	Crafoord Auktioner Lund
4	Finland	Helsinki	Stockholms Auktionsverk Helsinki	45	Sweden	Lysekil	Lysekils Auktionsbyrå
5	Germany	Bocholt–Suderwick	Rheinveld Auktionen	46	Sweden	Malmö	Limhamns Auktionsbyrå
6	Germany	Bonn	Auction Now	47	Sweden	Malmö	Crafoord Auktioner Malmö
7	Germany	Chemnitz	Auktionshaus Bossard	48	Sweden	Malmö	Stockholms Auktionsverk Malmö
8	Germany	Cologne	Stockholms Auktionsverk Köln	49	Sweden	Malmö	Garpenhus Auktioner
9	Germany	Düsseldorf	Stockholms Auktionsverk Düsseldorf	50	Sweden	Mora	TOKA Auktionshus
10	Germany	Frankfurt/Main	Auktionshaus Blank	51	Sweden	Motala	Auktionshuset Thörner & Ek
11	Germany	Hamburg	Stockholms Auktionsverk Hamburg	52	Sweden	Norrköping	Gomér & Andersson Norrköping
12	Germany	Hamburg	Colombos	53	Sweden	Norrköping	RA Auktionsverket Norrköping
13	Germany	Hannover	HannoVerum	54	Sweden	Norrtälje	Roslagens Auktionsverk
14	Germany	Mannheim	Auktionshaus Stuber's Hammerschlag	55	Sweden	Nyköping	Gomér & Andersson Nyköping
15	Germany	Mannheim	Kunst- und Auktionshaus Kleinhenz	56	Sweden	Oskarshamn	Auktionshuset Thelin & Johansson
16	Spain	Barcelona	Arce Auctions	57	Sweden	Sandviken	Handelslagret Auktionsservice
17	Spain	Barcelona	Barcelona Auctions	58	Sweden	Stockholm	Formstad Auktioner
18	Spain	Barcelona	Balclis	59	Sweden	Stockholm	Stockholms Auktionsverk Sickla
19	Sweden	Borås	Borås Auktionshall	60	Sweden	Stockholm	Stockholms Auktionsverk Magasin 5
20	Sweden	Gothenburg	Stockholms Auktionsverk Göteborg	61	Sweden	Stockholm	Stockholms Auktionsverk Fine Art
21	Sweden	Gothenburg	Connoisseur Bokauktioner	62	Sweden	Stockholm	Crafoord Auktioner Stockholm
22	Sweden	Gothenburg	Göteborgs Auktionsverk	63	Sweden	Stockholm	Walter Borg
23	Sweden	Halmstad	Halmstads Auktionskammare	64	Sweden	Stockholm	Mauritz Widforss
24	Sweden	Halmstad	Tisas	65	Sweden	Stockholm	Auktionshuset Kolonn
25	Sweden	Helsingborg	Stockholms Auktionsverk Helsingborg	66	Sweden	Sundsvall	Stadsauktion Sundsvall
26	Sweden	Helsingborg	Helsingborgs Auktionskammare	67	Sweden	Trelleborg	Markus Auktioner
27	Sweden	Henån	Auktionshuset STO Bohuslän	68	Sweden	Umeå	Norrlands Auktionsverk
28	Sweden	Hudiksvall	Hälsinglands Auktionsverk	69	Sweden	Uppsala	Uppsala Auktionskammare
29	Sweden	Höganäs	Höganäs Auktionsverk	70	Sweden	Varberg	Varberg Auktionskammare
30	Sweden	Höör	Höörs Auktionshall	71	Sweden	Vänersborg	Auktionsmagasinet Vänersborg
31	Sweden	Jönköping	Gomér & Andersson Jönköping	72	Sweden	Växjö	Växjö Auktionskammare
32	Sweden	Kalmar	Auktionskammaren Sydost Kalmar	73	Sweden	Ängelholm	Auktionsverket Engelholm
33	Sweden	Kalmar	Auktionsfirma Kenneth Svensson	74	Sweden	Örebro	Örebro Stadsauktioner
34	Sweden	Kalmar	Kalmar Auktionsverk	75	UK	Bath	Ma San Auction
35	Sweden	Karlshamn	Ekenbergs	76	UK	Crewkerne	Lawrences Auctioneers
36	Sweden	Karlstad	Karlstad Hammarö Auktionsverk	77	UK	London	Lots Road Auctions
37	Sweden	Katrineholm	Södermanlands Auktionsverk	78	UK	Sherborne	Acreman St Auctioneers & Valuers
38	Sweden	Laholm	Laholms Auktionskammare	79	UK	Sherborne	Rumsey's Auctioneers
39	Sweden	Landskrona	Skånes Auktionsverk	80	UK	Southend on Sea	Chalkwell Auctions
40	Sweden	Lindesberg	Wedevågs Auktionshus	81	UK	Stowmarket	Bishop & Miller
41	Sweden	Linghem	Sajab Vintage	82	UK	Surrey	Young's Auctions

Table B.1: Auction houses on Auctionet by country and city.

	Non-concurrent		Concurrent	
	Mean	s.d.	Mean	s.d.
Observations	157,648		119,388	
$SoldFor_a$(€)	298.1	3341.0	207.5	1195.0
$Estimate_a$ (€)	332.6	3374.0	206.1	934.0
$Duration_a$ (days)	5.3	4.6	6.9	4.5
$Bids_a$	7.1	8.8	10.0	9.8
$NBidders_a$	2.6	2.1	3.5	2.4

Notes: Item-level means and standard deviations, computed separately for auctions that ran with a concurrent same-artist listing and those that did not.

Table B.2: Item-level summary statistics.

Dependent Var:	$SoldFor_a$		
Model:	(1)	(2)	(3)
Concurrent	14.613***		
num_conc=1		10.667**	
num_conc=2		12.553*	
num_conc=3-6		22.735***	
num_conc>6		24.873***	
conc. diff house			17.574***
$Estimate_a$	1.139***	1.139***	1.146***
$NumVisits_a$	0.045***	0.045***	0.046***
$NumImages_a$	-13.285***	-13.265***	-15.545***
$Resale_a$	-6.863	-6.813	-11.041*
$Bids_a$	18.607***	18.602***	18.579***
$NBidders_a$	-9.346***	-9.410***	-6.706***
$Duration_a$	-5.712***	-5.785***	-6.076***
Constant	-125.684***	-126.371***	-122.912***
Fit statistics			
Observations	237,327	237,327	191,109
R^2	0.866	0.866	0.866

Notes: Artist, Category, Auction House, Year, Month, and day-of-week fixed effects are included.
Significance: $^{***}p < 0.001$; $^{**}p < 0.01$; $^{*}p < 0.05$.

Table B.3: Correlational revenue effects.

C Matching Procedure: Full Details

Here, we provide the complete formal specification of the PSM procedure summarized in §5.

C.1 Candidate Pool Definitions

Let $\mathcal{A}^T$ denote treated auctions and $\mathcal{A}^{\text{conc}}$ all auctions whose artist has any concurrent activity in any category-genre combination. For treated auction a with onset w_a^* and episode end w_a^{**},

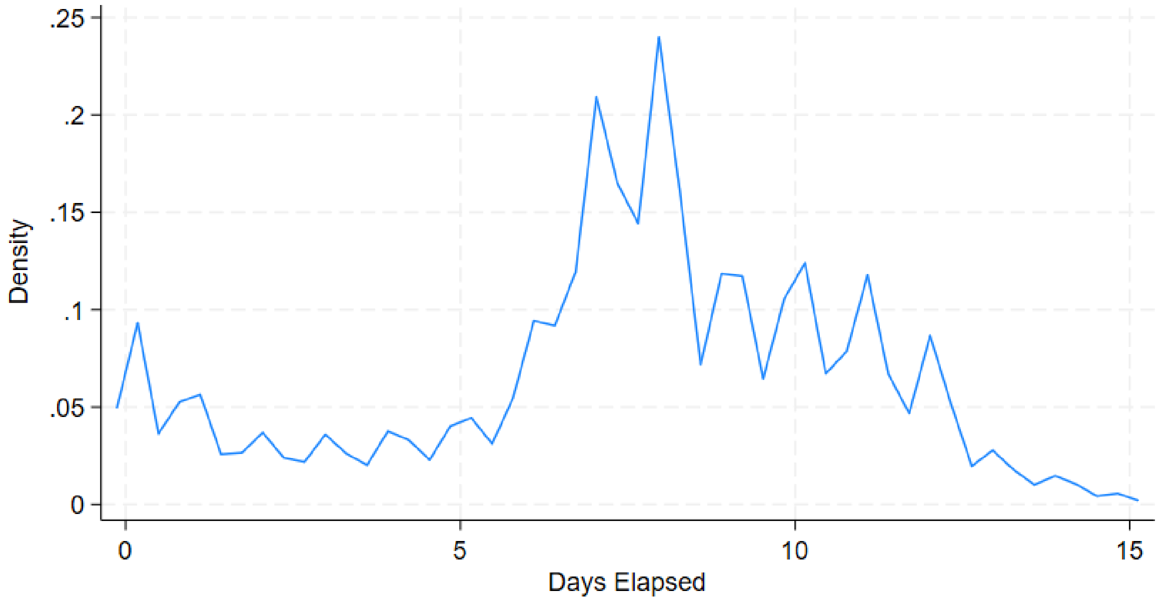

Figure B.3: Density distribution of auction duration (≤ 15 days).

the two candidate pools are:

$$\mathcal{C}'(a) = \left\{c \notin \mathcal{A}^T \cup \mathcal{A}^{\text{conc}} : \ |t_c^s - w_a^*| \leq 168\text{h}, \ \ i(c) \neq i(a), \ \ \text{cat}(c) = \text{cat}(a), \ \ t_c^e \geq w_a^{**}, \ \ n_c^{\text{pre}} \geq \underline{W}\right\}, \tag{4}$$

$$\mathcal{C}(a) = \left\{c \notin \mathcal{A}^T \cup \mathcal{A}^{\text{conc}} : \ |t_c^s - w_a^*| \leq 168\text{h}, \ \ i(c) \neq i(a), \ \ \text{cat}(c) \neq \text{cat}(a), \ \ t_c^e \geq w_a^{**}, \ \ n_c^{\text{pre}} \geq \underline{W}\right\}, \tag{5}$$

where n_c^{pre} is the number of 3-hour windows for control c strictly before w_a^* and $\underline{W} = 24$ is the pre-treatment window requirement of §5. Both pools impose the same non-concurrency requirement: $c \notin \mathcal{A}^T \cup \mathcal{A}^{\text{conc}}$ excludes not just treated items but all auctions by artists with any concurrent activity anywhere in the sample, so that neither control arm is contaminated by untreated-but-concurrent listings. The two pools differ only in the category restriction, $\text{cat}(c) = \text{cat}(a)$ for T' versus $\text{cat}(c) \neq \text{cat}(a)$ for C, which is what isolates the category-level spillover in Hypothesis 2.

C.2 Propensity Score Model

For each pool $\ell \in \{T', C\}$, we form a stacked sample of treated auctions ($D_a = 1$) and their pool-ℓ candidates ($D_c = 0$) and estimate a separate logistic model:

$$\hat{e}_a^{(\ell)} = \Pr(D_a = 1 \mid \mathbf{X}_a;\, \ell) = \Lambda\big(\mathbf{X}_a^\top \hat{\boldsymbol{\beta}}^{(\ell)}\big), \tag{6}$$

where $\Lambda(\cdot)$ is the logistic CDF. Estimating pool-specific models is important: the propensity score in the T' model captures treatment probability relative to same-category auctions, while the C

Panel A: Category composition						
Drawings	12,300					
Graphics	129,312					
Painting	171,856					
Photography	7,508					
Panel B: Auction characteristics						
Variable	Min.	1st Qu.	Median	Mean	3rd Qu.	Max.
$Estimate_a$	18.00	54.00	89.00	260.10	178.00	890,036.00
$Duration_a$	0.00	29.01	154.00	139.10	210.00	4604.00
$Bids_a$	1.00	1.00	4.00	8.03	12.00	162.00
$NBidders_a$	1.00	1.00	2.00	2.89	4.00	27.00
$SoldFor_a$	18.00	27.00	50.00	240.50	138.00	712,029.00

Notes: Here, for item auctioned off in a has $Estimate_a$ as the estimated selling price (€), $Duration_a$ is total time it is run for (hours), $Bids_a$ as the total number of bids it received, $NBidders_a$ is the total number of unique bidders, and $SoldFor_a$ is the final selling price (€).

Table B.4: Summary statistics for the full sample, before dropping about 43,940 items due to missing data, giving final sample of 277,036 items.

model does so relative to different-category auctions; pooling the two would blend structurally distinct covariate distributions and degrade within-pool balance.

The covariate vector $\mathbf{X}_a$ is computed from pre-treatment windows $w < w_a^*$ and comprises four groups:

(i) Cumulative pre-treatment bidding dynamics (running totals over all $w < w_a^*$):

$$\tilde{Bids}_a,\ N\tilde{Bidders}_a,\ Bid\tilde{Amount}_a^{mean},$$

that is, cumulative bids, cumulative unique bidders, and the mean bid amount to date.

(ii) Last-window activity (window $w_a^* - 1$ only):

$$Bids_a^{-1},\ NBidders_a^{-1},\ BidAmount_a^{mean,-1},\ BidAmount_a^{total,-1},$$

capturing bidding momentum immediately before treatment.

(iii) Activity intensity: an activity flag $h_a = \mathbf{1}[\tilde{Bids}_a > 0]$ and the pre-treatment bid rate $BidRate_a$, defined as cumulative bids per pre-treatment window.

(iv) Auction characteristics: $Estimate_a$ (log auction house estimate), y_a (start year), m_a (start month), $\mathbf{g}_a$ (genre indicators).

Auction *duration* is deliberately excluded from $\mathbf{X}_a$. Because the observed listing window is bounded below by the first recorded bid (§5), duration is partly an outcome of bidding activity rather than a pre-determined characteristic; matching on it would condition on a variable the treatment can move. Differences in lifecycle position are instead absorbed nonparametrically by the countdown-to-close fixed effects $\gamma_{r_{a\tau}}$ in Equation (1).

All bidding variables enter via $\log(1+\cdot)$ to accommodate right-skewness and improve linear index specification on the logit scale.

C.3 Caliper Matching on the Linear Predictor

We match on the linear predictor $\hat{\ell}_a^{(\ell)} = \mathbf{X}_a^\top \hat{\boldsymbol{\beta}}^{(\ell)}$ rather than the raw propensity score. Matching on the log-odds scale avoids distance compression near $(0,1)$ boundaries that would conflate pairs far apart in probability space (Austin and Stuart 2015). Control $c \in \mathcal{C}^{(\ell)}(a)$ is caliper-eligible if:

$$|\hat{\ell}_a^{(\ell)} - \hat{\ell}_c^{(\ell)}| \;\leq\; 0.10 \times \hat{\sigma}_{\text{ctrl}}^{(\ell)}, \tag{7}$$

where $\hat{\sigma}_{\text{ctrl}}^{(\ell)}$ is the standard deviation of $\hat{\ell}_c^{(\ell)}$ over all candidate controls in pool ℓ. The 0.10 SD caliper is stricter than the commonly adopted 0.20 threshold (Austin and Stuart 2015), reflecting our emphasis on close counterfactual matches. Among eligible candidates, greedy nearest-neighbor matching without replacement assigns each control to at most one treated auction per pool type. We retain up to $K = 5$ matched controls per pool.

C.4 Window Alignment and Panel Coverage

Because matched auctions start and end at different calendar times, we align all series within each triad using a relative index. Let $\iota_{a,w}$ be the sequential index of window w in auction a's panel, and let $\iota_a^* = \min\{\iota_{a,w} : w \geq w_{a_k}^*\}$ be the index of the first post-treatment window. The relative window index is:

$$\tau_{a,w} = \iota_{a,w} - \iota_a^*, \tag{8}$$

so $\tau = 0$ is the first treated window and $\tau = -1$ is the reference period for event-study normalization. To ensure all three arms of each triad share a common observation range, we restrict to the intersection:

$$\tau \in \big[\max(\underline{w}_T, \underline{w}_{T'}, \underline{w}_C),\ \min(\bar{w}_T, \bar{w}_{T'}, \bar{w}_C)\big], \tag{9}$$

where, for arm $\ell \in \{T, T', C\}$ of triad k, $\underline{w}_\ell$ and $\bar{w}_\ell$ denote the first and last relative windows observed for that arm. We require each triad to satisfy the same pre-treatment window requirement used throughout, $|\max(\underline{w}_T, \underline{w}_{T'}, \underline{w}_C)| \geq \underline{W} = 24$. The estimation window spans $\tau \in [-24, 36]$.

C.5 Matching Statistics

Variable	Before matching			After matching			Improvement
	T Mean	C Mean	SMD	T Mean	C Mean	SMD	(%)
$\tilde{Bids}_a$	0.080	0.070	0.150	0.060	0.070	-0.150	-1.54
$N\tilde{Bidders}_a$	0.050	0.040	0.160	0.040	0.050	-0.160	-3.32
$Bid\tilde{Amount}_a^{mean}$	1.110	0.860	0.240	0.870	1.030	-0.150	36.06
$Bids_a^{-1}$	0.080	0.030	0.160	0.030	0.040	-0.030	78.51
$NBidders_a^{-1}$	0.060	0.020	0.170	0.030	0.040	-0.040	76.13
$BidAmount_a^{mean,-1}$	0.310	0.120	0.160	0.140	0.190	-0.050	72.38
$BidAmount_a^{total,-1}$	0.320	0.120	0.160	0.140	0.200	-0.050	72.65
$h_a = \mathbf{1}[\tilde{Bids}_a > 0]$	0.710	0.510	0.450	0.600	0.660	-0.130	70.25
$BidRate_a$	1.140	0.690	0.470	0.830	1.010	-0.180	60.66
$Estimate_a$	4.920	4.860	0.070	4.840	4.890	-0.070	4.98
y_a	2020.540	2020.360	0.070	2020.890	2020.890	-0.000	98.88
m_a	6.580	6.520	0.020	6.560	6.560	-0.000	88.20

Notes: Values are log-transformed. SMD denotes the standardized mean difference between treated and control auctions. Improvement is the percentage reduction in absolute imbalance after matching, calculated relative to the pre-matching standardized mean difference. Genre indicators are omitted for brevity.

Table C.1: Covariate balance before and after Propensity-Score Matching: Comparison between Treated (T) and Control (C) groups.

Our matching strategy produces 4950 triads, amounting to 4950 $Treated$ items, 12,517 $SameCategory$ items, and 13,056 Control$_a$ items.

Tables C.1 and C.2 report balance against the different-category pool C—the omitted baseline in Equation (1), and therefore the comparison that carries our main coefficient—and against the same-category pool T', respectively. The two tables tell a similar story. Before matching, the largest standardized differences in both pools appear in pre-treatment activity, especially the activity indicator (SMD = 0.45 against C, 0.43 against T') and the pre-treatment bid rate (0.47 and 0.46), confirming that auctions that go on to receive a concurrent sibling were already more active beforehand—precisely the selection our design must neutralize. Matching removes most of this gap. Against T', the activity indicator improves by 80.28%, the bid rate by 70.52%, and the last-window bidding variables by roughly 78%; against C, the corresponding improvements are 70.25%, 60.66%, and 72–79%. Auction timing is balanced almost exactly in both pools (y_a and m_a improve by 88–99%), and the log estimate is well balanced against T' (SMD = -0.02).

Two qualifications are worth stating plainly. First, balance is markedly better on *recent* bidding momentum than on *cumulative* pre-treatment activity. Against the C pool, the three cumulative measures—$\tilde{Bids}_a$, $N\tilde{Bidders}_a$, and $Bid\tilde{Amount}_a^{mean}$—retain post-matching stan-

Variable	Before matching			After matching			Improvement
	T Mean	T' Mean	SMD	T Mean	T' Mean	SMD	(%)
$\tilde{Bids}_a$	0.080	0.070	0.140	0.060	0.070	-0.110	18.84
$N\tilde{Bidders}_a$	0.050	0.040	0.150	0.040	0.050	-0.130	17.07
$Bid\tilde{Amount}_a^{mean}$	1.110	0.860	0.230	0.900	1.010	-0.100	57.90
$Bids_a^{-1}$	0.080	0.030	0.160	0.030	0.050	-0.030	78.26
$NBidders_a^{-1}$	0.060	0.020	0.170	0.030	0.040	-0.040	78.57
$BidAmount_a^{mean,-1}$	0.310	0.130	0.160	0.150	0.190	-0.040	78.19
$BidAmount_a^{total,-1}$	0.320	0.130	0.160	0.150	0.200	-0.040	78.15
$h_a = \mathbf{1}[\tilde{Bids}_a > 0]$	0.710	0.510	0.430	0.610	0.650	-0.080	80.28
$BidRate_a$	1.140	0.710	0.460	0.860	0.980	-0.130	70.52
$Estimate_a$	4.920	4.850	0.080	4.860	4.880	-0.020	74.57
y_a	2020.540	2020.360	0.070	2020.900	2020.910	-0.000	98.61
m_a	6.580	6.520	0.020	6.510	6.520	-0.000	93.69

Notes: Values are log-transformed. SMD denotes the standardized mean difference between treated and same-category control auctions. Improvement is the percentage reduction in absolute imbalance after matching, calculated relative to the pre-matching standardized mean difference. Genre indicators are omitted for brevity.

Table C.2: Covariate balance before and after Propensity-Score Matching: Comparison between Treated (T) and Same-Category Control (T') groups.

dardized differences of -0.150, -0.160, and -0.150, above the conventional 0.10 threshold; for the first two the absolute imbalance is essentially unchanged by matching (improvements of -1.54% and -3.32%) and merely changes sign, so that matched controls are now marginally *more* active cumulatively than treated auctions. The same covariates retain differences of -0.110 and -0.130 against T'. Second, the sign of the residual imbalance works against finding our result rather than for it: the surviving gap leaves controls with slightly higher cumulative pre-treatment bidding, which biases the estimated treatment effect downward. Three features of the design bear directly on the remaining imbalance. The post-matching trimming rule above discards triads whose pre-onset bidding gap is large; triad fixed effects absorb any time-invariant level difference within a matched set; and the event-study estimates in §5.3.2 test the residual concern directly by asking whether treated and control trajectories were already diverging before onset. We provide aggregate statistics of the items that become part of our main analyses in Table C.3.

D Form Proximity via DINOv2 Embeddings

A central moderator in our mechanism analysis (§6, Hypothesis 5) is the *form* proximity between the focal item and a concurrent listing by the same artist. Quantifying form proximity in fine

Panel A: Category composition						
Drawings	1,008					
Graphics	11,137					
Painting	14,745					
Photography	502					
Panel B: Auction characteristics						
Variable	Min.	1st Qu.	Median	Mean	3rd Qu.	Max.
$Estimate_a$	27.00	71.00	107.00	252.30	179.00	220,000.00
$Duration_a$	73.00	169.00	192.03	199.44	231.67	841.77
$Bids_a$	1.00	3.00	7.00	10.09	15.00	103.00
$NBidders_a$	1.00	2.00	3.00	3.43	5.00	18.00
$SoldFor_a$	18.00	36.00	80.00	236.30	196.00	225,005.00

Notes: Here, for item auctioned off in a has $Estimate_a$ as the estimated selling price (€), $Duration_a$ is total time it is run for (hours), $Bids_a$ as the total number of bids it received, $NBidders_a$ is the total number of unique bidders, and $SoldFor_a$ is the final selling price (€).

Table C.3: Summary statistics for the matched analysis sample.

art is non-trivial: works by a single artist typically share palette, composition, brushwork, and subject matter to varying degrees, and a useful similarity measure must be sensitive to these mid- and high-level attributes rather than to low-level statistics (e.g., raw pixel intensity, average color, or photographic capture conditions). Hand-coded stylistic categories are infeasible at our sample scale and would involve substantial coder subjectivity. Supervised representations from ImageNet-trained CNNs (e.g., ResNet, VGG) are an alternative, but their feature spaces are organized around object-class boundaries ("cat" vs. "dog") and are known to under-weight stylistic and compositional variation that is precisely what distinguishes one painting from another (Caron et al. 2021).

We therefore use `DINOv2`, a self-supervised vision transformer released by Oquab et al. (2023) that learns image representations purely from a curated pretraining corpus of ~142M natural images without class labels. Because DINOv2 is trained with a self-distillation objective rather than a categorical classification loss, the resulting embedding space organizes images by holistic visual content, and the model has been shown to deliver state-of-the-art performance on dense prediction, instance retrieval, and fine-grained discrimination tasks — including art and cultural-heritage retrieval benchmarks — without any task-specific fine-tuning (Oquab et al. 2023). During DINOv2's self-supervised training, the classification (`[CLS]`) token's output is optimized to represent the core semantic content of an image. This combination of (i) self-supervised, label-free training, (ii) sensitivity to fine-grained stylistic variation, and (iii) strong zero-shot transfer to out-of-distribution domains makes DINOv2 a particularly apt choice for measuring form proximity among artworks for which no domain-specific labeled corpus exists.

Implementation. For each item a in our matched panel of treated and concurrent listings, we use the platform's primary listing photograph as the canonical image. We load the pretrained `facebook/dinov2-base` checkpoint via the HuggingFace `transformers` library, which exposes the model with a 768-dimensional hidden state and a 14×14 patch grid over 224×224 inputs. Each image is opened with `PIL`, converted to RGB to handle grayscale and four-channel inputs uniformly, and passed through the model's `AutoImageProcessor`, which performs the standard DINOv2 preprocessing pipeline (resize to the shorter side, center crop to 224×224, and normalize with the model's training-time mean/variance). We extract the embedding from the `[CLS]` token of the final hidden state, $e_a = h^{(L)}_{[\mathrm{CLS}]} \in \mathbb{R}^{768}$, which by construction aggregates information across all image patches and is the representation recommended by Oquab et al. (2023) for image-level tasks. For each treated–concurrent pair (a, a') we compute the cosine similarity $s_{a,a'} = \langle e_a, e_{a'} \rangle / (\|e_a\| \, \|e_{a'}\|) \in [-1, 1]$. Inference is performed in evaluation mode (`model.eval()` and `torch.no_grad()`) on GPU when available; pairs for which either image is missing or fails to decode are flagged and excluded from similarity-moderated regressions (these constitute fewer than 2% of pairs). The empirical distribution of $s_{a,a'}$ across our pair sample is right-skewed and concentrated in $[0.4, 0.85]$, reflecting that paired items are by construction by the same artist and therefore share substantial visual structure. Because absolute values on the cosine scale are not economically interpretable, we discretize $s_{a,a'}$ into sample quintiles for the regression specifications in §6; this also accommodates the non-monotonic (inverted-U) prediction of H5 without imposing a parametric functional form.

Alternative similarity grouping. The quintile discretization is an equal-count split and thus arbitrary. To check whether it obscures natural groupings, we re-partition the DINOv2 scores by optimal univariate clustering (Wang and Song 2011), which places break points to minimize within-group variance for a given number of groups k. We find no latent classes: the optimal break points fall on adjacent values of the similarity support with no separating gaps, and the Bayesian Information Criterion selects a single component. Similarity is therefore a smooth continuum, and any discretization is a presentational convenience.

Human validation. To assess whether DINOv2 cosine similarity aligns with human perception, we validated the measure against similarity ratings elicited from human participants. We drew a random sample of 50 painting pairs and administered a survey in Qualtrics in which two research assistants each completed all 50 trials independently. On each trial, the two images of a pair were presented side by side, and the participant rated how similar the pair appeared on a five-point Likert scale (1 = "Not at all similar," 2 = "Slightly similar," 3 = "Moderately similar," 4 = "Very similar," 5 = "Extremely similar"). Unlike Zhang et al. (2022), who rate the quality of single Airbnb images on a seven-point scale, we adopt the five-point scale to reflect the greater complexity of comparing image *pairs* rather than judging single images. The response scale was identical across trials, so that only the image pair varied from item to item; participants first viewed an instruction page describing the task and the meaning of the scale, and responses were recorded and exported automatically. The two raters' scores are highly consistent, correlating at 0.88. Averaging the two participants' ratings for each pair and correlating this human similarity score with the corresponding DINOv2 cosine similarity yields a correlation of 0.71. The embedding-based measure thus closely tracks human judgments of form proximity, supporting its use as our similarity moderator.

E Details for Survival Analyses

The reserve and estimate prices represent critical milestones in an auction's lifecycle. Reaching these thresholds signals market validation and can trigger psychological anchoring effects that influence subsequent bidding behavior (Beggs and Graddy 1997). Similarly, the arrival of new bidders represents a discrete event that fundamentally alters competitive dynamics. For each of these outcomes, we define a time-to-event process where the "event" is the first occurrence of the threshold being crossed during the post-treatment period.

Let $\mathcal{S}_a$ denote the time, measured in relative windows since treatment onset ($\tau = 0$), until auction a first experiences the event, with probability density function $f(\cdot)$ and cumulative distribution function $F(\cdot)$. The hazard function, defined as $h(\tau) = f(\tau)/\{1 - F(\tau)\}$, represents the instantaneous rate at which the event occurs at τ, conditional on the event not having occurred earlier. In our context, a higher hazard indicates a faster transition to the event—precisely the acceleration effect we hypothesize concurrent auctions will induce. We reserve T, T', and C for the three arms of a matched triad throughout, and use $\mathcal{S}_a$ for the event time.

We employ the Cox proportional hazards model (Cox 1972), which relates the hazard function to covariates without requiring parametric assumptions about the baseline hazard. The specification is exactly Equation (3) of §5, reproduced here with its components spelled out:

$$h_a(\tau \mid \cdot) = h_{0,Cat(a)}(\tau) \exp\Big(\beta_1 \, \text{Treated}_a + \beta_2 \, \text{SameCategory}_a + \boldsymbol{\psi}'\mathbf{X}_{a\tau} + \boldsymbol{\eta}'\mathbf{D}_{a\tau} + \theta_{k(a)}\Big), \qquad \tau \geq 0, \tag{10}$$

where $h_{0,Cat(a)}(\cdot)$ is a category-stratified baseline hazard, allowing paintings, graphics, drawings, and photographs to differ arbitrarily in the temporal dynamics with which they reach price thresholds; $\mathbf{X}_{a\tau}$ collects the time-varying controls of Equation (1) with coefficient vector $\boldsymbol{\psi}$; $\mathbf{D}_{a\tau}$ collects day-of-week, hour, month, and year dummies with coefficient vector $\boldsymbol{\eta}$, absorbing systematic calendar variation in bidding intensity; and $\theta_{k(a)}$ is a triad-level shared frailty (a Gamma-distributed random effect) that plays the role of the triad clustering in our DiD specification. The exponentiated coefficients e^{β_1} and e^{β_2} are hazard ratios (HRs); a hazard ratio greater than one indicates a higher instantaneous rate of event occurrence, that is, a shorter expected time to the event.

Risk set, exclusions, and censoring. We restrict the sample identified through the PSM in §5 to the post-treatment period ($\tau \geq 0$), because our focus is on whether treatment accelerates outcomes *after* concurrent auctions begin; including pre-treatment periods would conflate baseline differences across pools with treatment-induced acceleration. Every auction in a matched triad enters the risk set at $\tau = 0$ and is treated as an interval-censored series of Δ-hour windows, with time-varying covariates updated at each window boundary in counting-process (start, stop, event) form. An auction leaves the risk set at the first window in which its event occurs. Auctions that never experience the event are *right-censored* at the earlier of (i) the last window of their own listing, that containing t_a^e, and (ii) the right edge of the common estimation window, $\tau = 36$; censoring is therefore administrative and, conditional on the covariates and the category stratum, uninformative about the latent event time. Because matched auctions close at different calendar times, arms of the same triad can contribute different numbers of at-risk windows; the shared frailty $\theta_{k(a)}$ absorbs the resulting within-triad dependence. Covariates that mechanically define an event are excluded from that event's model: $ReserveMet_{a\tau}$ does not enter the $ReserveMet$ model, and the $NewBidderEntry$ model replaces the contemporaneous cumulative bidder count with its one-window lag $NBidders_{a,\tau-1}$, so that no regressor is a deterministic function of the outcome at the same instant.

F Moderators in Mechanism Testing

Moderator	**Construction**	**Hypothesis**
$\text{EarlyStage}'_\tau$, $\text{LateStage}'_\tau$	Indicators on the *concurrent* auction's clock: equal to 1 when at least one same-artist concurrent listing has $r_{a'\tau} > 12\text{h}$ or $r_{a'\tau} \leq 12\text{h}$ in window τ.	H3
$\text{Bids}'_{a,\tau-1}$, $\text{NewBidders}'_{a,\tau-1}$, ${\Delta^{\text{Mean}}}'_{a,\tau-1}$, ${\Delta^{\text{Total}}}'_{a,\tau-1}$	One-window lags of the concurrent auction's bid count, new-bidder count, mean bid increment, and total bid increment (each log-transformed); paired with the matching focal-auction outcome.	H4
$\text{Similarity}_{(a,a')} \in \{1,\ldots,5\}$	Sample quintile of cosine similarity between DINOv2 `[CLS]` embeddings (`facebook/dinov2-base`, 768-d) of the focal and concurrent item images; entered as five levels.	H5
$\text{EstimateLevel}_a \in \{1,\ldots,5\}$	Sample quintile of the focal item's pre-sale estimate, from 1 (lowest) to 5 (highest); fixed at listing and entered as five levels. A continuous counterpart, $\log \text{Estimate}_a$, is reported alongside.	H6

Table F.1: Moderator variables: Construction and mapped hypotheses.

G Expanded Results

	Dependent Variable			
	$NewBidders_{a\tau}$	$Bids_{a\tau}$	$\Delta_{a\tau}^{Mean}$	$\Delta_{a\tau}^{Total}$
	(1)	(2)	(3)	(4)
Treatment Effects				
Treated$_a$	0.000	-0.004^{***}	-0.011^{**}	-0.011^{**}
	(0.001)	(0.001)	(0.004)	(0.004)
SameCategory$_a$	0.000	0.000	-0.001	-0.001
	(0.000)	(0.000)	(0.002)	(0.002)
POST$_\tau$ × Treated$_a$	0.006^{***}	0.010^{***}	0.034^{***}	0.035^{***}
	(0.001)	(0.003)	(0.008)	(0.008)
POST$_\tau$ × SameCategory$_a$	0.000	0.000	-0.002	-0.002
	(0.000)	(0.001)	(0.004)	(0.004)
Controls				
$ReserveMet_{a\tau}$	0.055^{***}	0.061^{***}	0.247^{***}	0.249^{***}
	(0.003)	(0.006)	(0.021)	(0.022)
$NBidders_{a,\tau-1}$	-0.027^{***}			
	(0.001)			
$NBidders_{a\tau}$		0.033^{***}	0.099^{***}	0.102^{***}
		(0.002)	(0.006)	(0.006)
$AuctionAge_{a\tau}$	0.000^{**}	0.000^{***}	-0.001^{***}	-0.001^{***}
	(0.000)	(0.000)	(0.000)	(0.000)
$(AuctionAge_{a\tau})^2$	0.000	0.000	0.000	0.000
	(0.000)	(0.000)	(0.000)	(0.000)
Fixed Effects				
$\gamma_{k(a)}$	Yes	Yes	Yes	Yes
γ_τ	Yes	Yes	Yes	Yes
$\gamma_{r_{a\tau}}$	Yes	Yes	Yes	Yes
γ_{DOW}	Yes	Yes	Yes	Yes
γ_H	Yes	Yes	Yes	Yes
γ_M	Yes	Yes	Yes	Yes
γ_Y	Yes	Yes	Yes	Yes
γ_{Cat}	Yes	Yes	Yes	Yes
$\gamma_{S(a)}$	Yes	Yes	Yes	Yes
Observations	$1,233,876$	$1,233,876$	$1,233,876$	$1,233,876$
Adj. R^2	0.077	0.107	0.079	0.080
Log-Likelihood	$1,295,527.500$	$313,298.600$	$-1,358,988.900$	$-1,372,095.300$

Notes: Observations are at the auction-relative time level ($a \times \tau$). Standard errors (in parentheses) are clustered at the auction triad and relative-window levels. Significance: $^{***}p < 0.001$; $^{**}p < 0.01$; $^{*}p < 0.05$.

Table G.1: Effect of concurrent auctions on bidding outcomes: Difference-in-Differences estimates.

	Dependent Variable			
	$NewBidders_{a\tau}$	$Bids_{a\tau}$	$\Delta_{a\tau}^{Mean}$	$\Delta_{a\tau}^{Total}$
	(1)	(2)	(3)	(4)
Treatment Effects				
Treated_a	-0.001^{*}	0.000	0.008	0.008
	(0.000)	(0.001)	(0.004)	(0.004)
SameCategory_a	0.000	0.000	-0.001	-0.001
	(0.000)	(0.000)	(0.002)	(0.002)
$\text{POST}_\tau \times \text{Treated}_a$	0.006^{***}	0.016^{***}	0.055^{***}	0.056^{***}
	(0.001)	(0.002)	(0.008)	(0.008)
$\text{POST}_\tau \times \text{SameCategory}_a$	0.000	0.000	-0.001	-0.001
	(0.000)	(0.001)	(0.004)	(0.004)
Fixed Effects				
$\gamma_{k(a)}$	Yes	Yes	Yes	Yes
γ_τ	Yes	Yes	Yes	Yes
$\gamma_{r_{a\tau}}$	Yes	Yes	Yes	Yes
γ_{DOW}	Yes	Yes	Yes	Yes
γ_H	Yes	Yes	Yes	Yes
γ_M	Yes	Yes	Yes	Yes
γ_Y	Yes	Yes	Yes	Yes
γ_{Cat}	Yes	Yes	Yes	Yes
$\gamma_{S(a)}$	Yes	Yes	Yes	Yes
Observations	$1,233,876$	$1,233,876$	$1,233,876$	$1,233,876$
Adj. R^2	0.032	0.073	0.049	0.051
Log-Likelihood	$1,266,199.000$	$290,062.000$	$-1,378,405.200$	$-1,391,661.300$

Notes: Observations are at the auction-relative time level ($a \times \tau$). Standard errors (in parentheses) are clustered at the auction triad and relative-window levels. Significance: $^{***}p < 0.001$; $^{**}p < 0.01$; $^{*}p < 0.05$.

Table G.2: Effect of concurrent auctions on bidding outcomes: Difference-in-Differences estimates without controls.

	Dependent Variable			
	$NewBidders_{a\tau}$ (1)	$Bids_{a\tau}$ (2)	$\Delta_{a\tau}^{Mean}$ (3)	$\Delta_{a\tau}^{Total}$ (4)
Treatment Effects				
Treated_a	-0.001	-0.005^{***}	-0.013^{***}	-0.013^{***}
	(0.001)	(0.001)	(0.004)	(0.004)
SameCategory_a	0.000	0.000	-0.001	-0.001
	(0.000)	(0.000)	(0.002)	(0.002)
$\text{POST}_\tau \times \text{Treated}_a$	0.007^{***}	0.011^{***}	0.041^{***}	0.041^{***}
	(0.001)	(0.003)	(0.011)	(0.011)
$\text{POST}_\tau \times \text{SameCategory}_a$	0.000	0.000	-0.003	-0.003
	(0.000)	(0.001)	(0.004)	(0.004)
$(\text{POST}_\tau \times \text{Treated}_a \times$	-0.001	-0.001	-0.005	-0.005
$NConcurrent_{(a')})$	(0.001)	(0.001)	(0.005)	(0.005)
Controls				
$ReserveMet_{a\tau}$	0.054^{***}	0.061^{***}	0.246^{***}	0.248^{***}
	(0.003)	(0.006)	(0.021)	(0.022)
$NBidders_{a,\tau-1}$	-0.026^{***}			
	(0.001)			
$NBidders_{a\tau}$		0.033^{***}	0.102^{***}	0.104^{***}
		(0.002)	(0.006)	(0.006)
$AuctionAge_{a\tau}$	0.000^{**}	0.000^{***}	-0.001^{***}	-0.001^{***}
	(0.000)	(0.000)	(0.000)	(0.000)
$(AuctionAge_{a\tau})^2$	0.000	0.000	0.000	0.000
	(0.000)	(0.000)	(0.000)	(0.000)
Fixed Effects				
$\gamma_{k(a)}$	Yes	Yes	Yes	Yes
γ_τ	Yes	Yes	Yes	Yes
$\gamma_{r_{a\tau}}$	Yes	Yes	Yes	Yes
γ_{DOW}	Yes	Yes	Yes	Yes
γ_H	Yes	Yes	Yes	Yes
γ_M	Yes	Yes	Yes	Yes
γ_Y	Yes	Yes	Yes	Yes
$\gamma_{S(a)}$	Yes	Yes	Yes	Yes
Observations	1,233,876	1,233,876	1,233,876	1,233,876
R^2	0.081	0.112	0.083	0.084
Log-Likelihood	1,295,177.000	313,276.000	−1,359,103.600	−1,372,208.300

Notes: Observations are at the auction-relative time level ($a \times \tau$). Standard errors (in parentheses) are clustered at the auction triad and relative-window levels. Significance: $^{***}p < 0.001$; $^{**}p < 0.01$; $^{*}p < 0.05$.

Table G.3: Impact of number of concurrent items.

	Hazard Ratio of Event Occurrence		
	$ReserveMet_{a\tau}$ (1)	$EstimateMet_{a\tau}$ (2)	$NewBidderEntry_{a\tau}$ (3)
Treatment Effects			
Treated$_a$	1.797***	1.681***	3.136***
	(0.024)	(0.056)	(0.036)
SameCategory$_a$	0.992	0.906	1.058
	(0.021)	(0.052)	(0.035)
Controls			
$AuctionAge_{a\tau}$	0.962***	0.945***	0.947***
	(0.001)	(0.002)	(0.002)
$(AuctionAge_{a\tau})^2$	1.000***	1.000***	1.000***
	(0.000)	(0.000)	(0.000)
$NBidders_{a\tau}$	2.369***	3.677***	
	(0.011)	(0.025)	
$NBidders_{a,\tau-1}$			2.219***
			(0.016)
Fixed Effects & Strata			
$\theta_{k(a)}$ (triad frailty)	Yes	Yes	Yes
γ_{DOW}	Yes	Yes	Yes
γ_H	Yes	Yes	Yes
γ_M	Yes	Yes	Yes
γ_Y	Yes	Yes	Yes
γ_{Cat}	Yes	Yes	Yes
Number of Items	27,392	27,392	27,392
Events	13,201	2,781	6,107
Event Rate	48.2%	10.2%	22.3%
Log-Likelihood	-106,310	-21,076	-46,944
LR Test (df)	20,728 (1,026)	9,409 (1,352)	13,454 (1,465)

Notes: Analysis is restricted to the post treatment period (relative window $\geq$ 0). Hazard ratios greater than one indicate a higher instantaneous rate of event occurrence (treatment accelerates the outcome). Covariates that mechanically define the event are excluded: $ReserveMet_{a\tau}$ does not enter column (1), and column (3) uses the one-window lag $NBidders_{a,\tau-1}$ in place of the contemporaneous cumulative bidder count. Standard errors are reported in parentheses. Models are estimated with category specific baseline hazards (stratification) and triad level random effects (frailty). Event rate is the proportion of items experiencing the event during the observation period. Significance: $^{***}p < 0.001$; $^{**}p < 0.01$; $^{*}p < 0.05$.

Table G.4: Treatment effects on time to reserve met, estimate met, and new bidder entry: Cox proportional hazards models.

	Dependent Variable			
	$NewBidders_{a\tau}$	$Bids_{a\tau}$	$\Delta_{a\tau}^{Mean}$	$\Delta_{a\tau}^{Total}$
	(1)	(2)	(3)	(4)
Treatment Effects				
Treated_a	0.000	-0.004^{***}	-0.011^{***}	-0.011^{***}
	(0.000)	(0.001)	(0.003)	(0.003)
SameCategory_a	0.000	0.000	-0.001	-0.001
	(0.000)	(0.000)	(0.002)	(0.002)
$\text{POST}_\tau \times \text{Treated}_a \times$	0.006^{***}	0.009^{***}	0.034^{***}	0.034^{***}
EarlyStage'_τ	(0.001)	(0.001)	(0.005)	(0.005)
$\text{POST}_\tau \times \text{Treated}_a \times$	0.019^{***}	0.026^{***}	0.050^{*}	0.052^{*}
LateStage'_τ	(0.004)	(0.008)	(0.022)	(0.022)
$\text{POST}_\tau \times \text{SameCategory}_a$	0.000	0.000	-0.002	-0.002
	(0.000)	(0.001)	(0.003)	(0.003)
Controls				
$ReserveMet_{a\tau}$	0.055^{***}	0.061^{***}	0.247^{***}	0.249^{***}
	(0.001)	(0.001)	(0.004)	(0.004)
$NBidders_{a,\tau-1}$	-0.027^{***}			
	(0.000)			
$NBidders_{a\tau}$		0.033^{***}	0.099^{***}	0.102^{***}
		(0.001)	(0.002)	(0.002)
$AuctionAge_{a\tau}$	0.000^{***}	0.000^{***}	-0.001^{***}	-0.001^{***}
	(0.000)	(0.000)	(0.000)	(0.000)
$(AuctionAge_{a\tau})^2$	0.000	0.000	0.000	0.000
	(0.000)	(0.000)	(0.000)	(0.000)
Fixed Effects				
$\gamma_{k(a)}$	Yes	Yes	Yes	Yes
γ_τ	Yes	Yes	Yes	Yes
$\gamma_{r_{a\tau}}$	Yes	Yes	Yes	Yes
γ_{DOW}	Yes	Yes	Yes	Yes
γ_H	Yes	Yes	Yes	Yes
γ_M	Yes	Yes	Yes	Yes
γ_Y	Yes	Yes	Yes	Yes
γ_{Cat}	Yes	Yes	Yes	Yes
$\gamma_{S(a)}$	Yes	Yes	Yes	Yes
Observations	$1,233,876$	$1,233,876$	$1,233,876$	$1,233,876$
Adj. R^2	0.077	0.107	0.079	0.080
Log-Likelihood	$1,295,570.1$	$313,314.8$	$-1,358,988.1$	$-1,372,094.3$

Notes: Observations are at the auction-relative time level ($a \times \tau$). Standard errors (in parentheses) are clustered at the auction triad and relative-window levels. Significance: $^{***}p < 0.001$; $^{**}p < 0.01$; $^{*}p < 0.05$.

Table G.5: Heterogeneous treatment effects by concurrent auction stage.

	Dependent Variable			
	$NewBidders_{a\tau}$ (1)	$Bids_{a\tau}$ (2)	$\Delta^{Mean}_{a\tau}$ (3)	$\Delta^{Total}_{a\tau}$ (4)
Treatment Effects				
Treated_a	-0.001	-0.005^{***}	-0.013^{***}	-0.013^{***}
	(0.001)	(0.001)	(0.004)	(0.004)
SameCategory_a	0.000	0.000	-0.001	-0.001
	(0.000)	(0.000)	(0.002)	(0.002)
$\text{POST}_\tau \times \text{Treated}_a$	0.007^{***}	0.010^{**}	0.040^{***}	0.040^{***}
	(0.001)	(0.003)	(0.011)	(0.011)
$\text{POST}_\tau \times \text{SameCategory}_a$	0.000	0.000	-0.003	-0.003
	(0.000)	(0.001)	(0.004)	(0.004)
$(\text{POST}_\tau \times \text{Treated}_a \times NewBidders_{a',\tau-1})$	0.004			
	(0.004)			
$(\text{POST}_\tau \times \text{Treated}_a \times Bids_{a',\tau-1})$		0.012^{**}		
		(0.004)		
$(\text{POST}_\tau \times \text{Treated}_a \times \Delta^{Mean}_{a',\tau-1})$			0.007^{*}	
			(0.004)	
$(\text{POST}_\tau \times \text{Treated}_a \times \Delta^{Total}_{a',\tau-1})$				0.007
				(0.004)
Controls				
$ReserveMet_{a\tau}$	0.054^{***}	0.061^{***}	0.246^{***}	0.248^{***}
	(0.003)	(0.006)	(0.021)	(0.022)
$NBidders_{a,\tau-1}$	-0.026^{***}			
	(0.001)			
$NBidders_{a\tau}$		0.033^{***}	0.102^{***}	0.104^{***}
		(0.002)	(0.006)	(0.006)
$AuctionAge_{a\tau}$	0.000^{**}	0.000^{***}	-0.001^{***}	-0.001^{***}
	(0.000)	(0.000)	(0.000)	(0.000)
$(AuctionAge_{a\tau})^2$	0.000	0.000	0.000	0.000
	(0.000)	(0.000)	(0.000)	(0.000)
$ConcurrentItems_{a,\tau-1}$	-0.001	-0.001	-0.006	-0.006
	(0.001)	(0.001)	(0.005)	(0.005)
Fixed Effects				
$\gamma_{k(a)}$	Yes	Yes	Yes	Yes
γ_τ	Yes	Yes	Yes	Yes
$\gamma_{r_{a\tau}}$	Yes	Yes	Yes	Yes
γ_{DOW}	Yes	Yes	Yes	Yes
γ_H	Yes	Yes	Yes	Yes
γ_M	Yes	Yes	Yes	Yes
γ_Y	Yes	Yes	Yes	Yes
$\gamma_{S(a)}$	Yes	Yes	Yes	Yes
Observations	$1,233,876$	$1,233,876$	$1,233,876$	$1,233,876$
Adj. R^2	0.076	0.107	0.079	0.080
Log-Likelihood	$1,295,179.700$	$313,288.500$	$-1,359,098.800$	$-1,372,203.600$

Notes: Observations are at the auction-relative time level ($a \times \tau$). Standard errors (in parentheses) are clustered at the auction triad and relative-window levels. Significance: $^{***}p < 0.001$; $^{**}p < 0.01$; $^{*}p < 0.05$.

Table G.6: Impact of concurrent auction dynamics on focal auction. We use lagged variables for the concurrent auction in order to avoid issues related to simultaneity.

	Dependent Variable			
	$NewBidders_{a\tau}$ (1)	$Bids_{a\tau}$ (2)	$\Delta^{Mean}_{a\tau}$ (3)	$\Delta^{Total}_{a\tau}$ (4)
Treatment Effects				
Treated_a	-0.001^{*}	-0.006^{***}	-0.022^{***}	-0.023^{***}
	(0.001)	(0.001)	(0.004)	(0.005)
SameCategory_a	0.000	0.000	−0.001	−0.001
	(0.000)	(0.000)	(0.002)	(0.002)
$\text{POST}_\tau \times \text{Treated}_a$	-0.003^{**}	-0.014^{***}	-0.032^{***}	-0.034^{***}
	(0.001)	(0.002)	(0.009)	(0.009)
$\text{POST}_\tau \times \text{SameCategory}_a$	0.000	0.000	0.000	0.000
	(0.000)	(0.001)	(0.003)	(0.003)
$\text{POST}_\tau \times ReserveMet_{a\tau}$	-0.018^{**}	-0.038^{**}	-0.166^{***}	-0.167^{***}
	(0.006)	(0.013)	(0.048)	(0.049)
$\text{Treated}_a \times ReserveMet_{a\tau}$	0.007^{*}	0.012^{*}	0.087^{***}	0.086^{***}
	(0.003)	(0.006)	(0.021)	(0.021)
$\text{SameCategory}_a \times ReserveMet_{a\tau}$	−0.001	−0.001	0.003	0.003
	(0.001)	(0.001)	(0.005)	(0.005)
$\text{POST}_\tau \times \text{Treated}_a \times ReserveMet_{a\tau}$	0.020^{***}	0.057^{***}	0.125^{***}	0.130^{***}
	(0.004)	(0.006)	(0.022)	(0.023)
$\text{POST}_\tau \times \text{SameCategory}_a \times ReserveMet_{a\tau}$	0.002	0.000	−0.007	−0.008
	(0.001)	(0.002)	(0.008)	(0.008)
Controls				
$ReserveMet_{a\tau}$	0.062^{***}	0.075^{***}	0.312^{***}	0.314^{***}
	(0.006)	(0.012)	(0.046)	(0.047)
$NBidders_{a,\tau-1}$	-0.027^{***}			
	(0.001)			
$NBidders_{a\tau}$		0.033^{***}	0.100^{***}	0.102^{***}
		(0.002)	(0.006)	(0.006)
$AuctionAge_{a\tau}$	0.000^{***}	0.000^{***}	-0.001^{***}	-0.001^{***}
	(0.000)	(0.000)	(0.000)	(0.000)
$(AuctionAge_{a\tau})^2$	0.000	0.000	0.000	0.000
	(0.000)	(0.000)	(0.000)	(0.000)
Fixed Effects				
$\gamma_{k(a)}$	Yes	Yes	Yes	Yes
γ_τ	Yes	Yes	Yes	Yes
$\gamma_{r_{a\tau}}$	Yes	Yes	Yes	Yes
γ_{DOW}	Yes	Yes	Yes	Yes
γ_H	Yes	Yes	Yes	Yes
γ_M	Yes	Yes	Yes	Yes
γ_Y	Yes	Yes	Yes	Yes
γ_{Cat}	Yes	Yes	Yes	Yes
$\gamma_{S(a)}$	Yes	Yes	Yes	Yes
Observations	1,233,876	1,233,876	1,233,876	1,233,876
Adj. R^2	0.079	0.110	0.081	0.083
Log-Likelihood	1,296,996.200	314,872.400	−1,357,346.300	−1,370,451.500

Notes: Observations are at the auction-relative time level ($a \times \tau$). Standard errors (in parentheses) are clustered at the auction triad and relative-window levels. Significance: $^{***}p < 0.001$; $^{**}p < 0.01$; $^{*}p < 0.05$.

Table G.7: Effects of concurrent auctions and reserve met status.

	Dependent Variable			
	$NewBidders_{a\tau}$	$Bids_{a\tau}$	$\Delta^{Mean}_{a\tau}$	$\Delta^{Total}_{a\tau}$
	(1)	(2)	(3)	(4)
Treatment Effects				
Treated_a	0.000	-0.004^{***}	-0.011^{**}	-0.011^{**}
	(0.001)	(0.001)	(0.004)	(0.004)
SameCategory_a	0.000	0.000	-0.001	-0.001
	(0.000)	(0.000)	(0.002)	(0.002)
$\text{POST}_\tau \times \text{Treated}_a \times$	0.006^{***}	0.008^{***}	0.032^{***}	0.032^{***}
EarlyStage_τ	(0.001)	(0.002)	(0.007)	(0.007)
$\text{POST}_\tau \times \text{Treated}_a \times$	0.012	0.023	0.054	0.057
LateStage_τ	(0.007)	(0.021)	(0.056)	(0.058)
$\text{POST}_\tau \times \text{SameCategory}_a \times$	0.000	0.000	-0.002	-0.002
EarlyStage_τ	(0.000)	(0.001)	(0.004)	(0.004)
$\text{POST}_\tau \times \text{SameCategory}_a \times$	-0.002	0.001	-0.016	-0.016
LateStage_τ	(0.007)	(0.020)	(0.056)	(0.058)
Controls				
$ReserveMet_{a\tau}$	0.055^{***}	0.061^{***}	0.247^{***}	0.249^{***}
	(0.003)	(0.006)	(0.021)	(0.022)
$NBidders_{a,\tau-1}$	-0.027^{***}			
	(0.001)			
$NBidders_{a\tau}$		0.033^{***}	0.099^{***}	0.102^{***}
		(0.002)	(0.006)	(0.006)
$AuctionAge_{a\tau}$	0.000^{**}	0.000^{***}	-0.001^{***}	-0.001^{***}
	(0.000)	(0.000)	(0.000)	(0.000)
$(AuctionAge_{a\tau})^2$	0.000	0.000	0.000	0.000
	(0.000)	(0.000)	(0.000)	(0.000)
Fixed Effects				
$\gamma_{k(a)}$	Yes	Yes	Yes	Yes
γ_τ	Yes	Yes	Yes	Yes
$\gamma_{r_{a\tau}}$	Yes	Yes	Yes	Yes
γ_{DOW}	Yes	Yes	Yes	Yes
γ_H	Yes	Yes	Yes	Yes
γ_M	Yes	Yes	Yes	Yes
γ_Y	Yes	Yes	Yes	Yes
γ_{Cat}	Yes	Yes	Yes	Yes
$\gamma_{S(a)}$	Yes	Yes	Yes	Yes
Observations	1,233,876	1,233,876	1,233,876	1,233,876
Adj. R^2	0.077	0.108	0.079	0.0803
Log-Likelihood	1,295,547.6	313,312.9	$-1,358,984.8$	$-1,372,090.6$

Notes: Observations are at the auction-relative time level ($a \times \tau$). Early Stage defined as period prior to last 12 hours of auction; Late Stage as 12 hours. Standard errors (in parentheses) are clustered at the auction triad and relative-window levels. Significance: $^{***}p < 0.001$; $^{**}p < 0.01$; $^{*}p < 0.05$.

Table G.8: Heterogeneous effects by focal auction stage.

	Dependent Variable			
	$NewBidders_{a\tau}$	$Bids_{a\tau}$	$\Delta^{Mean}_{a\tau}$	$\Delta^{Total}_{a\tau}$
	(1)	(2)	(3)	(4)
Treatment Effects				
Treated_a	0.003^{***}	-0.006^{***}	-0.008	-0.008
	(0.001)	(0.001)	(0.006)	(0.006)
SameCategory_a	0.005^{***}	0.001	0.019^{***}	0.019^{***}
	(0.000)	(0.001)	(0.004)	(0.004)
$\text{POST}_\tau \times \text{SameCategory}_a$	-0.001	0.000	-0.004	-0.005
	(0.001)	(0.002)	(0.007)	(0.007)
$(\text{POST}_\tau \times \text{Treated}_a \times$	0.006^{*}	0.011^{*}	0.037^{*}	0.036^{*}
$Similarity_{(a,a')=1})$	(0.002)	(0.005)	(0.017)	(0.018)
$(\text{POST}_\tau \times \text{Treated}_a \times$	0.006^{**}	0.015^{**}	0.037^{*}	0.039^{*}
$Similarity_{(a,a')=2})$	(0.002)	(0.005)	(0.018)	(0.019)
$(\text{POST}_\tau \times \text{Treated}_a \times$	0.013^{***}	0.022^{**}	0.086^{**}	0.087^{**}
$Similarity_{(a,a')=3})$	(0.003)	(0.007)	(0.029)	(0.029)
$(\text{POST}_\tau \times \text{Treated}_a \times$	0.008^{**}	0.017^{*}	0.038	0.040
$Similarity_{(a,a')=4})$	(0.003)	(0.007)	(0.024)	(0.024)
$(\text{POST}_\tau \times \text{Treated}_a \times$	0.003	0.014^{*}	0.075^{***}	0.076^{***}
$Similarity_{(a,a')=5})$	(0.002)	(0.007)	(0.022)	(0.022)
Controls				
$ReserveMet_{a\tau}$	0.055^{***}	0.063^{***}	0.250^{***}	0.252^{***}
	(0.003)	(0.006)	(0.024)	(0.025)
$NBidders_{a,\tau-1}$	-0.026^{***}			
	(0.001)			
$NBidders_{a\tau}$		0.032^{***}	0.102^{***}	0.104^{***}
		(0.003)	(0.008)	(0.008)
$AuctionAge_{a\tau}$	0.000^{**}	0.000^{***}	-0.001^{***}	-0.001^{***}
	(0.000)	(0.000)	(0.000)	(0.000)
$(AuctionAge_{a\tau})^2$	0.000	0.000	0.000	0.000
	(0.000)	(0.000)	(0.000)	(0.000)
Fixed Effects				
$\gamma_{k(a)}$	*Yes*	*Yes*	*Yes*	*Yes*
γ_τ	*Yes*	*Yes*	*Yes*	*Yes*
$\gamma_{r_{a\tau}}$	*Yes*	*Yes*	*Yes*	*Yes*
γ_{DOW}	*Yes*	*Yes*	*Yes*	*Yes*
γ_H	*Yes*	*Yes*	*Yes*	*Yes*
γ_M	*Yes*	*Yes*	*Yes*	*Yes*
γ_Y	*Yes*	*Yes*	*Yes*	*Yes*
Observations	321,201	321,201	321,201	321,201
Adj. R^2	0.078	0.114	0.083	0.085
Log-Likelihood	339,578.200	86,234.900	$-351,383.500$	$-354,811.900$

Notes: Observations are at the auction-relative time level ($a \times \tau$). $\text{POST}_\tau \times \text{Treated}_a$, γ_{Cat}, and $\gamma_{S(a)}$ are not included on account of multicollinearity. Standard errors (in parentheses) are clustered at the auction triad and relative-window levels. Significance: $^{***}p < 0.001$; $^{**}p < 0.01$; $^{*}p < 0.05$.

Table G.9: Impact of concurrent item similarity with focal item on focal auction dynamics across 5 levels. Analyses restricted to one focal painting to one concurrent painting comparisons.

	Dependent Variable							
	$NewBidders_{a\tau}$		$Bids_{a\tau}$		$\Delta^{Mean}_{a\tau}$		$\Delta^{Total}_{a\tau}$	
	(1)	(2)	(3)	(4)	(5)	(6)	(7)	(8)
Treatment Effects								
Treated_a	0.003^{***}	0.003^{***}	-0.006^{***}	-0.006^{***}	-0.008	-0.008	-0.009	-0.008
	(0.001)	(0.001)	(0.001)	(0.001)	(0.006)	(0.006)	(0.006)	(0.006)
SameCategory_a	0.005^{***}	0.005^{***}	0.001	0.001	0.019^{***}	0.019^{***}	0.019^{***}	0.019^{***}
	(0.000)	(0.000)	(0.001)	(0.001)	(0.004)	(0.004)	(0.004)	(0.004)
$\text{POST}_\tau \times \text{Treated}_a$	0.008^{***}	0.004	0.014^{*}	0.003	0.030	0.019	0.030	0.017
	(0.002)	(0.004)	(0.006)	(0.009)	(0.022)	(0.038)	(0.022)	(0.038)
$\text{POST}_\tau \times \text{SameCategory}_a$	-0.001	-0.001	0.000	0.000	-0.004	-0.004	-0.005	-0.005
	(0.001)	(0.001)	(0.002)	(0.002)	(0.007)	(0.007)	(0.007)	(0.007)
$(\text{POST}_\tau \times \text{Treated}_a \times$ $Similarity_{(a,a')})$	-0.003	0.025	0.005	0.072	0.064	0.130	0.066	0.143
	(0.005)	(0.024)	(0.014)	(0.053)	(0.052)	(0.209)	(0.052)	(0.211)
$(\text{POST}_\tau \times \text{Treated}_a \times$ $Similarity^2_{(a,a')})$		-0.034		-0.080		-0.079		-0.092
		(0.030)		(0.064)		(0.243)		(0.245)
Controls								
$ReserveMet_{a\tau}$	0.055^{***}	0.055^{***}	0.063^{***}	0.063^{***}	0.250^{***}	0.250^{***}	0.252^{***}	0.252^{***}
	(0.003)	(0.003)	(0.006)	(0.006)	(0.024)	(0.024)	(0.025)	(0.025)
$NBidders_{a\tau}$			0.032^{***}	0.032^{***}	0.102^{***}	0.102^{***}	0.105^{***}	0.105^{***}
			(0.003)	(0.003)	(0.008)	(0.008)	(0.008)	(0.008)
$NBidders_{a,\tau-1}$	-0.026^{***}	-0.026^{***}						
	(0.001)	(0.001)						
$AuctionAge_{a\tau}$	0.000^{**}	0.000^{**}	0.000^{***}	0.000^{***}	-0.001^{***}	-0.001^{***}	-0.001^{***}	-0.001^{***}
	(0.000)	(0.000)	(0.000)	(0.000)	(0.000)	(0.000)	(0.000)	(0.000)
$(AuctionAge_{a\tau})^2$	0.000	0.000	0.000	0.000	0.000	0.000	0.000	0.000
	(0.000)	(0.000)	(0.000)	(0.000)	(0.000)	(0.000)	(0.000)	(0.000)
Fixed Effects								
$\gamma_{k(a)}$	*Yes*	*Yes*	*Yes*	*Yes*	*Yes*	*Yes*	*Yes*	*Yes*
γ_τ	*Yes*	*Yes*	*Yes*	*Yes*	*Yes*	*Yes*	*Yes*	*Yes*
$\gamma_{r_{a\tau}}$	*Yes*	*Yes*	*Yes*	*Yes*	*Yes*	*Yes*	*Yes*	*Yes*
γ_{DOW}	*Yes*	*Yes*	*Yes*	*Yes*	*Yes*	*Yes*	*Yes*	*Yes*
γ_H	*Yes*	*Yes*	*Yes*	*Yes*	*Yes*	*Yes*	*Yes*	*Yes*
γ_M	*Yes*	*Yes*	*Yes*	*Yes*	*Yes*	*Yes*	*Yes*	*Yes*
γ_Y	*Yes*	*Yes*	*Yes*	*Yes*	*Yes*	*Yes*	*Yes*	*Yes*
Observations	321,201	321,201	321,201	321,201	321,201	321,201	321,201	321,201
Adj. R^2	0.07767	0.07768	0.11352	0.11354	0.08325	0.08324	0.08489	0.08489
Log-Likelihood	339,565.3	339,567.8	86,231.6	86,234.4	$-351,388.9$	$-351,388.7$	$-354,817.1$	$-354,816.8$

Notes: Observations are at the auction-relative time level ($a \times \tau$). γ_{Cat} and $\gamma_{S(a)}$ are not included on account of multicollinearity. Standard errors (in parentheses) are clustered at the auction triad and relative-window levels. Significance: $^{***}p < 0.001$; $^{**}p < 0.01$; $^{*}p < 0.05$.

Table G.10: Impact of concurrent item similarity with focal item on focal auction dynamics, continuous specification. Analyses restricted to one focal painting to one concurrent painting comparisons.

	Dependent Variable			
	$NewBidders_{a\tau}$	$Bids_{a\tau}$	$\Delta^{Mean}_{a\tau}$	$\Delta^{Total}_{a\tau}$
	(1)	(2)	(3)	(4)
Treatment Effects				
Treated_a	-0.001	-0.006^{***}	-0.021^{***}	-0.022^{***}
	(0.001)	(0.001)	(0.004)	(0.004)
SameCategory_a	0.000	-0.001	-0.001	-0.001
	(0.000)	(0.001)	(0.003)	(0.003)
$\text{POST}_\tau \times \text{SameCategory}_a$	0.000	0.000	0.001	0.000
	(0.001)	(0.001)	(0.005)	(0.005)
$(\text{POST}_\tau \times \text{Treated}_a \times$	0.006^{**}	0.005	0.024	0.025
$Similarity_{(a,a')=1})$	(0.002)	(0.004)	(0.014)	(0.014)
$(\text{POST}_\tau \times \text{Treated}_a \times$	0.006^{***}	0.008	0.018	0.019
$Similarity_{(a,a')=2})$	(0.002)	(0.004)	(0.013)	(0.014)
$(\text{POST}_\tau \times \text{Treated}_a \times$	0.009^{***}	0.015^{***}	0.059^{***}	0.060^{***}
$Similarity_{(a,a')=3})$	(0.002)	(0.004)	(0.017)	(0.017)
$(\text{POST}_\tau \times \text{Treated}_a \times$	0.005^{**}	0.008	0.027	0.026
$Similarity_{(a,a')=4})$	(0.002)	(0.004)	(0.015)	(0.016)
$(\text{POST}_\tau \times \text{Treated}_a \times$	0.005^{**}	0.013^{**}	0.057^{***}	0.058^{***}
$Similarity_{(a,a')=5})$	(0.002)	(0.004)	(0.014)	(0.014)
Controls				
$ReserveMet_{a\tau}$	0.055^{***}	0.064^{***}	0.253^{***}	0.255^{***}
	(0.001)	(0.001)	(0.005)	(0.005)
$NBidders_{a,\tau-1}$	-0.025^{***}			
	(0.001)			
$NBidders_{a\tau}$		0.033^{***}	0.106^{***}	0.108^{***}
		(0.001)	(0.003)	(0.003)
$AuctionAge_{a\tau}$	0.000^{***}	0.000^{***}	-0.001^{***}	-0.001^{***}
	(0.000)	(0.000)	(0.000)	(0.000)
$(AuctionAge_{a\tau})^2$	0.000	0.000	0.000	0.000
	(0.000)	(0.000)	(0.000)	(0.000)
Fixed Effects				
$\gamma_{k(a)}$	Yes	Yes	Yes	Yes
γ_τ	Yes	Yes	Yes	Yes
$\gamma_{r_{a\tau}}$	Yes	Yes	Yes	Yes
γ_{DOW}	Yes	Yes	Yes	Yes
γ_H	Yes	Yes	Yes	Yes
γ_M	Yes	Yes	Yes	Yes
γ_Y	Yes	Yes	Yes	Yes
Observations	661,181	661,181	661,181	661,181
Adj. R^2	0.076	0.109	0.081	0.082
Log-Likelihood	698,976.900	178,925.200	$-718,750.600$	$-725,761.900$

Notes: Observations are at the auction-relative time level ($a \times \tau$). $\text{POST}_\tau \times \text{Treated}_a$, γ_{Cat}, and $\gamma_{S(a)}$ are not included on account of multicollinearity. Standard errors (in parentheses) are clustered at the auction triad and relative-window levels. Significance: $^{***}p < 0.001$; $^{**}p < 0.01$; $^{*}p < 0.05$.

Table G.11: Impact of concurrent item similarity with focal item on focal auction dynamics across 5 levels. Analyses with comparisons across all categories and number of pairs. Mean value of similarity is used when more than one concurrent item is present.

	Dependent Variable			
	$NewBidders_{a\tau}$	$Bids_{a\tau}$	$\Delta_{a\tau}^{Mean}$	$\Delta_{a\tau}^{Total}$
	(1)	(2)	(3)	(4)
Treatment Effects				
Treated_a	-0.001	-0.004^{**}	-0.014^{**}	-0.014^{**}
	(0.001)	(0.002)	(0.005)	(0.005)
SameCategory_a	0.000	0.000	-0.002	-0.002
	(0.000)	(0.000)	(0.002)	(0.002)
$\text{POST}_\tau \times \text{SameCategory}_a$	0.000	0.000	-0.002	-0.002
	(0.000)	(0.001)	(0.004)	(0.004)
$(\text{POST}_\tau \times \text{Treated}_a \times$	0.002	-0.014^{***}	-0.045^{***}	-0.047^{***}
$(EstimateLevel_a = 1))$	(0.001)	(0.003)	(0.010)	(0.011)
$(\text{POST}_\tau \times \text{Treated}_a \times$	0.007^{***}	0.006	0.004	0.004
$(EstimateLevel_a = 2))$	(0.001)	(0.003)	(0.009)	(0.010)
$(\text{POST}_\tau \times \text{Treated}_a \times$	0.010^{***}	0.016^{***}	0.037^{**}	0.037^{**}
$(EstimateLevel_a = 3))$	(0.002)	(0.004)	(0.012)	(0.013)
$(\text{POST}_\tau \times \text{Treated}_a \times$	0.008^{***}	0.018^{***}	0.056^{***}	0.057^{***}
$(EstimateLevel_a = 4))$	(0.002)	(0.004)	(0.014)	(0.014)
$(\text{POST}_\tau \times \text{Treated}_a \times$	0.003^{*}	0.024^{***}	0.122^{***}	0.124^{***}
$(EstimateLevel_a = 5))$	(0.001)	(0.004)	(0.017)	(0.017)
Controls				
$ReserveMet_{a\tau}$	0.056^{***}	0.063^{***}	0.262^{***}	0.264^{***}
	(0.003)	(0.006)	(0.021)	(0.022)
$NBidders_{a,\tau-1}$	-0.028^{***}			
	(0.001)			
$NBidders_{a\tau}$		0.032^{***}	0.086^{***}	0.088^{***}
		(0.003)	(0.006)	(0.006)
$AuctionAge_{a\tau}$	0.000^{**}	0.000^{***}	-0.001^{***}	-0.001^{***}
	(0.000)	(0.000)	(0.000)	(0.000)
$(AuctionAge_{a\tau})^2$	0.000	0.000	0.000	0.000
	(0.000)	(0.000)	(0.000)	(0.000)
Fixed Effects				
$\gamma_{k(a)}$	Yes	Yes	Yes	Yes
γ_τ	Yes	Yes	Yes	Yes
$\gamma_{r_{a\tau}}$	Yes	Yes	Yes	Yes
γ_{DOW}	Yes	Yes	Yes	Yes
γ_H	Yes	Yes	Yes	Yes
γ_M	Yes	Yes	Yes	Yes
γ_Y	Yes	Yes	Yes	Yes
γ_{Cat}	Yes	Yes	Yes	Yes
$\gamma_{S(a)}$	Yes	Yes	Yes	Yes
Observations	1,233,876	1,233,876	1,233,876	1,233,876
Adj. R^2	0.079	0.109	0.083	0.084
Log-Likelihood	1,297,088.700	314,451.200	$-1,356,475.500$	$-1,369,613.100$

Notes: Observations are at the auction-relative time level ($a \times \tau$). $EstimateLevel_a$ and its two-way interactions are excluded for brevity. $\text{POST}_\tau \times \text{Treated}_a$ is omitted from the specification so that all five estimate levels enter as separate triple interactions. Standard errors (in parentheses) are clustered at the auction triad and relative-window levels. Significance: $^{***}p < 0.001$; $^{**}p < 0.01$; $^{*}p < 0.05$.

Table G.12: Heterogeneous effects of concurrency by pre-sale estimate quintile: Triple-Difference estimates.

	Dependent Variable			
	$NewBidders_{a\tau}$ (1)	$Bids_{a\tau}$ (2)	$\Delta_{a\tau}^{Mean}$ (3)	$\Delta_{a\tau}^{Total}$ (4)
Treatment Effects				
Treated_a	-0.001	0.009	0.027	0.028
	(0.002)	(0.005)	(0.022)	(0.023)
SameCategory_a	0.000	0.000	-0.002	-0.002
	(0.000)	(0.000)	(0.002)	(0.002)
$\text{POST}_\tau \times \text{Treated}_a$	0.006	-0.052^{***}	-0.275^{***}	-0.282^{***}
	(0.003)	(0.009)	(0.046)	(0.047)
$\text{POST}_\tau \times \text{SameCategory}_a$	0.000	0.000	-0.002	-0.003
	(0.000)	(0.001)	(0.004)	(0.004)
$\text{POST}_\tau \times Estimate_a$	-0.001^{*}	0.000	0.004	0.004
	(0.000)	(0.001)	(0.004)	(0.004)
$(\text{POST}_\tau \times \text{Treated}_a \times$	0.000	0.013^{***}	0.064^{***}	0.065^{***}
$Estimate_a)$	(0.001)	(0.002)	(0.010)	(0.010)
Controls				
$ReserveMet_{a\tau}$	0.056^{***}	0.063^{***}	0.264^{***}	0.266^{***}
	(0.003)	(0.006)	(0.021)	(0.022)
$NBidders_{a,\tau-1}$	-0.028^{***}			
	(0.001)			
$NBidders_{a\tau}$		0.032^{***}	0.082^{***}	0.085^{***}
		(0.003)	(0.006)	(0.006)
$AuctionAge_{a\tau}$	0.000^{**}	0.000^{***}	-0.001^{***}	-0.001^{***}
	(0.000)	(0.000)	(0.000)	(0.000)
$(AuctionAge_{a\tau})^2$	0.000	0.000^{***}	0.000^{**}	0.000^{**}
	(0.000)	(0.000)	(0.000)	(0.000)
Fixed Effects				
$\gamma_{k(a)}$	Yes	Yes	Yes	Yes
γ_τ	Yes	Yes	Yes	Yes
$\gamma_{r_{a\tau}}$	Yes	Yes	Yes	Yes
γ_{DOW}	Yes	Yes	Yes	Yes
γ_H	Yes	Yes	Yes	Yes
γ_M	Yes	Yes	Yes	Yes
γ_Y	Yes	Yes	Yes	Yes
γ_{Cat}	Yes	Yes	Yes	Yes
$\gamma_{S(a)}$	Yes	Yes	Yes	Yes
Observations	$1,233,876$	$1,233,876$	$1,233,876$	$1,233,876$
Adj. R^2	0.079	0.109	0.083	0.085
Log-Likelihood	$1,297,130.200$	$314,364.900$	$-1,356,100.100$	$-1,369,248.300$

Notes: Observations are at the auction-relative time level ($a \times \tau$). Standard errors (in parentheses) are clustered at the auction triad and relative-window levels. Significance: $^{***}p < 0.001$; $^{**}p < 0.01$; $^{*}p < 0.05$.

Table G.13: Heterogeneous effects of concurrency in the pre-sale estimate, continuous specification: Triple-Difference estimates.

Model	Specification	$ReserveMet_{a\tau}$	$EstimateMet_{a\tau}$	$NewBidderEntry_{a\tau}$
Panel A: Treated$_a$ (T) vs Different Category (C)				
(1)	Baseline	1.706***	2.201***	2.975***
		(0.022)	(0.046)	(0.031)
(2)	+ Controls	1.769***	1.815***	3.134***
		(0.023)	(0.048)	(0.032)
(3)	+ Category Strata	1.748***	1.854***	3.154***
		(0.023)	(0.049)	(0.033)
(4)	+ Hour Strata	1.692***	1.796***	2.873***
		(0.024)	(0.050)	(0.033)
(5)	+ Triad Frailty	1.780***	1.678***	3.194***
		(0.024)	(0.056)	(0.036)
(6)	Full Specification	1.797***	1.681***	3.136***
		(0.024)	(0.056)	(0.036)
Panel B: Same Category$_a$ (T') vs Different Category (C)				
(1)	Baseline	0.989	0.906*	1.049
		(0.020)	(0.047)	(0.032)
(2)	+ Controls	0.993	0.959	1.052
		(0.020)	(0.047)	(0.032)
(3)	+ Category Strata	0.976	0.947	1.063
		(0.021)	(0.048)	(0.033)
(4)	+ Hour Strata	0.983	0.945	1.050
		(0.021)	(0.048)	(0.033)
(5)	+ Triad Frailty	0.990	0.889*	1.051
		(0.022)	(0.053)	(0.035)
(6)	Full Specification	0.992	0.906	1.058
		(0.021)	(0.052)	(0.035)
	Events / Observations	13,201 / 27,392	2,781 / 27,392	6,107 / 27,392

Notes: Hazard ratios from Cox proportional hazards models. Values > 1 indicate faster time to event. Model (6) includes day, hour, month, year fixed effects; category-specific baseline hazards; and triad-level frailty (random effects). Standard errors are reported in parentheses. Significance: $^{***}p < 0.001$; $^{**}p < 0.01$; $^{*}p < 0.05$.

Table G.14: Treatment effects across model specifications and outcomes. Full specification estimates are as per the results from Table G.4.

H Extension: Concurrency Removal

§5 defines treatment onset as $w_a^* = \min\{w : \text{concurrent}_{a,w} > 0\}$ and the concurrency episode's end as $w_a^{**} = \max\{w : \text{concurrent}_{a,w} > 0\}$, noting that the baseline sample restricts to auctions whose w_a^{**} falls at or beyond the focal auction's own close. Here we construct the complementary sample described there: treated auctions a for which (i) w_a^{**} occurs strictly before a's own close, guaranteeing a genuine post-removal, non-concurrent interval, and (ii) at least $\underline{W} = 24$ pre-treatment windows precede w_a^*, exactly as in the baseline design. We place no restriction on the number of concurrent auctions present at any w, nor on the number of distinct concurrent partners across the episode: a may acquire and lose several concurrent partners, simultaneously or in sequence, before w_a^{**}, which is simply the window in which the last such partner closes—allowing for interior windows in which concurrency briefly returns to zero between one partner's close and the next partner's onset.

Two departures from the baseline design are required. First, the requirement that concurrency end before the focal auction closes mechanically bounds the sibling exposure a treated auction can receive: the median treated auction in the unrestricted reversal sample faces a single sibling with 15 hours of remaining life, against five siblings with 171 hours in the baseline sample, and 57% of unrestricted episodes involve a sibling that attracts no bid at all. Because co-disclosure operates on observable bidding history, episodes without one cannot test it. We therefore retain treated auctions for which at least one concurrent listing attracted at least one bid over at least eight overlapping windows (24h).

Matching follows Appendix C without modification: pool-specific logistic propensity scores estimated on pre-onset (pre-w_a^*) covariates only, matched on the linear predictor with caliper $\delta = 0.10$ SD, $K = 5$ nearest neighbors per pool, greedy without replacement. Candidate eligibility is unchanged in form but now anchors on w_a^{**} as the removal point rather than as persistent concurrency: candidates must remain active through the window in which the focal auction's concurrency episode—however many partners it comprised—ends. Because removal, unlike onset, cannot itself be matched on—it is a later, sample-defined event realized only for treated auctions—all matching covariates remain measured strictly before w_a^*, exactly as in the baseline design. Matching yields 630 treated auctions matched to up to five SameCategory_a (1933 total) and up to five Control_a (2047 total) auctions per triad.

Let $\rho_a = w_a^{**} - w_a^*$ denote the removal point on the relative grid, so that removal occurs at $\tau = \rho_a$. We re-estimate Equation (1) with POST_τ replaced by two mutually exclusive phase indicators, $\text{Concurrent}_\tau = \mathbf{1}[0 \le \tau < \rho_a]$ and $\text{PostRemoval}_\tau = \mathbf{1}[\tau \ge \rho_a]$ ($\tau < 0$ omitted), each interacted with Treated_a and SameCategory_a:

$$
\begin{aligned}
Y_{a\tau} = {} & \beta_1 \,\text{Concurrent}_\tau + \beta_2 \,\text{PostRemoval}_\tau + \beta_3 \,\text{Treated}_a + \beta_4 \,\text{SameCategory}_a \\
& + \beta_5 \,(\text{Concurrent}_\tau \times \text{Treated}_a) + \beta_6 \,(\text{PostRemoval}_\tau \times \text{Treated}_a) \\
& + \beta_7 \,(\text{Concurrent}_\tau \times \text{SameCategory}_a) + \beta_8 \,(\text{PostRemoval}_\tau \times \text{SameCategory}_a) \\
& + \boldsymbol{\delta}'\mathbf{X}_{a\tau} + \gamma_{k(a)} + \gamma_{r_{a\tau}} + \gamma_{r'_{a\tau}} + \gamma_{DOW} + \gamma_H + \gamma_M + \gamma_Y + \gamma_{Cat} + \gamma_{S(a)} + \varepsilon_{a\tau},
\end{aligned}
\tag{11}
$$

where $\mathbf{X}_{a\tau}$ and every fixed effect except two are as in Equation (1). The addition is $\gamma_{r'_{a\tau}}$, a countdown-to-removal fixed effect ($r'_{a\tau} = \rho_a - \tau$, binned at Δ-hour resolution); the omission is γ_τ, which is collinear with it within triad. Standard errors remain clustered on k and τ. β_5 is comparable to the $\text{POST}_\tau \times \text{Treated}_a$ coefficient of Equation (1); $\beta_6 - \beta_5$, obtained from the estimated variance-covariance matrix, isolates the incremental effect of removal net of any onset effect that persists.

Table H.1 reports estimates from 262,103 auction-window observations. All four onset interactions with Treated_a are positive and significant: new bidder entry rises 0.4% ($p < 0.05$), bids 0.9% ($p < 0.01$), and mean and total increments 2.9% and 3.0% ($p < 0.05$). Every post-removal interaction is indistinguishable from zero, so the $\beta_6 - \beta_5$ contrast is negative on all four outcomes: the onset gain does not survive the sibling's close. The SameCategory_a interactions depart from the baseline pattern. During the concurrent phase they are null on entry (0.001, ns) but positive on the three intensity outcomes (0.007, 0.025, 0.025, all $p < 0.001$), and null post-removal throughout. The artist-specific intensity effect is therefore the difference $\beta_5 - \beta_7$, which is small relative to β_5; the entry effect, by contrast, is artist-specific in full. We note that this asymmetry does not appear in the baseline sample, where SameCategory_a interactions are null across outcomes.

	Dependent Variable			
	$NewBidders_{a\tau}$	$Bids_{a\tau}$	$\Delta_{a\tau}^{Mean}$	$\Delta_{a\tau}^{Total}$
	(1)	(2)	(3)	(4)
Treated_a	−0.002	0.000	0.001	0.001
	(0.001)	(0.002)	(0.006)	(0.006)
SameCategory_a	−0.001	−0.002*	−0.004	−0.005
	(0.001)	(0.001)	(0.004)	(0.004)
$\text{Concurrent}_\tau \times \text{Treated}_a$	0.004*	0.009**	0.029*	0.030*
	(0.002)	(0.003)	(0.012)	(0.012)
$\text{PostRemoval}_\tau \times \text{Treated}_a$	0.001	0.002	0.019	0.017
	(0.002)	(0.006)	(0.019)	(0.019)
$\text{Concurrent}_\tau \times \text{SameCategory}_a$	0.001	0.007***	0.025***	0.025***
	(0.001)	(0.002)	(0.007)	(0.007)
$\text{PostRemoval}_\tau \times \text{SameCategory}_a$	0.000	0.002	0.004	0.004
	(0.002)	(0.004)	(0.013)	(0.013)
$ReserveMet_{a\tau}$	0.064***	0.016***	0.088***	0.087***
	(0.004)	(0.003)	(0.010)	(0.010)
$NBidders_{a,\tau-1}$	−0.034***			
	(0.002)			
$NBidders_{a\tau}$		0.048***	0.143***	0.147***
		(0.003)	(0.007)	(0.007)
$AuctionAge_{a\tau}$	0.000	0.000***	−0.001***	−0.001***
	(0.000)	(0.000)	(0.000)	(0.000)
$(AuctionAge_{a\tau})^2$	0.000***	0.000***	0.000***	0.000***
	(0.000)	(0.000)	(0.000)	(0.000)
Fixed Effects				
$\gamma_{k(a)}$	Yes	Yes	Yes	Yes
$\gamma_{r'_{a\tau}}$	Yes	Yes	Yes	Yes
$\gamma_{r_{a\tau}}$	Yes	Yes	Yes	Yes
γ_{DOW}	Yes	Yes	Yes	Yes
γ_H	Yes	Yes	Yes	Yes
γ_M	Yes	Yes	Yes	Yes
γ_Y	Yes	Yes	Yes	Yes
γ_{Cat}	Yes	Yes	Yes	Yes
$\gamma_{S(a)}$	Yes	Yes	Yes	Yes
Observations	262,103	262,103	262,103	262,103
Adj. R^2	0.084	0.128	0.092	0.094

Notes: Concurrent_τ and PostRemoval_τ are dropped due to multicollinearity. Standard errors (in parentheses) are clustered at the auction triad and relative-window levels. Significance: $^{***}p < 0.001$; $^{**}p < 0.01$; $^{*}p < 0.05$.

Table H.1: Concurrency removal, dose-restricted multi-concurrency sample: Onset and post-removal effects.

I Robustness

I.1 Event Study and Verification of Parallel Trends Assumption

	Dependent Variable			
	$Bids_{a\tau}$	$NewBidders_{a\tau}$	$\Delta^{Mean}_{a\tau}$	$\Delta^{Total}_{a\tau}$
	(1)	(2)	(3)	(4)
Treated$_a$ × relative window				
Treated$_a$ × $\mathbb{1}\{\tau = -24\}$	-0.003	-0.005**	-0.006	-0.006
	(0.003)	(0.002)	(0.012)	(0.012)
Treated$_a$ × $\mathbb{1}\{\tau = -23\}$	0.000	-0.002	0.000	0.001
	(0.003)	(0.001)	(0.011)	(0.011)
Treated$_a$ × $\mathbb{1}\{\tau = -22\}$	-0.005*	-0.004**	-0.018	-0.018
	(0.003)	(0.001)	(0.010)	(0.011)
Treated$_a$ × $\mathbb{1}\{\tau = -21\}$	0.000	-0.001	-0.008	-0.008
	(0.003)	(0.001)	(0.010)	(0.011)
Treated$_a$ × $\mathbb{1}\{\tau = -20\}$	0.002	-0.002	0.010	0.009
	(0.003)	(0.001)	(0.011)	(0.011)
Treated$_a$ × $\mathbb{1}\{\tau = -19\}$	-0.001	-0.004**	0.001	0.001
	(0.003)	(0.001)	(0.011)	(0.011)
Treated$_a$ × $\mathbb{1}\{\tau = -18\}$	-0.003	-0.003*	-0.016	-0.016
	(0.003)	(0.001)	(0.011)	(0.011)
Treated$_a$ × $\mathbb{1}\{\tau = -17\}$	-0.001	-0.001	0.006	0.005
	(0.003)	(0.001)	(0.011)	(0.011)
Treated$_a$ × $\mathbb{1}\{\tau = -16\}$	0.000	0.000	0.011	0.011
	(0.002)	(0.001)	(0.011)	(0.011)
Treated$_a$ × $\mathbb{1}\{\tau = -15\}$	-0.003	-0.002*	-0.012	-0.012
	(0.002)	(0.001)	(0.009)	(0.009)
Treated$_a$ × $\mathbb{1}\{\tau = -14\}$	0.006*	0.001	0.027**	0.028**
	(0.002)	(0.001)	(0.010)	(0.010)
Treated$_a$ × $\mathbb{1}\{\tau = -13\}$	0.004	0.000	0.016	0.016
	(0.002)	(0.001)	(0.010)	(0.010)
Treated$_a$ × $\mathbb{1}\{\tau = -12\}$	0.002	0.001	0.002	0.003
	(0.003)	(0.001)	(0.011)	(0.011)
Treated$_a$ × $\mathbb{1}\{\tau = -11\}$	0.001	0.000	0.005	0.005
	(0.002)	(0.001)	(0.011)	(0.011)
Treated$_a$ × $\mathbb{1}\{\tau = -10\}$	0.002	-0.002	0.004	0.003
	(0.003)	(0.001)	(0.012)	(0.012)
Treated$_a$ × $\mathbb{1}\{\tau = -9\}$	-0.001	-0.001	-0.003	-0.003
	(0.003)	(0.001)	(0.011)	(0.011)
Treated$_a$ × $\mathbb{1}\{\tau = -8\}$	-0.002	-0.001	-0.003	-0.003
	(0.002)	(0.001)	(0.011)	(0.011)
Treated$_a$ × $\mathbb{1}\{\tau = -7\}$	0.001	0.000	0.009	0.009
	(0.003)	(0.001)	(0.011)	(0.011)
Treated$_a$ × $\mathbb{1}\{\tau = -6\}$	-0.002	-0.001	0.000	-0.001
	(0.002)	(0.001)	(0.010)	(0.010)
Treated$_a$ × $\mathbb{1}\{\tau = -5\}$	0.000	0.001	0.003	0.003
	(0.003)	(0.001)	(0.011)	(0.011)
Treated$_a$ × $\mathbb{1}\{\tau = -4\}$	-0.005	-0.002	-0.016	-0.016
	(0.003)	(0.001)	(0.011)	(0.011)
Treated$_a$ × $\mathbb{1}\{\tau = -3\}$	-0.008***	0.001	-0.006	-0.007
	(0.002)	(0.001)	(0.012)	(0.012)
Treated$_a$ × $\mathbb{1}\{\tau = -2\}$	-0.001	0.003	0.016	0.017
	(0.004)	(0.002)	(0.015)	(0.015)
Treated$_a$ × $\mathbb{1}\{\tau = 0\}$	0.022***	0.014***	0.095***	0.096***
	(0.004)	(0.002)	(0.016)	(0.016)
Treated$_a$ × $\mathbb{1}\{\tau = 1\}$	0.012**	0.003	0.039**	0.040**
	(0.004)	(0.002)	(0.014)	(0.015)
Treated$_a$ × $\mathbb{1}\{\tau = 2\}$	0.010*	0.002	0.046**	0.047**

(continued on next page)

Table I.1 (continued)

	Dependent Variable			
	$Bids_{a\tau}$	$NewBidders_{a\tau}$	$\Delta^{Mean}_{a\tau}$	$\Delta^{Total}_{a\tau}$
	(1)	(2)	(3)	(4)
	(0.004)	(0.002)	(0.015)	(0.015)
$\text{Treated}_a \times \mathbb{1}\{\tau = 3\}$	0.012**	0.005*	0.049**	0.049**
	(0.004)	(0.002)	(0.016)	(0.016)
$\text{Treated}_a \times \mathbb{1}\{\tau = 4\}$	0.013**	0.007**	0.025	0.027
	(0.005)	(0.002)	(0.016)	(0.017)
$\text{Treated}_a \times \mathbb{1}\{\tau = 5\}$	0.005	0.006*	0.031	0.030
	(0.005)	(0.002)	(0.019)	(0.019)
$\text{Treated}_a \times \mathbb{1}\{\tau = 6\}$	0.013*	0.010***	0.049*	0.050*
	(0.006)	(0.003)	(0.019)	(0.020)
$\text{Treated}_a \times \mathbb{1}\{\tau = 7\}$	0.006	0.003	0.051**	0.049**
	(0.005)	(0.002)	(0.018)	(0.019)
$\text{Treated}_a \times \mathbb{1}\{\tau = 8\}$	0.016**	0.004	0.056**	0.055**
	(0.006)	(0.002)	(0.018)	(0.019)
$\text{Treated}_a \times \mathbb{1}\{\tau = 9\}$	0.029***	0.008**	0.100***	0.102***
	(0.006)	(0.002)	(0.020)	(0.020)
$\text{Treated}_a \times \mathbb{1}\{\tau = 10\}$	0.016**	0.007**	0.048*	0.049*
	(0.006)	(0.003)	(0.019)	(0.019)
$\text{Treated}_a \times \mathbb{1}\{\tau = 11\}$	0.011*	-0.001	0.047*	0.047*
	(0.006)	(0.002)	(0.020)	(0.021)
$\text{Treated}_a \times \mathbb{1}\{\tau = 12\}$	0.014*	0.005	0.045*	0.045*
	(0.007)	(0.003)	(0.021)	(0.022)
$\text{Treated}_a \times \mathbb{1}\{\tau = 13\}$	0.010	0.002	0.039	0.039
	(0.007)	(0.003)	(0.023)	(0.024)
$\text{Treated}_a \times \mathbb{1}\{\tau = 14\}$	0.012	0.003	0.062*	0.062*
	(0.008)	(0.003)	(0.026)	(0.026)
$\text{Treated}_a \times \mathbb{1}\{\tau = 15\}$	0.018*	0.007	0.063*	0.063*
	(0.008)	(0.003)	(0.025)	(0.026)
$\text{Treated}_a \times \mathbb{1}\{\tau = 16\}$	0.023**	0.007*	0.077***	0.079***
	(0.007)	(0.003)	(0.023)	(0.024)
$\text{Treated}_a \times \mathbb{1}\{\tau = 17\}$	0.019*	0.006	0.046	0.047
	(0.008)	(0.003)	(0.024)	(0.024)
$\text{Treated}_a \times \mathbb{1}\{\tau = 18\}$	0.018*	0.007*	0.065*	0.067*
	(0.008)	(0.003)	(0.026)	(0.027)
$\text{Treated}_a \times \mathbb{1}\{\tau = 19\}$	0.017*	0.002	0.049	0.051
	(0.008)	(0.003)	(0.027)	(0.028)
$\text{Treated}_a \times \mathbb{1}\{\tau = 20\}$	0.017	-0.001	0.060	0.063*
	(0.009)	(0.004)	(0.031)	(0.031)
$\text{Treated}_a \times \mathbb{1}\{\tau = 21\}$	0.018	-0.002	0.078*	0.077*
	(0.010)	(0.004)	(0.033)	(0.033)
$\text{Treated}_a \times \mathbb{1}\{\tau = 22\}$	0.028*	0.000	0.135***	0.135***
	(0.011)	(0.005)	(0.038)	(0.038)
$\text{Treated}_a \times \mathbb{1}\{\tau = 23\}$	0.012	0.002	0.072*	0.073*
	(0.011)	(0.004)	(0.036)	(0.037)
$\text{Treated}_a \times \mathbb{1}\{\tau = 24\}$	0.026*	0.007	0.093*	0.095*
	(0.011)	(0.005)	(0.036)	(0.037)
SameCategory$_a$ × relative window				
$\text{SameCategory}_a \times \mathbb{1}\{\tau = -24\}$	0.001	0.001	0.008	0.008
	(0.002)	(0.002)	(0.010)	(0.010)
$\text{SameCategory}_a \times \mathbb{1}\{\tau = -23\}$	-0.001	-0.001	-0.003	-0.003
	(0.002)	(0.001)	(0.009)	(0.009)
$\text{SameCategory}_a \times \mathbb{1}\{\tau = -22\}$	0.000	0.001	0.000	0.000
	(0.002)	(0.001)	(0.009)	(0.009)
$\text{SameCategory}_a \times \mathbb{1}\{\tau = -21\}$	-0.002	0.000	-0.004	-0.005
	(0.002)	(0.001)	(0.009)	(0.009)
$\text{SameCategory}_a \times \mathbb{1}\{\tau = -20\}$	0.001	-0.001	0.000	0.000
	(0.002)	(0.001)	(0.009)	(0.009)
$\text{SameCategory}_a \times \mathbb{1}\{\tau = -19\}$	-0.002	-0.002	-0.002	-0.002
	(0.002)	(0.001)	(0.009)	(0.009)
$\text{SameCategory}_a \times \mathbb{1}\{\tau = -18\}$	0.000	-0.001	-0.007	-0.007

(continued on next page)

Table I.1 (continued)

	Dependent Variable			
	$Bids_{a\tau}$	$NewBidders_{a\tau}$	$\Delta^{Mean}_{a\tau}$	$\Delta^{Total}_{a\tau}$
	(1)	(2)	(3)	(4)
	(0.002)	(0.001)	(0.010)	(0.010)
$\text{SameCategory}_a \times \mathbb{1}\{\tau = -17\}$	0.000	0.000	0.001	0.000
	(0.002)	(0.001)	(0.009)	(0.009)
$\text{SameCategory}_a \times \mathbb{1}\{\tau = -16\}$	-0.002	0.000	-0.001	-0.002
	(0.002)	(0.001)	(0.008)	(0.008)
$\text{SameCategory}_a \times \mathbb{1}\{\tau = -15\}$	-0.002	-0.001	-0.004	-0.004
	(0.002)	(0.001)	(0.008)	(0.008)
$\text{SameCategory}_a \times \mathbb{1}\{\tau = -14\}$	0.003	0.001	0.013	0.013
	(0.002)	(0.001)	(0.008)	(0.008)
$\text{SameCategory}_a \times \mathbb{1}\{\tau = -13\}$	-0.001	0.000	-0.010	-0.010
	(0.002)	(0.001)	(0.008)	(0.008)
$\text{SameCategory}_a \times \mathbb{1}\{\tau = -12\}$	0.001	0.001	-0.001	-0.001
	(0.002)	(0.001)	(0.009)	(0.009)
$\text{SameCategory}_a \times \mathbb{1}\{\tau = -11\}$	0.000	-0.001	-0.005	-0.004
	(0.002)	(0.001)	(0.009)	(0.009)
$\text{SameCategory}_a \times \mathbb{1}\{\tau = -10\}$	-0.002	0.000	-0.017*	-0.017
	(0.002)	(0.001)	(0.009)	(0.009)
$\text{SameCategory}_a \times \mathbb{1}\{\tau = -9\}$	-0.001	-0.001	-0.004	-0.004
	(0.002)	(0.001)	(0.008)	(0.008)
$\text{SameCategory}_a \times \mathbb{1}\{\tau = -8\}$	-0.001	0.000	-0.003	-0.003
	(0.002)	(0.001)	(0.008)	(0.008)
$\text{SameCategory}_a \times \mathbb{1}\{\tau = -7\}$	0.000	0.000	0.003	0.003
	(0.002)	(0.001)	(0.008)	(0.008)
$\text{SameCategory}_a \times \mathbb{1}\{\tau = -6\}$	-0.004*	-0.001	-0.013	-0.013
	(0.002)	(0.001)	(0.007)	(0.007)
$\text{SameCategory}_a \times \mathbb{1}\{\tau = -5\}$	0.000	-0.001	0.000	0.000
	(0.002)	(0.001)	(0.008)	(0.008)
$\text{SameCategory}_a \times \mathbb{1}\{\tau = -4\}$	-0.003	-0.001	-0.005	-0.006
	(0.002)	(0.001)	(0.008)	(0.008)
$\text{SameCategory}_a \times \mathbb{1}\{\tau = -3\}$	0.001	0.000	0.001	0.001
	(0.002)	(0.001)	(0.009)	(0.009)
$\text{SameCategory}_a \times \mathbb{1}\{\tau = -2\}$	0.001	-0.001	0.006	0.006
	(0.002)	(0.001)	(0.009)	(0.009)
$\text{SameCategory}_a \times \mathbb{1}\{\tau = 0\}$	0.002	0.001	0.011	0.011
	(0.002)	(0.001)	(0.009)	(0.009)
$\text{SameCategory}_a \times \mathbb{1}\{\tau = 1\}$	0.002	0.002*	0.007	0.007
	(0.002)	(0.001)	(0.009)	(0.009)
$\text{SameCategory}_a \times \mathbb{1}\{\tau = 2\}$	-0.002	-0.001	-0.012	-0.012
	(0.002)	(0.001)	(0.009)	(0.009)
$\text{SameCategory}_a \times \mathbb{1}\{\tau = 3\}$	0.004	0.000	0.012	0.012
	(0.002)	(0.001)	(0.009)	(0.010)
$\text{SameCategory}_a \times \mathbb{1}\{\tau = 4\}$	0.001	-0.001	-0.005	-0.005
	(0.003)	(0.001)	(0.010)	(0.010)
$\text{SameCategory}_a \times \mathbb{1}\{\tau = 5\}$	-0.004	0.000	-0.023*	-0.024*
	(0.003)	(0.001)	(0.011)	(0.011)
$\text{SameCategory}_a \times \mathbb{1}\{\tau = 6\}$	-0.002	0.002	-0.005	-0.006
	(0.003)	(0.001)	(0.011)	(0.011)
$\text{SameCategory}_a \times \mathbb{1}\{\tau = 7\}$	-0.001	0.000	0.000	0.000
	(0.003)	(0.001)	(0.011)	(0.011)
$\text{SameCategory}_a \times \mathbb{1}\{\tau = 8\}$	-0.001	0.000	-0.002	-0.003
	(0.003)	(0.001)	(0.011)	(0.011)
$\text{SameCategory}_a \times \mathbb{1}\{\tau = 9\}$	0.004	0.002	0.012	0.013
	(0.003)	(0.001)	(0.012)	(0.012)
$\text{SameCategory}_a \times \mathbb{1}\{\tau = 10\}$	0.001	0.002	-0.009	-0.009
	(0.003)	(0.001)	(0.012)	(0.012)
$\text{SameCategory}_a \times \mathbb{1}\{\tau = 11\}$	0.000	0.000	-0.006	-0.006
	(0.003)	(0.001)	(0.012)	(0.012)
$\text{SameCategory}_a \times \mathbb{1}\{\tau = 12\}$	-0.001	-0.001	-0.010	-0.010
	(0.003)	(0.001)	(0.013)	(0.013)
$\text{SameCategory}_a \times \mathbb{1}\{\tau = 13\}$	-0.006	-0.001	-0.023	-0.024

(continued on next page)

Table I.1 (continued)

	Dependent Variable			
	$Bids_{a\tau}$	$NewBidders_{a\tau}$	$\Delta^{Mean}_{a\tau}$	$\Delta^{Total}_{a\tau}$
	(1)	(2)	(3)	(4)
	(0.004)	(0.002)	(0.014)	(0.014)
$\text{SameCategory}_a \times \mathbb{1}\{\tau = 14\}$	-0.013***	-0.004*	-0.046***	-0.047***
	(0.004)	(0.002)	(0.014)	(0.014)
$\text{SameCategory}_a \times \mathbb{1}\{\tau = 15\}$	-0.008*	-0.002	-0.043**	-0.044**
	(0.004)	(0.002)	(0.015)	(0.015)
$\text{SameCategory}_a \times \mathbb{1}\{\tau = 16\}$	0.004	0.003	0.027	0.028
	(0.004)	(0.002)	(0.015)	(0.015)
$\text{SameCategory}_a \times \mathbb{1}\{\tau = 17\}$	-0.002	0.000	-0.008	-0.009
	(0.004)	(0.002)	(0.015)	(0.015)
$\text{SameCategory}_a \times \mathbb{1}\{\tau = 18\}$	0.001	0.001	0.000	0.001
	(0.004)	(0.002)	(0.016)	(0.016)
$\text{SameCategory}_a \times \mathbb{1}\{\tau = 19\}$	-0.002	0.000	-0.007	-0.007
	(0.004)	(0.002)	(0.017)	(0.018)
$\text{SameCategory}_a \times \mathbb{1}\{\tau = 20\}$	-0.001	-0.001	-0.008	-0.007
	(0.005)	(0.002)	(0.019)	(0.019)
$\text{SameCategory}_a \times \mathbb{1}\{\tau = 21\}$	0.010	0.004	0.038	0.038
	(0.005)	(0.002)	(0.020)	(0.021)
$\text{SameCategory}_a \times \mathbb{1}\{\tau = 22\}$	-0.009	-0.005	-0.023	-0.025
	(0.006)	(0.003)	(0.022)	(0.023)
$\text{SameCategory}_a \times \mathbb{1}\{\tau = 23\}$	-0.007	-0.001	-0.023	-0.022
	(0.006)	(0.002)	(0.021)	(0.021)
$\text{SameCategory}_a \times \mathbb{1}\{\tau = 24\}$	-0.001	0.000	0.004	0.003
	(0.006)	(0.002)	(0.023)	(0.023)
Fixed Effects				
$\gamma_{k(a)}$	Yes	Yes	Yes	Yes
γ_{τ}	Yes	Yes	Yes	Yes
$\gamma_{r_{a\tau}}$	Yes	Yes	Yes	Yes
Observations	1,176,317	1,176,317	1,176,317	1,176,317
Adj. R^2	0.06503	0.03225	0.04349	0.04453
Log-Likelihood	310,468.6	1,225,979.1	-1,295,276.4	-1,307,488.5

Table I.1: Event study: Treatment and category matched effects by relative auction window.

Notes: Observations are at the auction-relative time level ($a \times \tau$). Table shortened until $\tau = 24$ for brevity. Standard errors (in parentheses) are clustered at the auction triad level. Significance: $^{***}p < 0.001$; $^{**}p < 0.01$; $^{*}p < 0.05$.

I.2 Placebo Event Study Using Pure Controls

We further assess the validity of the event-time design using a placebo event study estimated only on pure control auctions C. This exercise asks whether the event-time construction itself generates apparent post-treatment effects in auctions that are not exposed to the treatment. If the estimated treatment effects in the main analysis were driven primarily by mechanical auction lifecycle dynamics, market-wide shocks, or the way relative time is constructed, then similar post-treatment changes should appear even among pure controls. Conversely, the absence of a comparable post-treatment break among C auctions supports the interpretation that the main estimates capture treatment-specific changes in auction dynamics.

For each outcome, we estimate the following specification on the sample of pure control auctions only:

$$Y_{a\tau} = \sum_{\ell \neq -1} \beta_\ell \mathbb{1}[\tau = \ell] + \delta ReserveMet_{a\tau} + \gamma_a + \gamma_{T(a)-\tau} + \gamma_{DOW} + \gamma_H + \gamma_M + \gamma_Y + \gamma_{Cat} + \varepsilon_{a\tau},$$

where τ indexes relative time windows and the omitted category is $\tau = -1$. Because the sample includes only pure controls, there is no actual treatment in this regression. The coefficients β_ℓ therefore trace the event-time dynamics of untreated auctions relative to the period immediately before the assigned treatment time. A placebo failure would occur if the pure control group displayed a sharp and persistent post-period increase around $\tau = 0$, similar to the pattern observed for treated auctions.

The placebo event-study plots are reported in Figure I.1. The results do not show a treatment-like discontinuity for the pure control group. For the number of bids, the pre-period coefficients are positive at earlier relative windows but decline smoothly as the omitted period approaches. Around the treatment cutoff, the coefficients are close to zero, and the post-period profile does not exhibit a sustained upward shift. For new bidder entry, the post-period coefficients are generally small and often negative, which is inconsistent with the positive post-treatment increase observed for treated auctions. The bid-increment outcomes show a similar pattern: there is no sharp positive break at the treatment threshold, and the post-period coefficients fluctuate around zero with wider confidence intervals at longer horizons.

The presence of some statistically significant coefficients in the placebo event study should not be interpreted as evidence of a placebo treatment effect. These coefficients reflect relative-window differences within pure controls compared with the omitted period $\tau = -1$. Auction outcomes naturally evolve over the lifecycle of an auction, and some relative-window coefficients may differ from the reference period even in the absence of treatment. The relevant diagnostic is whether the untreated controls display a discrete and persistent post-treatment pattern that mirrors the treated event-study response. They do not. Instead, the placebo profiles suggest smooth pre-period dynamics, no immediate post-treatment jump, and increasingly noisy estimates at long post-treatment horizons where support is thinner.

This placebo exercise therefore supports the identification strategy. The main treatment effects are unlikely to be artifacts of the event-time normalization or common auction lifecycle dynamics, because the same event-time procedure applied to untreated control auctions does not produce a comparable positive post-treatment response. Together with the T' versus C comparison and the pooled synthetic-control robustness check, the placebo event study strengthens the interpretation that the observed increases in bidding activity and bid increments are specific to treated auctions exposed to concurrent auction activity.

	Dependent Variable			
	$Bids_{a\tau}$ (1)	$NewBidders_{a\tau}$ (2)	$\Delta_{a\tau}^{Mean}$ (3)	$\Delta_{a\tau}^{Total}$ (4)
Treatment Effects				
POST_τ	-2.150	-1.240	-9.543	-7.044
	(2.466)	(1.123)	(9.865)	(9.962)
Controls				
$ReserveMet_{a\tau}$	0.090***	0.033***	0.336***	0.340***
	(0.001)	(0.000)	(0.003)	(0.003)
Fixed Effects				
$\gamma_{k(a)}$	Yes	Yes	Yes	Yes
$\gamma_{r_{a\tau}}$	Yes	Yes	Yes	Yes
γ_{DOW}	Yes	Yes	Yes	Yes
γ_H	Yes	Yes	Yes	Yes
γ_M	Yes	Yes	Yes	Yes
γ_Y	Yes	Yes	Yes	Yes
γ_{Cat}	Yes	Yes	Yes	Yes
Observations	523,363	523,363	523,363	523,363
R^2	0.08357	0.04304	0.06795	0.06865

Notes: Observations are at the auction-relative time level ($a \times \tau$). γ_τ is dropped. Standard errors (in parentheses) are clustered at the auction triad level. Significance: $^{***}p < 0.001$; $^{**}p < 0.01$; $^{*}p < 0.05$.

Table I.2: Placebo test for items in group C. $Post_\tau$ takes value 1 when corresponding treated item in a triad k gets concurrency.

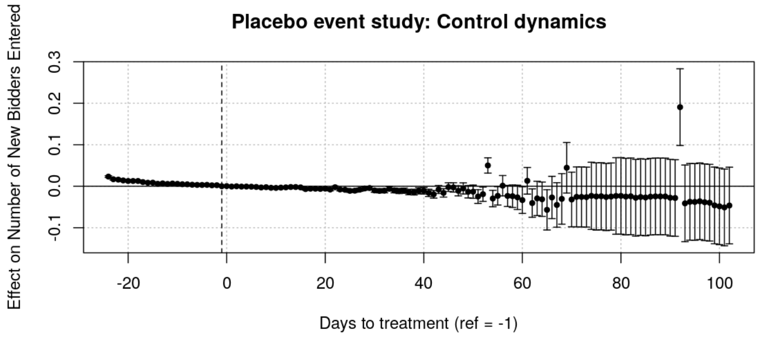

(a) For $NewBidders_{a\tau}$.

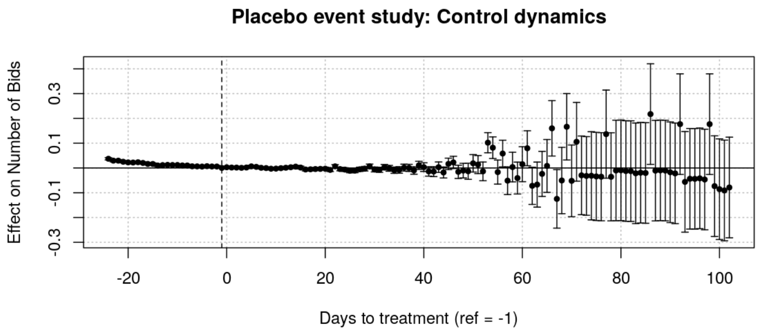

(b) For $Bids_{a\tau}$.

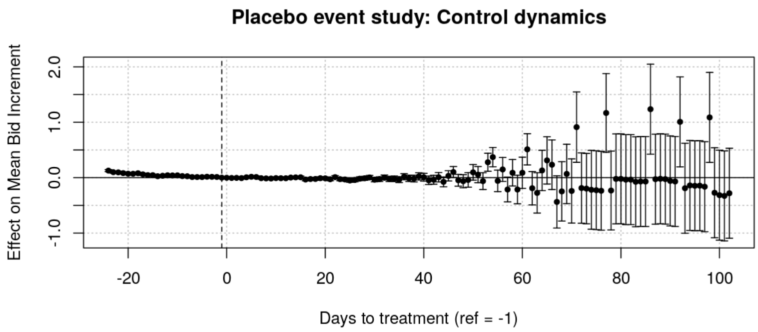

(c) For $\Delta_{a\tau}^{Mean}$.

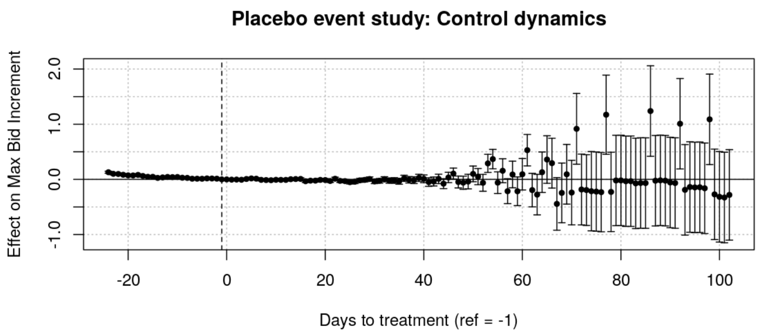

(d) For $\Delta_{a\tau}^{Total}$.

Notes: Graphs show estimated coefficients for event analyses for control auctions across relative time windows (relative window -1) along with 95% confidence intervals. Control auction dynamics are not statistically different from 0 in the post treatment period, providing further validation for our control selection and no SUTVA violation.

Figure I.1: Placebo analyses.

I.3 Synthetic Control Method as Robustness

We complement the main DiD analysis with a synthetic-control-style robustness exercise (Abadie 2021). The purpose of this analysis is to assess whether the same qualitative pattern appears when the treated auctions are compared to an empirically constructed donor benchmark. Whereas the DiD specification estimates treatment effects after conditioning on a rich set of fixed effects, the synthetic-control approach compares the post-treatment trajectory of treated auctions to the observed trajectory of matched control auctions in the donor pool.

Our implementation follows the comparison structure of the main analysis. Specifically, we estimate two pooled counterfactual comparisons. First, for the treated auctions T, we use only the pure control auctions C as the donor group. Second, as a placebo-style comparison, we compare the contemporaneous comparison auctions T' against the same pure control group C. This mirrors the logic of the main empirical design: if the estimated post-treatment increase reflects the effect of focal exposure to concurrent auctions rather than a broad time-varying shock affecting all matched auctions, then we should observe a positive post-treatment gap for T relative to C, but not for T' relative to C.

For each outcome $Y_{a\tau}$, we aggregate outcomes by relative time window and treatment status. Let $\bar{Y}_\tau^T$ denote the average outcome for treated auctions at relative time τ, and let $\bar{Y}_\tau^C$ denote the corresponding average outcome for pure control auctions. The pooled synthetic-control-style gap for the treated group is then

$$\widehat{\Delta}_\tau^{T-C} = \bar{Y}_\tau^T - \bar{Y}_\tau^C.$$

Analogously, for the comparison-group diagnostic, we compute

$$\widehat{\Delta}_\tau^{T'-C} = \bar{Y}_\tau^{T'} - \bar{Y}_\tau^C.$$

The average post-treatment gap is calculated as

$$\widehat{\text{ATT}}_{\text{SC}} = \frac{1}{N_{\text{post}}} \sum_{\tau \in \mathcal{W}_{\text{post}}} \widehat{\Delta}_\tau,$$

where $\mathcal{W}_{\text{post}}$ denotes the set of post-treatment relative time windows and $N_{\text{post}} = |\mathcal{W}_{\text{post}}|$. We report standard errors based on the time-series variation of the post-treatment gaps across relative-time windows,

$$SE(\widehat{\text{ATT}}_{\text{SC}}) = \frac{sd(\widehat{\Delta}_\tau : \tau \in \mathcal{W}_{\text{post}})}{\sqrt{N_{\text{post}}}}.$$

Thus, the reported standard errors should be interpreted as descriptive uncertainty in the average post-treatment gap across relative-time windows, rather than as full randomization-based synthetic control inference. This is appropriate for our purpose here: the exercise is used as a robustness check on the direction and specificity of the main DiD results.

The results are reported in Table I.3. The treated auctions exhibit positive post-treatment gaps relative to the pure control group across all four outcomes. For the number of bids, the estimated average post-treatment gap is 0.069 log points ($SE = 0.017$, $p < 0.001$). For new bidders, the estimated gap is 0.022 log points ($SE = 0.011$, $p = 0.051$), which is positive and marginally significant. The estimated gaps are substantially larger for bid increments: 0.229 log points for mean bid increments ($SE = 0.072$, $p = 0.002$) and 0.232 log points for total bid increments ($SE = 0.073$, $p = 0.002$). Expressed approximately in percentage terms, these estimates correspond to about a 7.2% increase in bids, a 2.2% increase in new bidders, a 25.7% increase in mean bid increments, and a 26.1% increase in max bid increments.

The comparison-group diagnostic provides an important falsification check. When we compare T' auctions to pure controls C, the post-treatment gaps are small and statistically insignificant across all outcomes. The estimated gap is 0.006 log points for bids ($p = 0.545$), -0.001 log points for new bidders ($p = 0.661$), 0.067 log points for mean bid increments ($p = 0.328$), and 0.067 log points for total bid increments ($p = 0.330$). These estimates suggest that the post-treatment increase is not a general feature of all matched comparison auctions. Rather, the increase is concentrated among the treated auctions.

Pre-treatment gaps are also small. For the treated-versus-control comparison, the average pre-treatment gap is -0.003 for bids, -0.001 for new bidders, -0.012 for mean bid increments, and -0.013 for total bid increments. For the T'-versus-C

diagnostic comparison, the corresponding pre-treatment gaps are close to zero as well. This pattern supports the validity of the donor comparison: before treatment, treated and control trajectories are closely aligned on average, while after treatment the treated auctions diverge positively from the controls.

The SC estimates are larger in magnitude than the corresponding DiD estimates. For example, the DiD estimate for bids is 0.010, while the pooled SC post-treatment gap is 0.069; for mean bid increments, the corresponding estimates are 0.035 and 0.229. We do not interpret this difference as a contradiction. The DiD estimates condition on a richer set of fixed effects and controls, while the pooled SC exercise uses relative-time averages to construct a transparent donor comparison. The key implication is that both approaches point in the same qualitative direction: treated auctions exhibit higher post-treatment bidding activity and bid increments, while the T' group does not exhibit a comparable increase relative to pure controls.

Overall, the synthetic-control-style robustness check reinforces the main DiD findings. The positive post-treatment gaps for T versus C, combined with near-zero and statistically insignificant gaps for T' versus C, support the interpretation that concurrent auction exposure increases bidding activity and bid escalation for the treated auctions, rather than merely reflecting a common time trend, auction lifecycle pattern, or broader market-level shock.

Outcome	T vs. C		T' vs. C	
	ATT	SE	ATT	SE
$NewBidders_{a\tau}$	$0.022^{\dagger}$	(0.011)	-0.001	(0.003)
$Bids_{a\tau}$	0.069^{***}	(0.017)	0.006	(0.010)
$\Delta^{Mean}_{a\tau}$	0.229^{**}	(0.072)	0.067	(0.068)
$\Delta^{Total}_{a\tau}$	0.232^{**}	(0.073)	0.067	(0.068)
Pre-treatment gap: $NewBidders_{a\tau}$	-0.001		0.000	
Pre-treatment gap: $Bids_{a\tau}$	-0.003		-0.001	
Pre-treatment gap: $\Delta^{Mean}_{a\tau}$	-0.012		-0.002	
Pre-treatment gap: $\Delta^{Total}_{a\tau}$	-0.013		-0.002	

Notes: The table reports average post-treatment gaps from the pooled synthetic-control-style comparison. The treated comparison uses pure controls C as the donor group. The placebo-style diagnostic compares T' auctions to the same pure control group C. Standard errors are calculated from the time-series variation of post-treatment gaps across relative-time windows. Significance: $^{***}p < 0.001$; $^{**}p < 0.01$; $^{*}p < 0.05$; $^{\dagger}p < 0.10$.

Table I.3: Pooled synthetic-control robustness results.

I.4 Estimation with Matched-Set Weights

We further re-estimate the baseline specification using matched-set weights so that differences in the number of treated, same-category control, and pure control observations within matched triads do not mechanically determine the estimating sample. The weighted estimates are, if anything, stronger than the baseline results: the coefficient on $\text{POST}_\tau \times \text{Treated}_a$ remains positive and highly significant across all four outcomes, increasing to 0.009 for new bidders, 0.013 for bids, 0.048 for mean bid increments, and 0.049 for total bid increments (all at $p < 0.001$). Furthermore, the coefficients for $\text{POST}_\tau \times \text{SameCategory}_a$ remain statistically insignificant. This further adds to the robustness for our results presented in Table 1.

	Dependent Variable			
	$NewBidders_{a\tau}$	$Bids_{a\tau}$	$\Delta^{Mean}_{a\tau}$	$\Delta^{Total}_{a\tau}$
	(1)	(2)	(3)	(4)
Treatment Effects				
Treated_a	-0.002^{**}	-0.005^{***}	-0.013^{**}	-0.013^{**}
	(0.001)	(0.001)	(0.004)	(0.004)
SameCategory_a	0.000	0.000	0.002	0.002
	(0.000)	(0.001)	(0.002)	(0.002)
$\text{POST}_\tau \times \text{Treated}_a$	0.009^{***}	0.013^{***}	0.048^{***}	0.049^{***}
	(0.001)	(0.003)	(0.011)	(0.011)
$\text{POST}_\tau \times \text{SameCategory}_a$	0.000	0.000	-0.003	-0.003
	(0.000)	(0.001)	(0.004)	(0.004)
Controls				
$ReserveMet_{a\tau}$	0.063^{***}	0.071^{***}	0.293^{***}	0.295^{***}
	(0.003)	(0.006)	(0.023)	(0.023)
$NBidders_{a,\tau-1}$	-0.031^{***}			
	(0.001)			
$NBidders_{a\tau}$		0.040^{***}	0.107^{***}	0.111^{***}
		(0.004)	(0.008)	(0.008)
$AuctionAge_{a\tau}$	0.000^{***}	0.000^{***}	-0.001^{***}	-0.001^{***}
	(0.000)	(0.000)	(0.000)	(0.000)
$(AuctionAge_{a\tau})^2$	0.000	0.000	0.000	0.000
	(0.000)	(0.000)	(0.000)	(0.000)
Fixed Effects				
$\gamma_{k(a)}$	Yes	Yes	Yes	Yes
γ_τ	Yes	Yes	Yes	Yes
$\gamma_{r_{a\tau}}$	Yes	Yes	Yes	Yes
γ_{DOW}	Yes	Yes	Yes	Yes
γ_H	Yes	Yes	Yes	Yes
γ_M	Yes	Yes	Yes	Yes
γ_Y	Yes	Yes	Yes	Yes
γ_{Cat}	Yes	Yes	Yes	Yes
$\gamma_{S(a)}$	Yes	Yes	Yes	Yes
Observations	$1,233,876$	$1,233,876$	$1,233,876$	$1,233,876$
Adj. R^2	0.096	0.134	0.100	0.102
Log-Likelihood	$1,292,759.600$	$310,618.700$	$-1,361,044.200$	$-1,374,168.000$

Notes: Observations are at the auction-relative time level ($a \times \tau$). The specification uses matched-set weights to adjust for differences in the number of treated, same-category control, and pure control observations within matched triads. Standard errors (in parentheses) are clustered at the auction triad and relative-window levels. Significance: $^{***}p < 0.001$; $^{**}p < 0.01$; $^{*}p < 0.05$.

Table I.4: Effect of concurrent auctions on bidding outcomes with matched-set weights.

I.5 Poisson Pseudo-Maximum Likelihood Estimation for Count Models

	Dependent Variable	
	$NewBidders_{a\tau}$	$Bids_{a\tau}$
	(1)	(2)
Treatment Effects		
Treated_a	-0.020	-0.094^{***}
	(0.041)	(0.020)
SameCategory_a	-0.061^{*}	0.001
	(0.028)	(0.013)
$\text{POST}_\tau \times \text{Treated}_a$	0.372^{***}	0.259^{***}
	(0.049)	(0.022)
$\text{POST}_\tau \times \text{SameCategory}_a$	0.056	0.031
	(0.040)	(0.017)
Controls		
$ReserveMet_{a\tau}$	4.936^{***}	1.925^{***}
	(0.023)	(0.011)
$NBidders_{a\tau}$		0.928^{***}
		(0.006)
$NBidders_{a,\tau-1}$	-3.154^{***}	
	(0.018)	
$AuctionAge_{a\tau}$	-0.004^{***}	-0.005^{***}
	(0.001)	(0.000)
$(AuctionAge_{a\tau})^2$	0.000^{***}	0.000^{***}
	(0.000)	(0.000)
Fixed Effects		
$\gamma_{k(a)}$	Yes	Yes
γ_τ	Yes	Yes
$\gamma_{r_{a\tau}}$	Yes	Yes
γ_{DOW}	Yes	Yes
γ_H	Yes	Yes
γ_M	Yes	Yes
γ_Y	Yes	Yes
γ_{Cat}	Yes	Yes
$\gamma_{S(a)}$	Yes	Yes
Observations	$1,171,063$	$1,213,738$
Log-Likelihood	$-50,176.600$	$-248,778.900$

Notes: This table reports Poisson pseudo-maximum likelihood estimates for the two count outcomes. Observations are at the auction-relative time level $(a \times \tau)$. Standard errors are reported in parentheses. Significance: $^{***}p < 0.001$; $^{**}p < 0.01$; $^{*}p < 0.05$.

Table I.5: PPML robustness test for count outcomes.

As an additional robustness check, we re-estimate the count-outcome specifications using Poisson pseudo-maximum likelihood (PPML). This addresses the concern that the main log-linear specification may be sensitive to the large mass of zero bidding outcomes, since PPML estimates the model in levels and naturally accommodates zero counts. The PPML results reinforce the baseline findings. The coefficient on $\text{POST}_\tau \times \text{Treated}_a$ is positive and highly significant for both new bidder entry and bidding frequency. Interpreted as semi-elasticities, the estimates imply an increase of approximately $e^{0.372} - 1 = 45.1\%$ in new bidder entry and $e^{0.259} - 1 = 29.5\%$ in bid counts following concurrency onset.

These estimates correspond to multiplicative increases in the conditional mean of the raw count, though these percentage magnitudes should be interpreted cautiously given the sparsity of auction-window bidding outcomes. The corresponding $\text{POST}_\tau \times \text{SameCategory}_a$ coefficients are smaller and statistically insignificant, indicating that the post-treatment increase is concentrated among treated auctions rather than among same-category comparison auctions.

I.6 Alternative Aggregation Windows

In this section, we provide results of estimating Equation 1 with auction window aggregation at 1 hour and 6 hour level. The results after redoing the matching in Tables I.6 and I.7 show that all results are replicated at these alternative aggregation levels, further providing robustness to the main results from Table 1 which uses a 3-hour level aggregation.

	Dependent Variable			
	$NewBidders_{a\tau}$ (1)	$Bids_{a\tau}$ (2)	$\Delta^{Mean}_{a\tau}$ (3)	$\Delta^{Total}_{a\tau}$ (4)
Treatment Effects				
Treated_a	0.000	-0.003^{***}	-0.006^{*}	-0.006^{*}
	(0.000)	(0.001)	(0.003)	(0.003)
SameCategory_a	0.001^{**}	-0.001^{*}	-0.002	-0.002
	(0.000)	(0.000)	(0.002)	(0.002)
$\text{POST}_\tau \times \text{Treated}_a$	0.003^{***}	0.004^{***}	0.016^{***}	0.016^{***}
	(0.000)	(0.001)	(0.004)	(0.004)
$\text{POST}_\tau \times \text{SameCategory}_a$	0.000	0.000	0.001	0.001
	(0.000)	(0.001)	(0.003)	(0.003)
Controls				
$ReserveMet_{a\tau}$	0.021^{***}	0.048^{***}	0.198^{***}	0.200^{***}
	(0.001)	(0.002)	(0.010)	(0.010)
$NBidders_{a,\tau-1}$	-0.009^{***}			
	(0.000)			
$NBidders_{a\tau}$		0.011^{***}	0.023^{***}	0.024^{***}
		(0.001)	(0.002)	(0.002)
$AuctionAge_{a\tau}$	0.000^{***}	0.000^{**}	0.000	0.000
	(0.000)	(0.000)	(0.000)	(0.000)
$(AuctionAge_{a\tau})^2$	0.000	0.000	0.000	0.000
	(0.000)	(0.000)	(0.000)	(0.000)
Fixed Effects				
$\gamma_{k(a)}$	Yes	Yes	Yes	Yes
γ_τ	Yes	Yes	Yes	Yes
$\gamma_{r_{a\tau}}$	Yes	Yes	Yes	Yes
γ_{DOW}	Yes	Yes	Yes	Yes
γ_H	Yes	Yes	Yes	Yes
γ_M	Yes	Yes	Yes	Yes
γ_Y	Yes	Yes	Yes	Yes
γ_{Cat}	Yes	Yes	Yes	Yes
$\gamma_{S(a)}$	Yes	Yes	Yes	Yes
Observations	704,814	704,814	704,814	704,814
Adj. R^2	0.060	0.113	0.076	0.077
Log-Likelihood	1,098,373.600	434,727.800	$-520,734.200$	$-527,812.000$

Notes: Observations are at the auction-relative time level ($a \times \tau$). Standard errors (in parentheses) are clustered at the auction triad and relative-window levels. Significance: $^{***}p < 0.001$; $^{**}p < 0.01$; $^{*}p < 0.05$.

Table I.6: Effect of concurrent auctions on bidding outcomes: At 60-minute window aggregation.

	Dependent Variable			
	$NewBidders_{a\tau}$	$Bids_{a\tau}$	$\Delta^{Mean}_{a\tau}$	$\Delta^{Total}_{a\tau}$
	(1)	(2)	(3)	(4)
Treatment Effects				
Treated_a	-0.002	-0.007^{***}	-0.014^{*}	-0.016^{*}
	(0.001)	(0.002)	(0.006)	(0.007)
SameCategory_a	0.000	-0.001	-0.002	-0.002
	(0.000)	(0.001)	(0.002)	(0.003)
$\text{POST}_\tau \times \text{Treated}_a$	0.010^{***}	0.020^{***}	0.054^{***}	0.068^{***}
	(0.002)	(0.005)	(0.013)	(0.015)
$\text{POST}_\tau \times \text{SameCategory}_a$	0.001	-0.001	-0.002	-0.003
	(0.001)	(0.002)	(0.006)	(0.007)
Controls				
$ReserveMet_{a\tau}$	0.072^{***}	0.113^{***}	0.382^{***}	0.459^{***}
	(0.006)	(0.014)	(0.044)	(0.053)
$NBidders_{a,\tau-1}$	-0.013^{***}			
	(0.001)			
$NBidders_{a\tau}$		0.061^{***}	0.156^{***}	0.184^{***}
		(0.006)	(0.012)	(0.014)
$AuctionAge_{a\tau}$	0.000	-0.001^{***}	-0.001^{***}	-0.001^{***}
	(0.000)	(0.000)	(0.000)	(0.000)
$(AuctionAge_{a\tau})^2$	0.000	0.000	0.000	0.000^{*}
	(0.000)	(0.000)	(0.000)	(0.000)
Fixed Effects				
$\gamma_{k(a)}$	Yes	Yes	Yes	Yes
γ_τ	Yes	Yes	Yes	Yes
$\gamma_{r_{a\tau}}$	Yes	Yes	Yes	Yes
γ_{DOW}	Yes	Yes	Yes	Yes
γ_H	Yes	Yes	Yes	Yes
γ_M	Yes	Yes	Yes	Yes
γ_Y	Yes	Yes	Yes	Yes
γ_{Cat}	Yes	Yes	Yes	Yes
$\gamma_{S(a)}$	Yes	Yes	Yes	Yes
Observations	624,982	624,982	624,982	624,982
Adj. R^2	0.078	0.157	0.124	0.126
Log-Likelihood	447,764.200	$-28,335.800$	$-772,718.300$	$-872,981.500$

Notes: Observations are at the auction-relative time level ($a \times \tau$). Standard errors (in parentheses) are clustered at the auction triad and relative-window levels. Significance: $^{***}p < 0.001$; $^{**}p < 0.01$; $^{*}p < 0.05$.

Table I.7: Effect of concurrent auctions on bidding outcomes: At 6-hour window aggregation.

I.7 Alternative Matching Parameters

In this section, we provide results of estimating Equation 1 by using a caliper of 0.25 and 1 standard deviation while generating matches. The results in Tables I.8 and I.9 show that all results are replicated with this alternative matching criteria, further providing robustness to the main results from Table 1 which uses a matching caliper of 0.1 standard deviation.

	Dependent Variable			
	$NewBidders_{a\tau}$ (1)	$Bids_{a\tau}$ (2)	$\Delta_{a\tau}^{Mean}$ (3)	$\Delta_{a\tau}^{Total}$ (4)
Treatment Effects				
Treated_a	0.000	−0.001	0.003	0.003
	(0.000)	(0.001)	(0.003)	(0.003)
SameCategory_a	0.000	−0.001	−0.001	−0.001
	(0.000)	(0.000)	(0.002)	(0.002)
$\text{POST}_\tau \times \text{Treated}_a$	0.004***	0.006***	0.021***	0.021***
	(0.000)	(0.001)	(0.004)	(0.004)
$\text{POST}_\tau \times \text{SameCategory}_a$	0.000	0.001	0.003	0.003
	(0.000)	(0.001)	(0.002)	(0.002)
Controls				
$ReserveMet_{a\tau}$	0.056***	0.062***	0.246***	0.248***
	(0.000)	(0.000)	(0.002)	(0.002)
$NBidders_{a\tau}$		0.030***	0.093***	0.096***
		(0.000)	(0.001)	(0.001)
$NBidders_{a,\tau-1}$	−0.026***			
	(0.000)			
$AuctionAge_{a\tau}$	0.000***	0.000***	−0.001***	−0.001***
	(0.000)	(0.000)	(0.000)	(0.000)
$(AuctionAge_{a\tau})^2$	0.000	0.000	0.000	0.000
	(0.000)	(0.000)	(0.000)	(0.000)
Fixed Effects				
$\gamma_{k(a)}$	Yes	Yes	Yes	Yes
γ_τ	Yes	Yes	Yes	Yes
$\gamma_{r_{a\tau}}$	Yes	Yes	Yes	Yes
γ_{DOW}	Yes	Yes	Yes	Yes
γ_H	Yes	Yes	Yes	Yes
γ_M	Yes	Yes	Yes	Yes
γ_Y	Yes	Yes	Yes	Yes
γ_{Cat}	Yes	Yes	Yes	Yes
$\gamma_{S(a)}$	Yes	Yes	Yes	Yes
Observations	1,700,004	1,700,004	1,700,004	1,700,004
Adj. R^2	0.072	0.101	0.077	0.079
Log-Likelihood	1,789,846.700	437,552.300	−1,836,985.600	−1,855,563.500

Notes: Observations are at the auction-relative time level ($a \times \tau$). Standard errors (in parentheses) are clustered at the auction triad and relative-window levels. Significance: $^{***}p < 0.001$; $^{**}p < 0.01$; $^{*}p < 0.05$.

Table I.8: Effect of concurrent auctions on bidding outcomes with alternative matching parameters (caliper of 0.25 SD).

	Dependent Variable			
	$NewBidders_{a\tau}$	$Bids_{a\tau}$	$\Delta^{Mean}_{a\tau}$	$\Delta^{Total}_{a\tau}$
	(1)	(2)	(3)	(4)
Treatment Effects				
Treated_a	-0.001^{*}	-0.003^{***}	-0.006^{**}	-0.007^{**}
	(0.000)	(0.001)	(0.002)	(0.002)
SameCategory_a	0.000	0.000	0.000	0.000
	(0.000)	(0.000)	(0.002)	(0.002)
$\text{POST}_\tau \times \text{Treated}_a$	0.006^{***}	0.009^{***}	0.032^{***}	0.033^{***}
	(0.000)	(0.001)	(0.003)	(0.004)
$\text{POST}_\tau \times \text{SameCategory}_a$	0.000	-0.001	-0.003	-0.003
	(0.000)	(0.001)	(0.002)	(0.002)
Controls				
$ReserveMet_{a\tau}$	0.053^{***}	0.060^{***}	0.240^{***}	0.242^{***}
	(0.000)	(0.000)	(0.002)	(0.002)
$NBidders_{a\tau}$		0.031^{***}	0.096^{***}	0.098^{***}
		(0.000)	(0.001)	(0.001)
$NBidders_{a,\tau-1}$	-0.026^{***}			
	(0.000)			
$AuctionAge_{a\tau}$	0.000^{***}	0.000^{***}	-0.001^{***}	-0.001^{***}
	(0.000)	(0.000)	(0.000)	(0.000)
$(AuctionAge_{a\tau})^2$	0.000	0.000	0.000	0.000
	(0.000)	(0.000)	(0.000)	(0.000)
Fixed Effects				
$\gamma_{k(a)}$	*Yes*	*Yes*	*Yes*	*Yes*
γ_τ	*Yes*	*Yes*	*Yes*	*Yes*
$\gamma_{r_{a\tau}}$	*Yes*	*Yes*	*Yes*	*Yes*
γ_{DOW}	*Yes*	*Yes*	*Yes*	*Yes*
γ_H	*Yes*	*Yes*	*Yes*	*Yes*
γ_M	*Yes*	*Yes*	*Yes*	*Yes*
γ_Y	*Yes*	*Yes*	*Yes*	*Yes*
γ_{Cat}	*Yes*	*Yes*	*Yes*	*Yes*
$\gamma_{S(a)}$	*Yes*	*Yes*	*Yes*	*Yes*
Observations	1,842,633	1,842,633	1,842,633	1,842,633
Adj. R^2	0.071	0.101	0.075	0.076
Log-Likelihood	1,949,083.800	469,708.200	$-2,024,088.400$	$-2,043,431.000$

Notes: Observations are at the auction-relative time level ($a \times \tau$). Standard errors (in parentheses) are clustered at the auction triad and relative-window levels. Significance: $^{***}p < 0.001$; $^{**}p < 0.01$; $^{*}p < 0.05$.

Table I.9: Effect of concurrent auctions on bidding outcomes with alternative matching parameters (caliper of 1 SD).

I.8 Alternative Matching Method: Using Mahalanobis Distances

	Dependent Variable			
	$NewBidders_{a\tau}$	$Bids_{a\tau}$	$\Delta^{Mean}_{a\tau}$	$\Delta^{Total}_{a\tau}$
	(1)	(2)	(3)	(4)
Treatment Effects				
Treated$_a$	0.002***	0.001	0.009***	0.009***
	(0.000)	(0.001)	(0.002)	(0.002)
SameCategory$_a$	0.000	0.000	0.001	0.001
	(0.000)	(0.000)	(0.001)	(0.001)
POST$_\tau$ × Treated$_a$	−0.001**	0.005***	0.012***	0.012***
	(0.000)	(0.001)	(0.003)	(0.003)
POST$_\tau$ × SameCategory$_a$	0.000	0.000	0.001	0.001
	(0.000)	(0.001)	(0.002)	(0.002)
Controls				
$ReserveMet_{a\tau}$	0.073***	0.062***	0.256***	0.258***
	(0.000)	(0.000)	(0.002)	(0.002)
$NBidders_{a,\tau-1}$	−0.032***			
	(0.000)			
$NBidders_{a\tau}$		0.036***	0.102***	0.105***
		(0.000)	(0.001)	(0.001)
$AuctionAge_{a\tau}$	0.000***	0.000***	0.000***	0.000***
	(0.000)	(0.000)	(0.000)	(0.000)
$(AuctionAge_{a\tau})^2$	0.000	0.000	0.000	0.000
	(0.000)	(0.000)	(0.000)	(0.000)
Fixed Effects				
$\gamma_{k(a)}$	Yes	Yes	Yes	Yes
γ_τ	Yes	Yes	Yes	Yes
$\gamma_{r_{a\tau}}$	Yes	Yes	Yes	Yes
γ_{DOW}	Yes	Yes	Yes	Yes
γ_H	Yes	Yes	Yes	Yes
γ_M	Yes	Yes	Yes	Yes
γ_Y	Yes	Yes	Yes	Yes
γ_{Cat}	Yes	Yes	Yes	Yes
$\gamma_{S(a)}$	Yes	Yes	Yes	Yes
Observations	1,663,141	1,663,141	1,663,141	1,663,141
Adj. R^2	0.090	0.122	0.097	0.099
Log-Likelihood	1,819,171.700	659,391.100	−1,483,589.000	−1,503,118.100

Notes: Observations are at the auction-relative time level ($a \times \tau$). Standard errors (in parentheses) are clustered at the auction triad and relative-window levels. Significance: $^{***}p < 0.001$; $^{**}p < 0.01$; $^{*}p < 0.05$.

Table I.10: Effect of concurrent auctions on bidding outcomes with Mahalanobis-distance matching.

Here, we utilize Mahalanobis distances to generate matched triads for our main analyses. The corresponding matching produces 4,973 triads: 4,973 *Treated* items matched with 19,215 *SameCategory* items and 19,397 Control$_a$ items, an average of 3.9 matches from each of the two pools per treated item. For the sake of brevity, we do not provide matching statistics, which are in line with those for our Propensity Score based matching from §C.5.

Table I.10 provides results of estimating Equation 1. We see that while the number of new bidders that join a treated auction drops a little (-0.001, $p < 0.001$), all other are positively impacted by the concurrency. Hence, bids increase by 0.005, and the mean and total bid increment amount by 0.012 each (all at $p < 0.001$). Hence, our main results with Propensity Score based matching are mostly replicated.

I.9 Alternative Dimensions of Overlap

	Dependent Variable			
	$NewBidders_{a\tau}$	$Bids_{a\tau}$	$\Delta^{Mean}_{a\tau}$	$\Delta^{Total}_{a\tau}$
	(1)	(2)	(3)	(4)
Treatment Effects				
Treated_a	-0.001	-0.005^{***}	-0.014^{**}	-0.014^{**}
	(0.001)	(0.001)	(0.004)	(0.004)
SameCategory_a	0.000	0.000	0.001	0.001
	(0.000)	(0.000)	(0.002)	(0.002)
$\text{POST}_\tau \times \text{Treated}_a$	0.005^{*}	0.003	0.025	0.024
	(0.002)	(0.006)	(0.018)	(0.018)
$\text{POST}_\tau \times \text{SameCategory}_a$	0.000	-0.001	-0.004	-0.005
	(0.000)	(0.001)	(0.004)	(0.004)
$(\text{POST}_\tau \times \text{Treated}_a \times$	0.001	0.008	0.011	0.013
$TypeOverlap_{(a,a')})$	(0.003)	(0.006)	(0.017)	(0.017)
Controls				
$ReserveMet_{a\tau}$	0.057^{***}	0.066^{***}	0.264^{***}	0.266^{***}
	(0.003)	(0.006)	(0.023)	(0.023)
$NBidders_{a,\tau-1}$	-0.027^{***}			
	(0.001)			
$NBidders_{a\tau}$		0.032^{***}	0.096^{***}	0.098^{***}
		(0.003)	(0.006)	(0.006)
$AuctionAge_{a\tau}$	0.000^{***}	0.000^{***}	-0.001^{***}	-0.001^{***}
	(0.000)	(0.000)	(0.000)	(0.000)
$(AuctionAge_{a\tau})^2$	0.000	0.000	0.000	0.000
	(0.000)	(0.000)	(0.000)	(0.000)
Fixed Effects				
$\gamma_{k(a)}$	Yes	Yes	Yes	Yes
γ_τ	Yes	Yes	Yes	Yes
$\gamma_{r_{a\tau}}$	Yes	Yes	Yes	Yes
γ_{DOW}	Yes	Yes	Yes	Yes
γ_H	Yes	Yes	Yes	Yes
γ_M	Yes	Yes	Yes	Yes
γ_Y	Yes	Yes	Yes	Yes
γ_{Cat}	Yes	Yes	Yes	Yes
$\gamma_{S(a)}$	Yes	Yes	Yes	Yes
Observations	$798,139$	$798,139$	$798,139$	$798,139$
Adj. R^2	0.079	0.107	0.080	0.082
Log-Likelihood	$838,806.700$	$211,508.800$	$-866,706.300$	$-875,192.700$

Notes: Observations are at the auction-relative time level ($a \times \tau$). Standard errors (in parentheses) are clustered at the auction triad level. Significance: $^{***}p < 0.001$; $^{**}p < 0.01$; $^{*}p < 0.05$.

Table I.11: Impact of concurrent item type overlap (for example, $type_a = type_{a'} =$ Painting).

	Dependent Variable			
	$NewBidders_{a\tau}$	$Bids_{a\tau}$	$\Delta^{Mean}_{a\tau}$	$\Delta^{Total}_{a\tau}$
	(1)	(2)	(3)	(4)
Treatment Effects				
Treated_a	-0.001	-0.005^{***}	-0.014^{**}	-0.014^{**}
	(0.001)	(0.001)	(0.004)	(0.004)
SameCategory_a	0.000	0.000	0.001	0.001
	(0.000)	(0.000)	(0.002)	(0.002)
$\text{POST}_\tau \times \text{Treated}_a$	0.006^{***}	0.009^{**}	0.031^{**}	0.032^{**}
	(0.001)	(0.003)	(0.010)	(0.011)
$\text{POST}_\tau \times \text{SameCategory}_a$	0.000	-0.001	-0.004	-0.005
	(0.000)	(0.001)	(0.004)	(0.004)
$(\text{POST}_\tau \times \text{Treated}_a \times$	0.001	0.003	0.007	0.008
$GenreOverlap_{(a,a')})$	(0.001)	(0.003)	(0.010)	(0.010)
Controls				
$ReserveMet_{a\tau}$	0.057^{***}	0.066^{***}	0.264^{***}	0.266^{***}
	(0.003)	(0.006)	(0.023)	(0.023)
$NBidders_{a,\tau-1}$	-0.027^{***}			
	(0.001)			
$NBidders_{a\tau}$		0.032^{***}	0.096^{***}	0.098^{***}
		(0.003)	(0.006)	(0.006)
$AuctionAge_{a\tau}$	0.000^{***}	0.000^{***}	-0.001^{***}	-0.001^{***}
	(0.000)	(0.000)	(0.000)	(0.000)
$(AuctionAge_{a\tau})^2$	0.000	0.000	0.000	0.000
	(0.000)	(0.000)	(0.000)	(0.000)
Fixed Effects				
$\gamma_{k(a)}$	Yes	Yes	Yes	Yes
γ_τ	Yes	Yes	Yes	Yes
$\gamma_{r_{a\tau}}$	Yes	Yes	Yes	Yes
γ_{DOW}	Yes	Yes	Yes	Yes
γ_H	Yes	Yes	Yes	Yes
γ_M	Yes	Yes	Yes	Yes
γ_Y	Yes	Yes	Yes	Yes
γ_{Cat}	Yes	Yes	Yes	Yes
$\gamma_{S(a)}$	Yes	Yes	Yes	Yes
Observations	798,139	798,139	798,139	798,139
Adj. R^2	0.079	0.107	0.080	0.082
Log-Likelihood	838,807.500	211,505.100	$-866,706.300$	$-875,192.800$

Notes: Observations are at the auction-relative time level ($a \times \tau$). Standard errors (in parentheses) are clustered at the auction triad and relative-window levels. Significance: $^{***}p < 0.001$; $^{**}p < 0.01$; $^{*}p < 0.05$.

Table I.12: Impact of concurrent item genre overlap (for example, $genre_a = genre_{a'}$ = Landscape).

	Dependent Variable			
	$NewBidders_{a\tau}$	$Bids_{a\tau}$	$\Delta^{Mean}_{a\tau}$	$\Delta^{Total}_{a\tau}$
	(1)	(2)	(3)	(4)
Treatment Effects				
Treated_a	-0.001	-0.005^{***}	-0.014^{**}	-0.014^{**}
	(0.001)	(0.001)	(0.004)	(0.004)
SameCategory_a	0.000	0.000	0.001	0.001
	(0.000)	(0.000)	(0.002)	(0.002)
$\text{POST}_\tau \times \text{Treated}_a$	0.007^{***}	0.011^{***}	0.037^{***}	0.038^{***}
	(0.001)	(0.003)	(0.010)	(0.010)
$\text{POST}_\tau \times \text{SameCategory}_a$	0.000	-0.001	-0.004	-0.005
	(0.000)	(0.001)	(0.004)	(0.004)
$(\text{POST}_\tau \times \text{Treated}_a \times$	-0.003^{*}	-0.003	-0.007	-0.008
$AuctionHouseOverlap_{(a,a')})$	(0.001)	(0.003)	(0.011)	(0.011)
Controls				
$ReserveMet_{a\tau}$	0.057^{***}	0.066^{***}	0.264^{***}	0.266^{***}
	(0.003)	(0.006)	(0.023)	(0.023)
$NBidders_{a,\tau-1}$	-0.027^{***}			
	(0.001)			
$NBidders_{a\tau}$		0.032^{***}	0.096^{***}	0.098^{***}
		(0.003)	(0.006)	(0.006)
$AuctionAge_{a\tau}$	0.000^{***}	0.000^{***}	-0.001^{***}	-0.001^{***}
	(0.000)	(0.000)	(0.000)	(0.000)
$(AuctionAge_{a\tau})^2$	0.000	0.000	0.000	0.000
	(0.000)	(0.000)	(0.000)	(0.000)
Fixed Effects				
$\gamma_{k(a)}$	Yes	Yes	Yes	Yes
γ_τ	Yes	Yes	Yes	Yes
$\gamma_{r_{a\tau}}$	Yes	Yes	Yes	Yes
γ_{DOW}	Yes	Yes	Yes	Yes
γ_H	Yes	Yes	Yes	Yes
γ_M	Yes	Yes	Yes	Yes
γ_Y	Yes	Yes	Yes	Yes
γ_{Cat}	Yes	Yes	Yes	Yes
$\gamma_{S(a)}$	Yes	Yes	Yes	Yes
Observations	798,139	798,139	798,139	798,139
Adj. R^2	0.079	0.107	0.080	0.082
Log-Likelihood	838,811.800	211,505.100	$-866,706.300$	$-875,192.700$

Notes: Observations are at the auction-relative time level ($a \times \tau$). Standard errors (in parentheses) are clustered at the auction triad and relative-window levels. Significance: $^{***}p < 0.001$; $^{**}p < 0.01$; $^{*}p < 0.05$.

Table I.13: Impact of concurrent item auction house overlap (for example, $AH_a = AH_{a'} =$ Barcelona Auctions).